Out of equilibrium dynamics of complex systems

Leticia F. Cugliandolo

Sorbonne Universités, Université Pierre et Marie Curie

Laboratoire de Physique Théorique et Hautes Energies

Institut Universitaire de France

leticia@lpthe.jussieu.fr

www.lpthe.jussieu.fr/˜leticia/seminars

Bangalore, India, 2021

Plan of Lectures

1. Introduction
2. Coarsening
3. Disorder
4. Active Matter
5. Integrability

Fourth lecture

Plan of Lectures

1. Introduction
2. Coarsening
3. Disorder
4. **Active Matter**
5. Integrability

Melting in two dimensional passive & active matter

Leticia F. Cugliandolo

Sorbonne Université

Institut Universitaire de France

leticia@lpthe.jussieu.fr

www.lpthe.jussieu.fr/˜leticia

Work in collaboration with

C. Caporusso, **G. Gonnella**, **P. Digregorio & I. Petrelli** (Bari, Italia)

A. Suma (Trieste, Italia, Philadelphia, USA, Bari, Italia)

D. Levis & I. Pagonabarraga (Barcelona, España & Lausanne, Suisse)

Aim

Better understanding of melting in two dimensions

Why $2d$?

Experimental realisations but in reality,

because it is interesting from a

fundamental viewpoint

a talk about a classical problem and a

timely active extension

Plan

1. Equilibrium phases : solidification/melting

   Special in two-dimensions

   Solid, hexatic & liquid phases

   Phase transitions

   Topological defects

2. Active matter

   Self-propelled Brownian disks in $2d$

   Phase diagram

   Solid, hexatic & liquid phases ; motility induced phase separation

   Topological defects

Plan

1. **Equilibrium phases : solidification/melting**

   Special in two-dimensions

   Solid, hexatic & liquid phases

   Phase transitions

   Topological defects

2. Active matter

   Self-propelled Brownian disks in $2d$

   Phase diagram

   Solid, hexatic & liquid phases ; motility induced phase separation

   Topological defects

Phases of matter

Solid, liquid and gas equilibrium phases

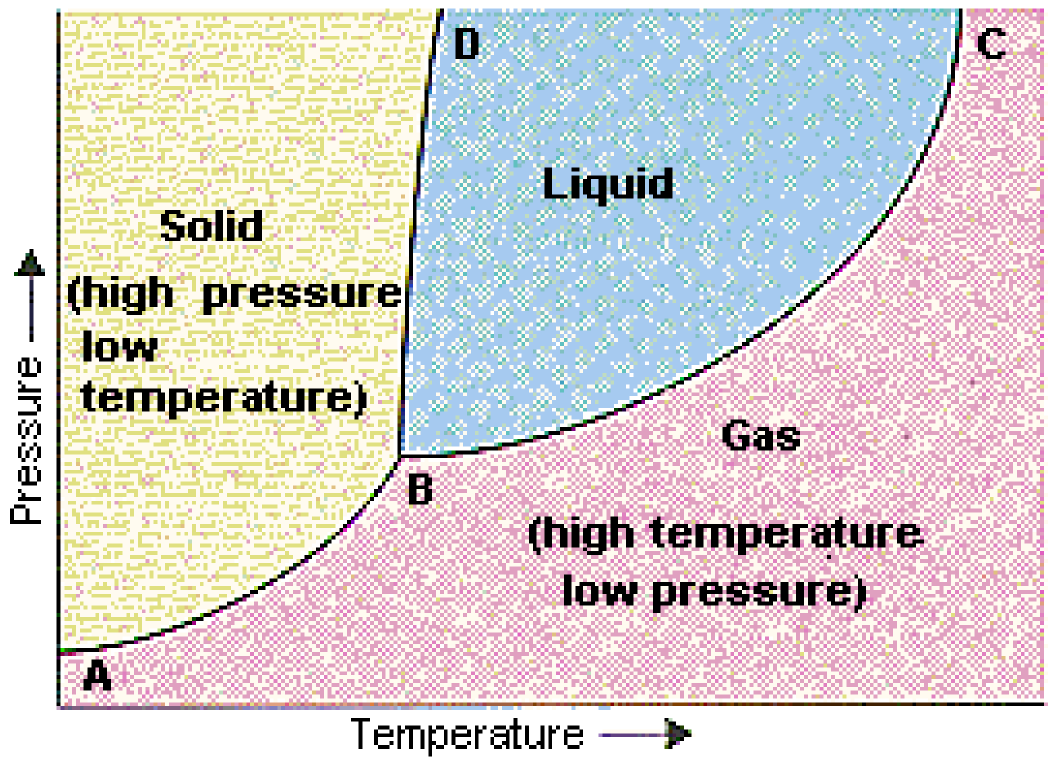

Typical & simple (P, T) phase diagram

Phases of matter

Solid, liquid and gas equilibrium phases

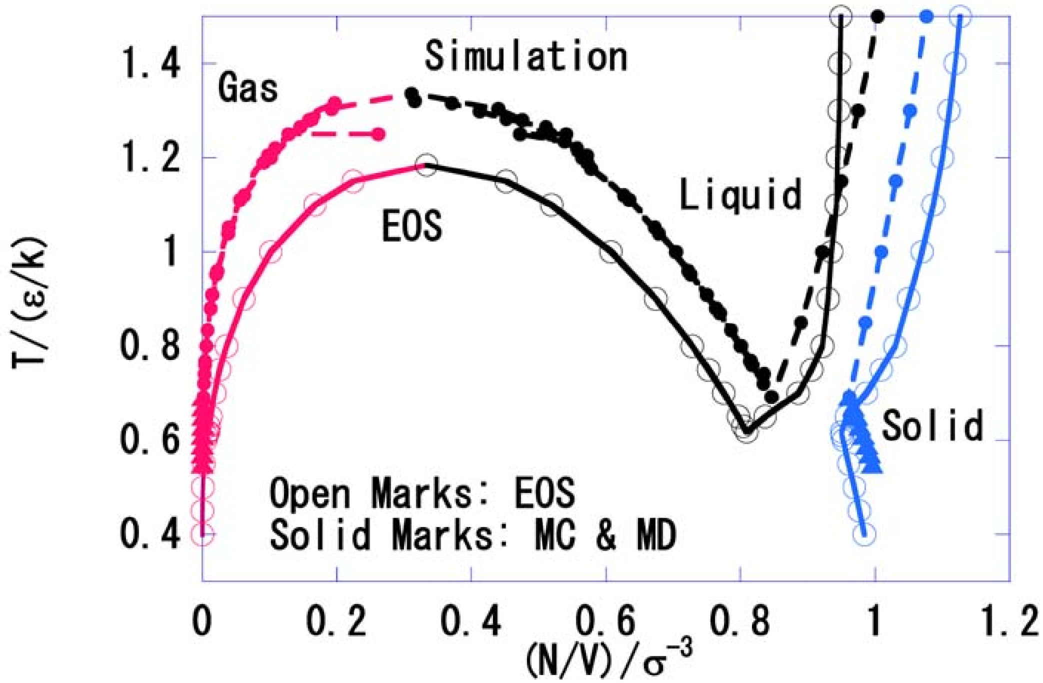

Typical & simple (ϕ, T) phase diagram

Lennard-Jones model system for Argon (more later)

Kataoka & Yamada, J. Comp. Chem. Jpn. 11, 81 (2012)

Equilibrium phases

Macroscopic properties

- A gas is an an air-like fluid substance which expands freely to fill any space available, irrespective of its quantity.
- A liquid is a substance that flows freely but is of constant volume, having a consistency like that of water or oil. It takes the shape of its container
- A solid is a material with non-vanishing shear modulus.
- A crystal is a system with long-range positional order.
  It has a periodic structure and its 'particles' are located close to the nodes of a lattice.

Phases and transitions

Names

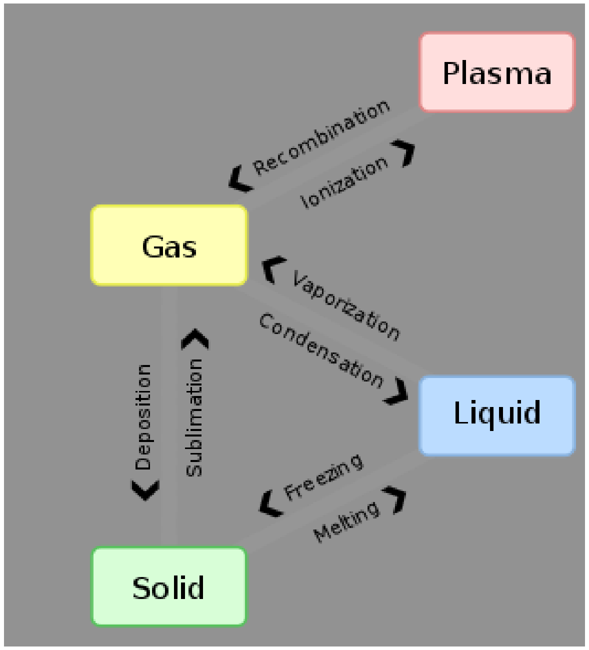

The states of matter have uniform physical properties in each phase. During a phase transition certain properties change, often discontinuously, as a result of the change of an external condition, such as temperature, pressure, or others.

Positional order

Local density properties

The (fluctuating) local particle number density

$$\rho(\boldsymbol{r}_0) = \sum_{i=1}^{N} \ \delta(\boldsymbol{r}_0 - \boldsymbol{r}_i)$$

with normalisation $\int d^d\boldsymbol{r}_0 \, \rho(\boldsymbol{r}_0) = N$. In a homogeneous system, the *coarse-grained* (averaged over a volume v) local density is constant $[[\rho(\boldsymbol{r}_0)]] = N/V$

Fluctuations

The density-density correlation function $C(\boldsymbol{r}+\boldsymbol{r}_0, \boldsymbol{r}_0) = \langle \rho(\boldsymbol{r}+\boldsymbol{r}_0)\rho(\boldsymbol{r}_0)\rangle$

The average $\langle \ldots \rangle$ is over configurations in a steady state

For homogeneous (independence of $\boldsymbol{r}_0$) and isotropic ($\boldsymbol{r} \mapsto |\boldsymbol{r}| = r$) cases, is simply $C(\boldsymbol{r}+\boldsymbol{r}_0, \boldsymbol{r}_0) = C(r)$

The double sum in $C(\boldsymbol{r}+\boldsymbol{r}_0, \boldsymbol{r}_0) = \langle \sum_{ij} \delta(\boldsymbol{r}+\boldsymbol{r}_0 - \boldsymbol{r}_i)\delta(\boldsymbol{r}_0 - \boldsymbol{r}_j)\rangle$ has contributions from $i = j$ and $i \neq j$: $C_{\text{self}} + C_{\text{diff}}$

Positional order

Local density properties

The density-density correlation function

$$C(\boldsymbol{r}+\boldsymbol{r}_0,\boldsymbol{r}_0) = \langle \rho(\boldsymbol{r}+\boldsymbol{r}_0)\rho(\boldsymbol{r}_0)\rangle = \sum_{ij}\langle \delta(\boldsymbol{r}+\boldsymbol{r}_0-\boldsymbol{r}_i)\delta(\boldsymbol{r}_0-\boldsymbol{r}_i)\rangle$$

is linked to the structure factor

$$S(\boldsymbol{q}) \equiv N^{-1}\langle\tilde{\rho}(\boldsymbol{q})\tilde{\rho}(-\boldsymbol{q})\rangle = \frac{1}{N}\langle\sum_{i=1}^{N}\sum_{j=1}^{N} e^{-\mathrm{i}\boldsymbol{q}\cdot(\boldsymbol{r}_i-\boldsymbol{r}_j)}\rangle$$

with $\tilde{\rho}(\boldsymbol{q})$ the Fourier transform of $\rho(\boldsymbol{r})$ by

$$N\,S(\boldsymbol{q}) \;=\; \int d^d\boldsymbol{r}_1 \int d^d\boldsymbol{r}_2\, C(\boldsymbol{r}_1,\boldsymbol{r}_2)\, e^{-\mathrm{i}\boldsymbol{q}\cdot(\boldsymbol{r}_1-\boldsymbol{r}_2)}$$

Exercise : prove it

Positional order

Local density properties

In isotropic cases, i.e. liquid phases, the pair correlation function

$$\frac{N}{V}\, g(r) = \text{average number of particles at distance } r$$

$$\text{from a tagged particle at } \boldsymbol{r}_0$$

is linked to the structure factor

$$S(\boldsymbol{q}) = \frac{1}{N}\langle \sum_{i=1}^{N} \sum_{j=1}^{N} e^{-\mathrm{i}\boldsymbol{q}\cdot(\boldsymbol{r}_i - \boldsymbol{r}_j)} \rangle$$

by

$$S(\boldsymbol{q}) = 1 + \frac{N}{V} \int d^d\boldsymbol{r}\; g(r) e^{-\mathrm{i}\boldsymbol{q}\cdot\boldsymbol{r}}$$

Peaks in $g(r)$ are related to peaks in $S(q)$. The first peak in $S(q)$ is at $q_0 = 2\pi/\Delta r$ where Δr is the distance between peaks in $g(r)$ (that is close to the inter particle distance as well).

Positional order

Gas vs. Liquid : pair correlations

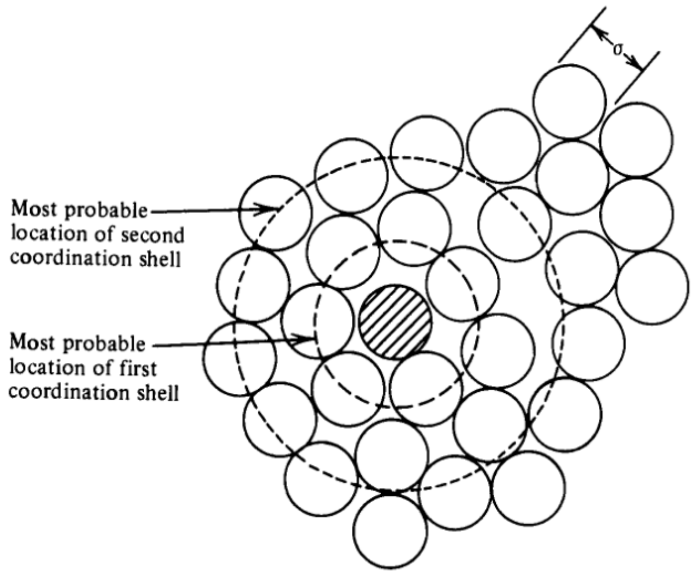

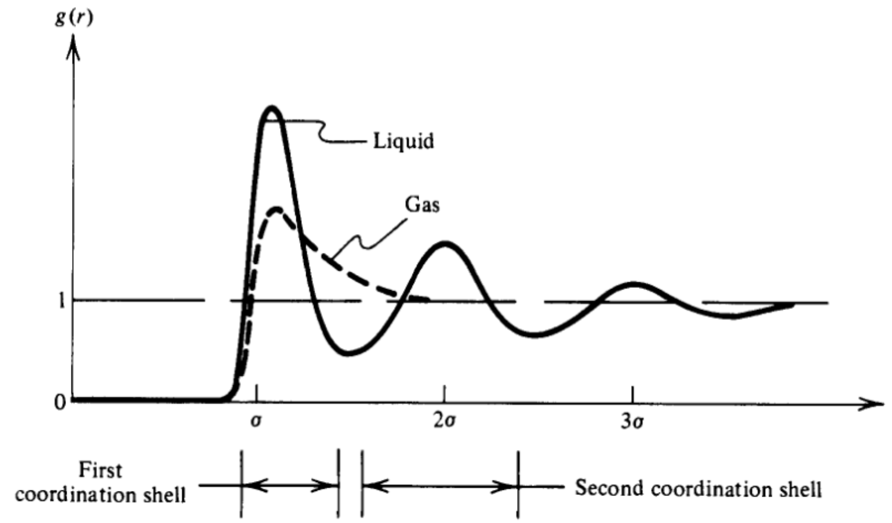

“Introduction to Modern Statistical Mechanics”, **Chandler** (OUP)

Positional order

Crystals, Liquids, Amorphous : structure factors

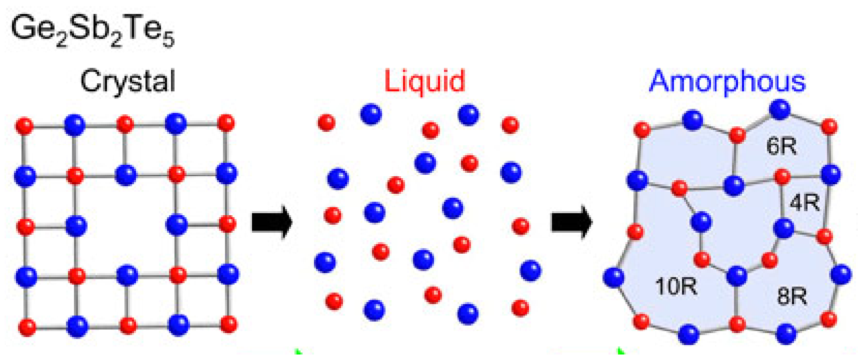

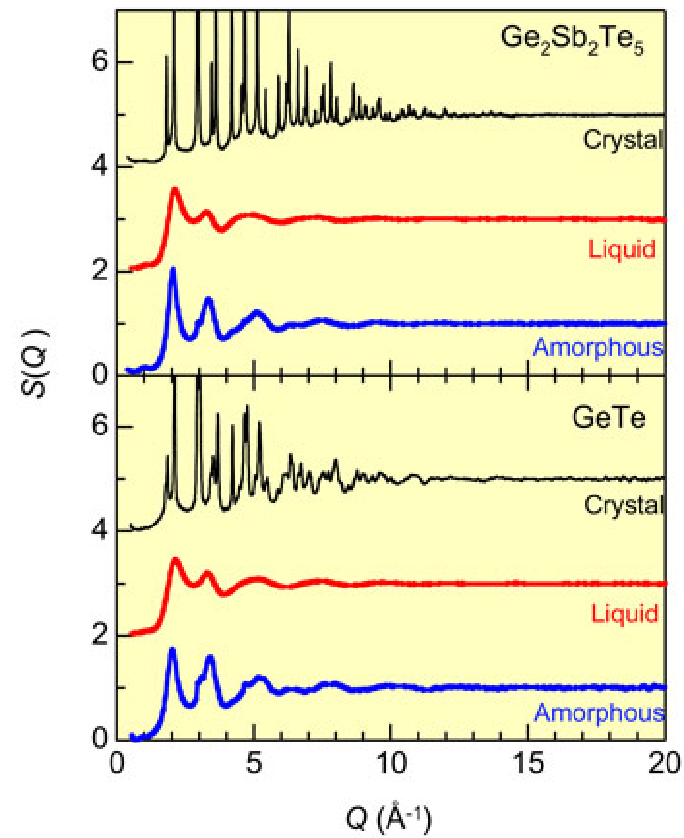

"RMC Analyses Solve High-Speed Phase-Change Mechanism"

Matsunaga, Kojima, Yamada, Kohara, Takata (2006)

Freezing

From liquid to solid: $3d$ nucleation & growth

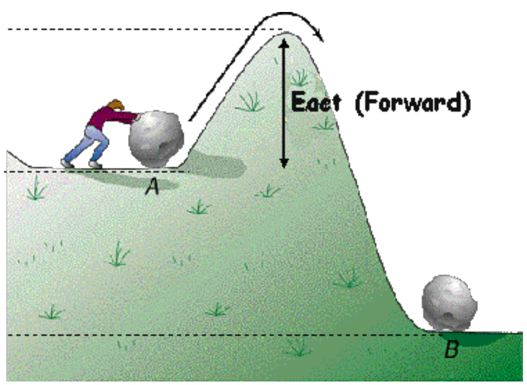

Nucleation barrier ΔF

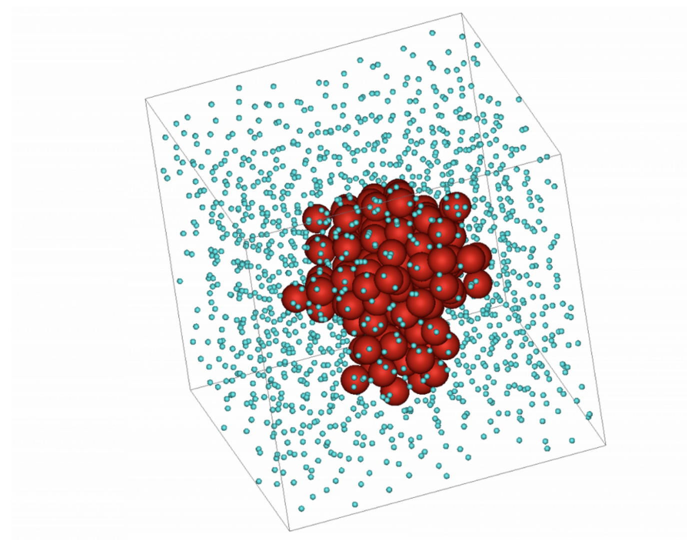

Example of crystalline nucleus

Left image borrowed from **González, Crystals 6, 46 (2016)**

right one from **L. Filion (Utrecht Univ)**

Melting

From solid to liquid: $3d$ nucleation & growth

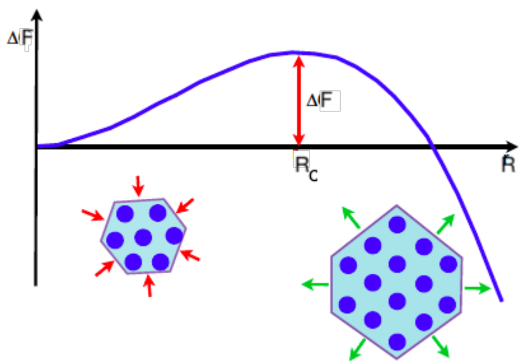

Nucleation barrier ΔF

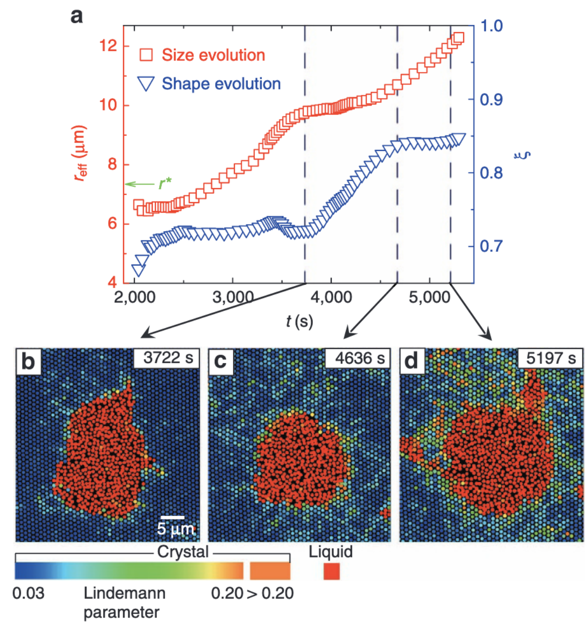

Example of liquid nucleus

Left image from **Gasser, J. Phys.: Cond. Matt. 21, 203101 (2009)**

right one from **Wang, Wang, Peng, Han, Nat. Comm. (2015)**

First order route

Nucleation & growth

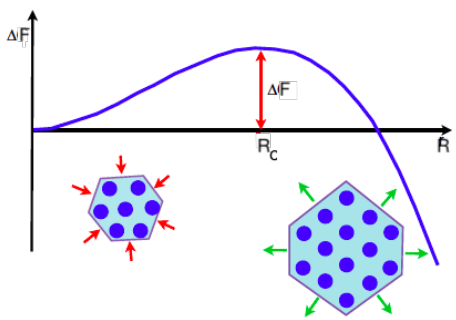

R radius of nucleus

Nucleation barrier $\Delta F(R)$

$$\equiv F_{\rm bubble}(R) - F_{\rm no\ bubble}(R)$$

$$\approx -\delta f\, R^d + s\, R^{d-1}$$

with maximum at

$$0 = \left. \frac{d\Delta F(R)}{dR} \right|_{R=R_c} \approx -\delta f\, R_c^{d-1} + s\, R_c^{d-2} \quad \Rightarrow$$

$$\boxed{R_c \approx \frac{s}{\delta f}} \qquad \text{and} \qquad \boxed{\Delta F(R_c) \approx \frac{s^d}{(\delta f)^{d-1}} \qquad \text{in} \;\; d \geq 2}$$

Crossing point $\Delta F(R^*) = 0$ with the same parameter dependence

$$0 = \Delta F(R^*) \approx -\delta f\, R^{*\,d} + s\, R^{*\,d-1} \quad \Rightarrow \quad \boxed{R^* \approx \frac{s}{\delta f}}$$

Freezing/Melting

but, this is not the route in $2d$

$T = 0$ Position & orientation order lost

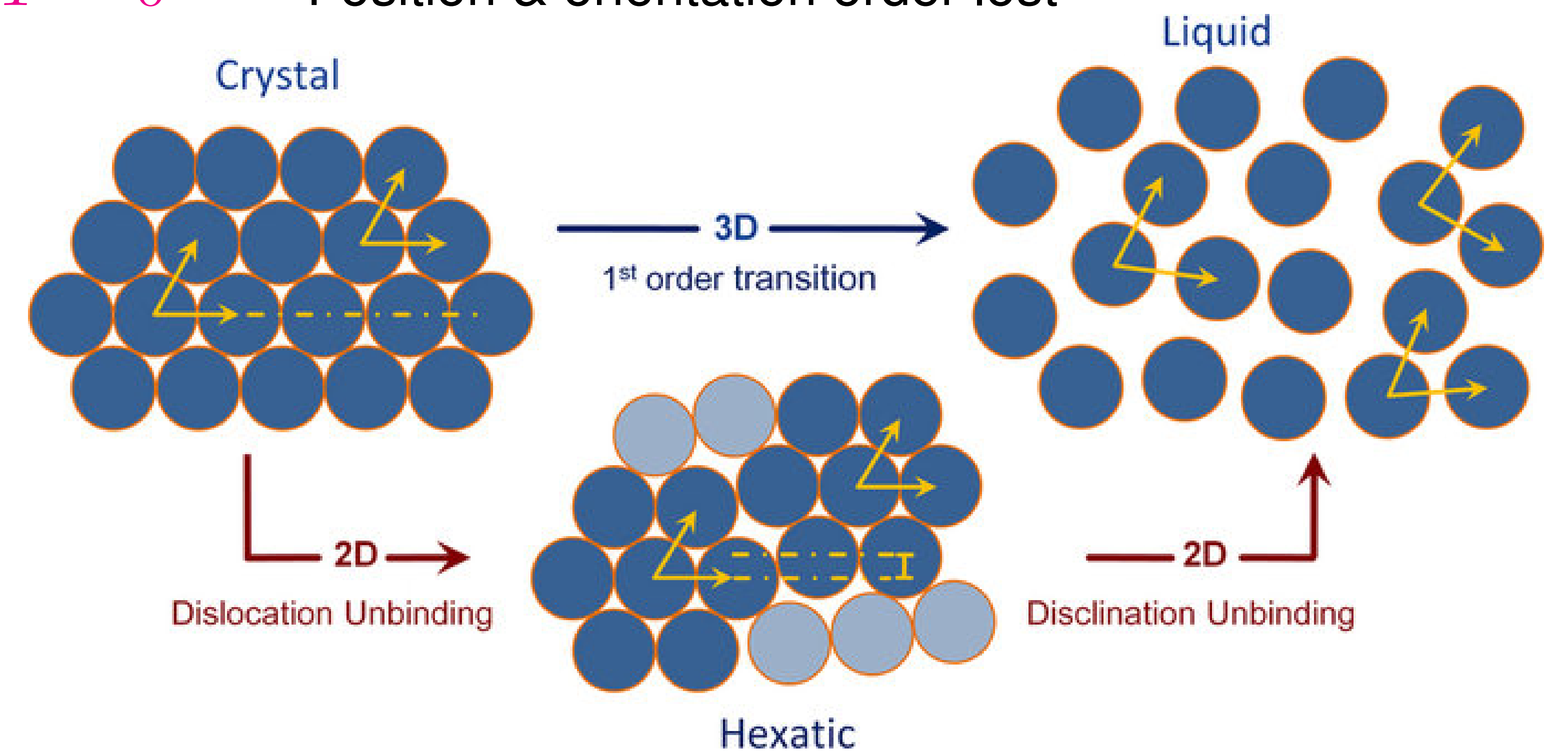

Orientation order preserved also lost

Image from **Pal, Kamal & Raghunathan, Sc. Rep. 6, 32313 (2016)**

Crystals vs. Solids

$3d$ *vs.* $2d$

- A solid is a material with non-vanishing shear modulus.
- A crystal is a system with long-range positional order.

  It has a periodic structure and its ‘particles’ are located close to the nodes of a lattice.

  The position fluctuations are bounded $\Delta^2 = \langle (\boldsymbol{r}_i - \boldsymbol{r}_i^{\rm latt}) \rangle < \infty$
- $2d$ solids exist but have a weaker ordering than $3d$ ones.
  - They are oriented crystals with no positional order.
  - Critical phase with algebraic relaxation of position correlations.
  - Phase transition *à la* Kosterlitz-Thouless (Nobel Prize).

Hard disks in $2d$

Zero temperature crystal : triangular lattice w/6 nearest neigh.

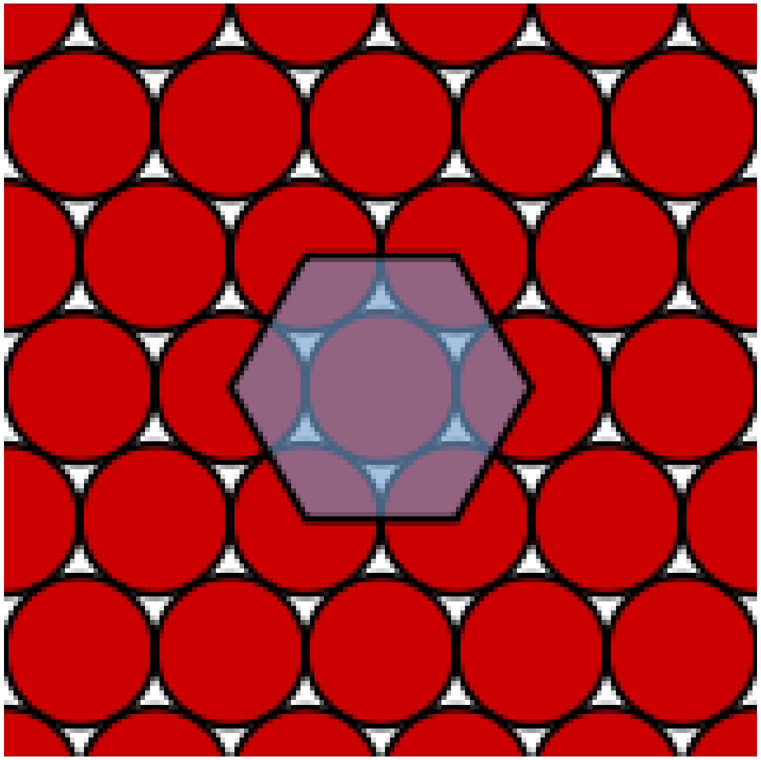

$d = 2$ packing fraction $\phi = S_{\text{occupied}}/S$ at close packing $\phi_{\text{cp}} \approx 0.91$

Harmonic solids

Peierls 30s: no finite T translational long-range order in $2d$

Consider a crystal made of atoms connected to their nearest-neighbours by Hooke springs. At finite T the atomic positions, ϕ_i, fluctuate, $\phi_i = \boldsymbol{R}_i + \boldsymbol{u}_i$, with $\boldsymbol{u}_i$ the local displacement from a regular lattice site at $\boldsymbol{R}_i$

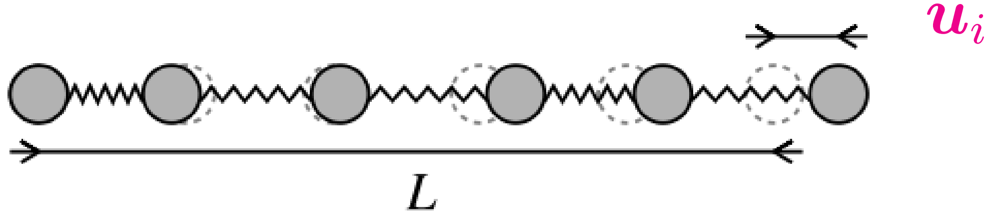

Open dashed: perfect lattice positions $\boldsymbol{R}_i$ Filled gray: actual positions ϕ_i

Does the long-range positional order (crystal) survive at finite T?

not in $d = 2$ since the mean-square displacement grows with distance

$$\Delta^2(\boldsymbol{r}) \equiv \langle (\boldsymbol{u}(\boldsymbol{r}) - \boldsymbol{u}(\boldsymbol{0}))^2 \rangle \simeq k_B T \ \ln r$$

Harmonic solids

Peierls calculation

Consider a crystal made of atoms connected to their nearest - neighbours by Hooke springs.

Perfect lattice positions $\boldsymbol{R}_i$

At finite temperature the actual particle positions are $\phi_{\boldsymbol{R}_i} = \boldsymbol{R}_i + \boldsymbol{u}_{\boldsymbol{R}_i}$.

The potential energy is

$$U = \frac{K}{2} \sum_{\langle ij \rangle} (\boldsymbol{u}_{\boldsymbol{R}_i} - \boldsymbol{u}_{\boldsymbol{R}_j})^2 \approx \frac{K}{2} \int d^d r \; [\nabla \boldsymbol{u}(\boldsymbol{r})]^2$$

Look at the displacement field, $\boldsymbol{u}(\boldsymbol{r}, t)$, in Fourier transform

$$\boldsymbol{u}(\boldsymbol{r}) = \int \frac{d^d \boldsymbol{q}}{(2\pi)^2} \; \tilde{u}(\boldsymbol{q}) \; e^{\mathrm{i}\boldsymbol{q}\cdot\boldsymbol{r}}$$

Harmonic solids

Peierls calculation

A quadratic Hamiltonian that can be diagonalised going to Fourier space

In the continuum limit

$$U = \frac{K}{2} \int d^d\boldsymbol{r} \, [\nabla \boldsymbol{u}(\boldsymbol{r})]^2 = \frac{K}{2} \int \frac{d^d\boldsymbol{q}}{(2\pi)^d} \, q^2 \, |\tilde{\boldsymbol{u}}(\boldsymbol{q})|^2$$

is the one of a set of independent harmonic oscillators (phonons).

Assuming canonical equilibrium at inverse temperature β, for each $\boldsymbol{q}$

$$\langle |\tilde{u}(\boldsymbol{q})|^2 \rangle \propto \frac{k_B T}{K q^2}$$

The density of states of the phonons (how many of them there are with q between q and $q + dq$) is $g(q) \propto q^{d-1}$

Harmonic solids

Peierls calculation

Let's go back to real space and compute the mean-square displacement

$$\Delta^2(\boldsymbol{r}) = \langle [\boldsymbol{u}(\boldsymbol{r}) - \boldsymbol{u}(\boldsymbol{0})]^2 \rangle$$

Using the equipartition result $\langle |\tilde{u}(\boldsymbol{q})|^2 \rangle \propto k_B T/(K q^2)$,

$$\Delta^2(\boldsymbol{r}) \;=\; \frac{k_B T}{K} \int d^d\boldsymbol{q}\, \frac{1 - \cos \boldsymbol{q} \cdot \boldsymbol{r}}{q^2} \;\approx\; \frac{k_B T}{K} \int_{1/r}^{1/a} dq\; q^{d-1}\, \frac{1}{q^2}$$

and

$$\Delta^2(\boldsymbol{r}) \equiv \langle (\boldsymbol{u}(\boldsymbol{r}) - \boldsymbol{u}(\boldsymbol{0}))^2 \rangle \simeq \frac{k_B T}{K} \begin{cases} r & d = 1 \\ \boxed{\ln r} & d = 2 \\ \text{cst} & d \geq 3 \end{cases}$$

Quasi long-range order in $d = 2$

Mermin-Wagner theorem

Consequences

Some continuous symmetry cannot be spontaneously broken in $2d$.

(The Hamiltonian $\frac{K}{2}\int d^d r\ [\nabla \boldsymbol{u}(\boldsymbol{r})]^2$ is invariant under global rotations of $\boldsymbol{u}$)

Corollary: a crystal with long-range order cannot exist at $T > 0$ in $d = 2$.

Reason: in low d fluctuations are more effective and inhibit order.

Quasi long-range positional order with algebraically decaying correlations is possible, $C(r) \simeq r^{-\eta}$.

Note the similarity with the $2d$ XY model of magnetism, $\boldsymbol{s}_i = (\cos\theta_i, \sin\theta_i)$

$$-\frac{H}{J} = \sum_{\langle ij \rangle} \boldsymbol{s}_i \cdot \boldsymbol{s}_j = \sum_{\langle ij \rangle} \cos\theta_{ij} \simeq \sum_{\langle ij \rangle} (1 - \frac{\theta_{ij}^2}{2}) \approx -\frac{1}{2}\int d^2 r\ [\boldsymbol{\nabla}\theta(\boldsymbol{r})]^2$$

Colloidal suspensions

Structure factor: from fuzzy peaks to a disk as T increases

$$S(\boldsymbol{q}) \equiv N^{-1}\langle \tilde{\rho}(\boldsymbol{q})\tilde{\rho}(-\boldsymbol{q})\rangle = \frac{1}{N}\sum_{i=1}^{N}\sum_{j=1}^{N}\langle e^{-\mathrm{i}\boldsymbol{q}\cdot(\boldsymbol{r}_i-\boldsymbol{r}_j)}\rangle$$

High T Low T

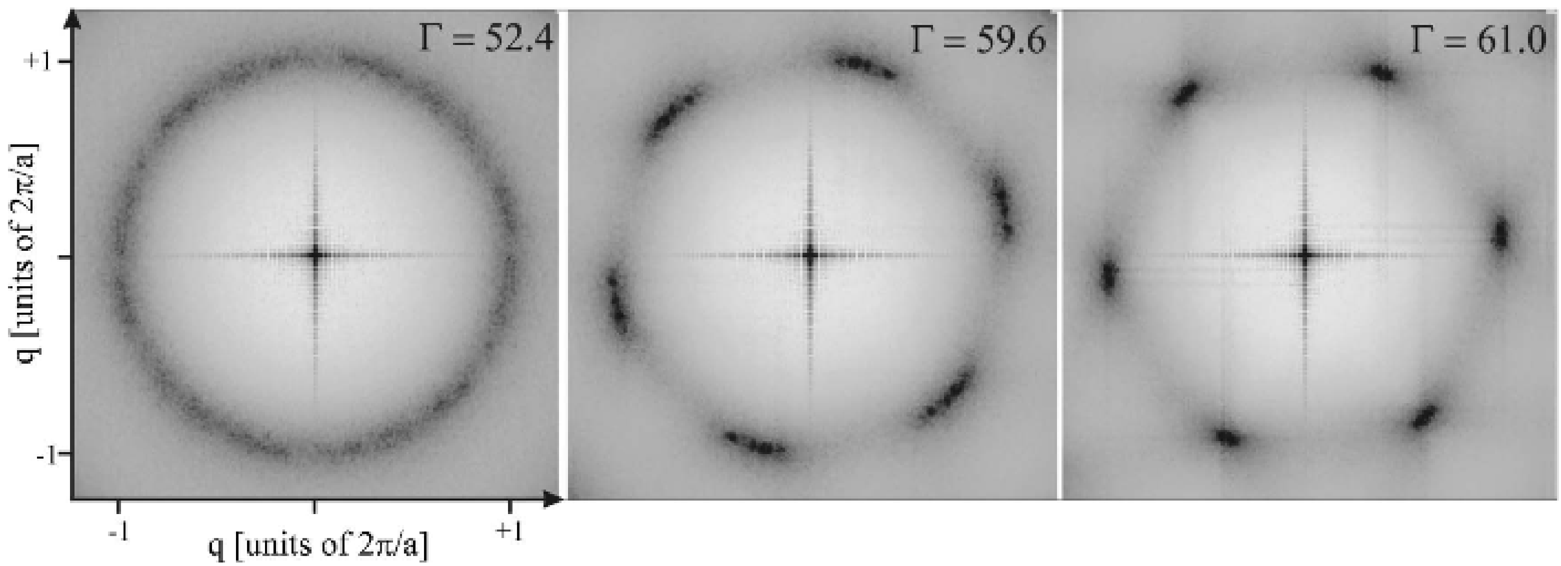

Liquid (later) Solid

Figure from **Keim, Maret and von Grünberg, PRE 75, 031402 (2007)**

Harmonic solids

Peierls 30s: but finite T orientational long-range order possible

Consider a crystal made of atoms connected to their nearest-neighbours by Hooke springs. At finite T the atomic positions, ϕ_i, fluctuate, $\phi_i = \boldsymbol{R}_i + \boldsymbol{u}_i$, with $\boldsymbol{u}_i$ the local displacement from a regular lattice site at $\boldsymbol{R}_i$

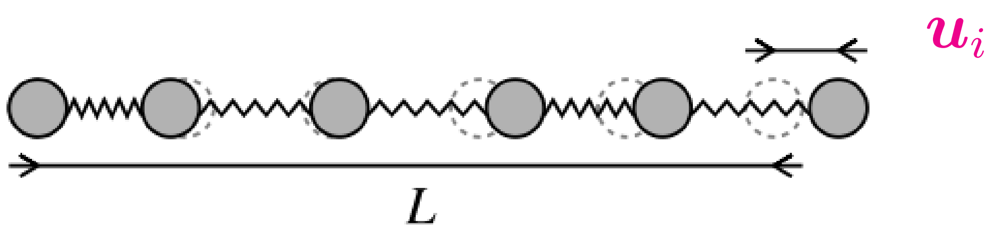

Dashed: perfect lattice positions $\boldsymbol{R}_i$ Gray: actual positions ϕ_i

Does the long-range orientational order (solid) survive at finite T?

yes, even in $d = 2$ since the correlation

$$C_{\text{orient}}(\boldsymbol{r}) \equiv \langle \boldsymbol{u}(\boldsymbol{r}) \cdot \boldsymbol{u}(\boldsymbol{0}) \rangle \to \text{cst}$$

Harmonic solids

No long-range translational but long-range orientational order

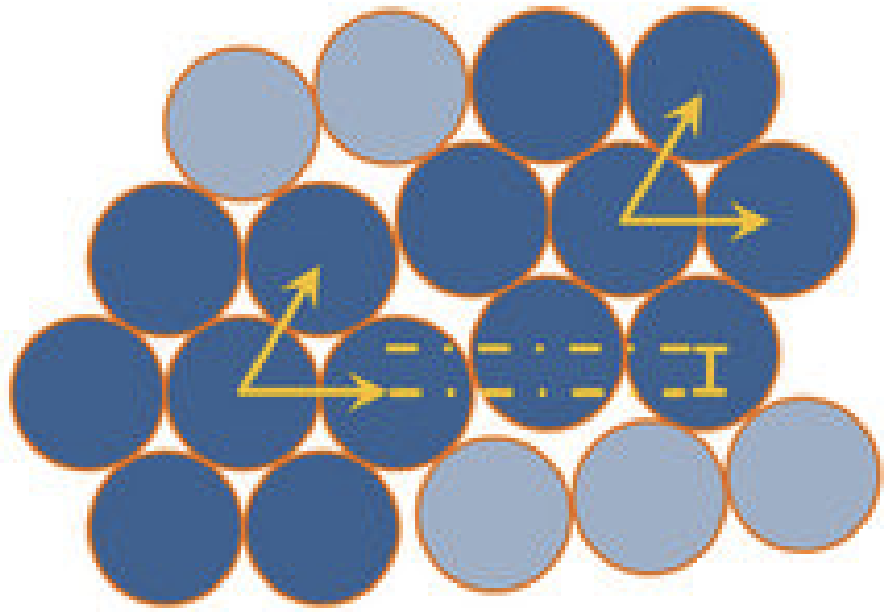

Angles preserved while no periodic order of the disks' centres.

How can one quantify orientational order in general ?

Neighbourhood

Voronoi tessellation to identify nearest-neighbours

A Voronoi diagram is induced by a set of points, called sites, that in our case are the centres of the disks.

The plane is subdivided into faces that correspond to the regions where one site is closest.

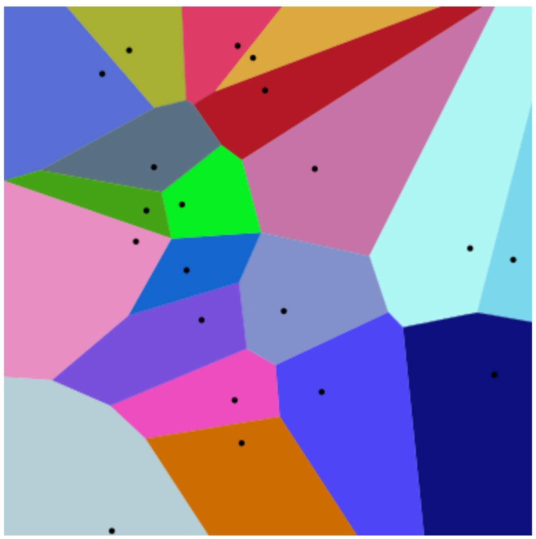

Focus on the central light-green face

All points within this region are closer to the dot within it than to any other dot on the plane

The region has five neighbouring cells from which it is separated by an edge

The grey zone has six neighbouring cells

Orientational order

Hexatic order parameter

The local (six) order parameter $\psi_{6_j} = \frac{1}{N_{\rm nn}^j} \sum_{k=1}^{N_{\rm nn}^j} e^{6{\rm i}\theta_{jk}}$ (vector)

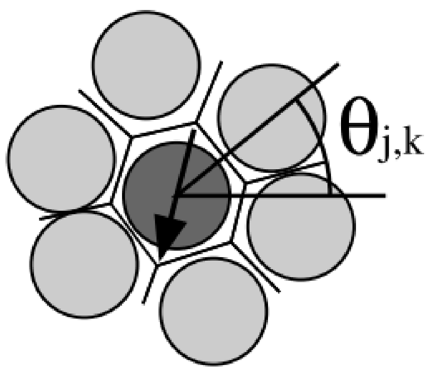

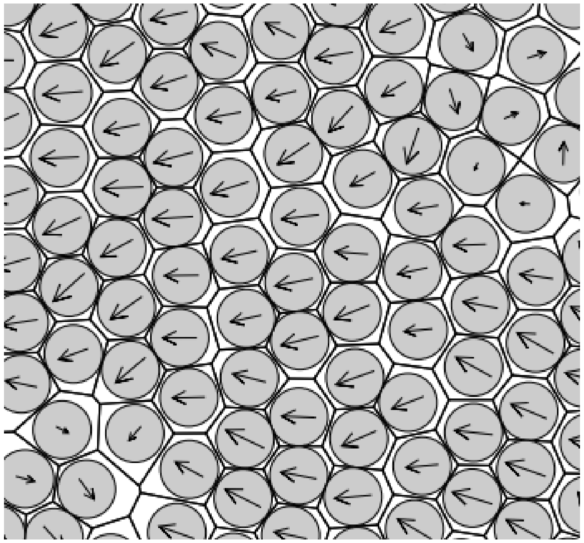

(For beads placed on the vertices of a triangular lattice, each bead j has six nearest-neighbours, $k = 1, \ldots, N_{\rm nn}^j = 6$, the angles verify $\Delta\theta_{jk} = \frac{2\pi}{6}$ and $\psi_{6_j} = 1$)

associates arrows (directions) to disks

and measures **orientational order**

Correlations & defects

Hexatic **Positional** ● **7 neighb** ● **5 neighb**

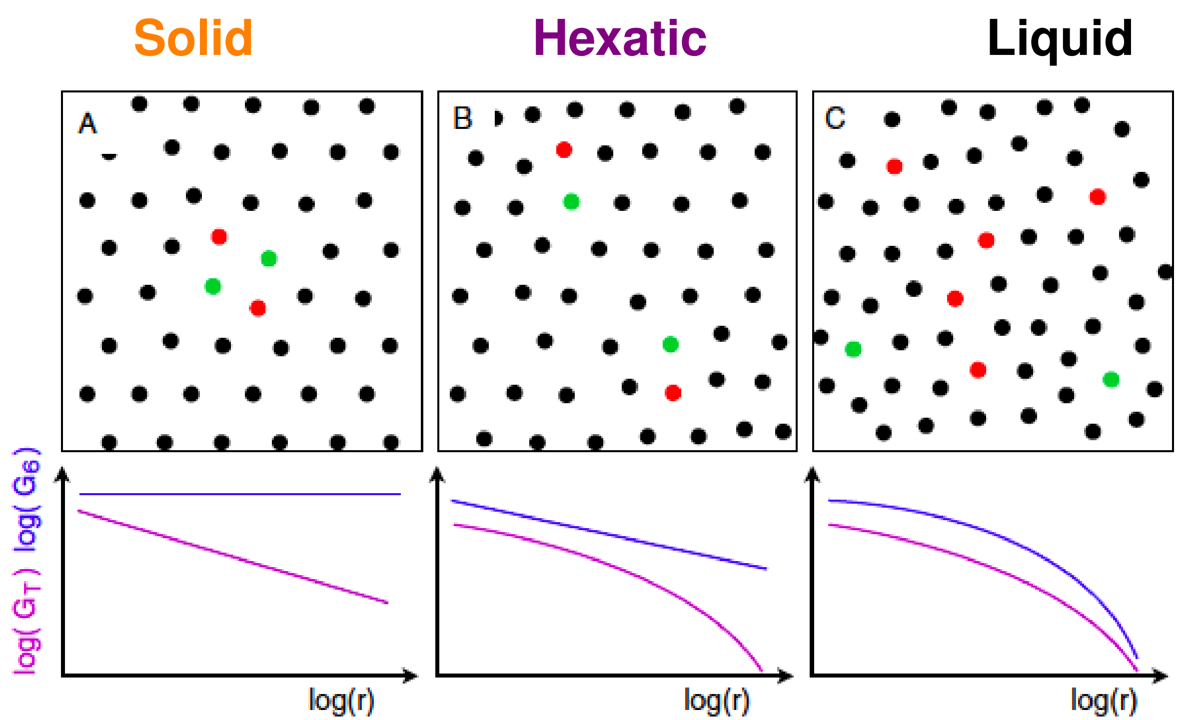

$$\text{long } r: \quad G(r) = \begin{cases} \text{ct} & r^{-\eta} \\ r^{-\eta_6} & e^{-r/\xi} \\ e^{-r/\xi_6} & e^{-r/\xi} \end{cases}$$

Solid	long range order
Hexatic	quasi long range order
Liquid	disorder

Sketches from **Gasser 10**

$2d$ colloidal suspensions

Hexatic correlation functions

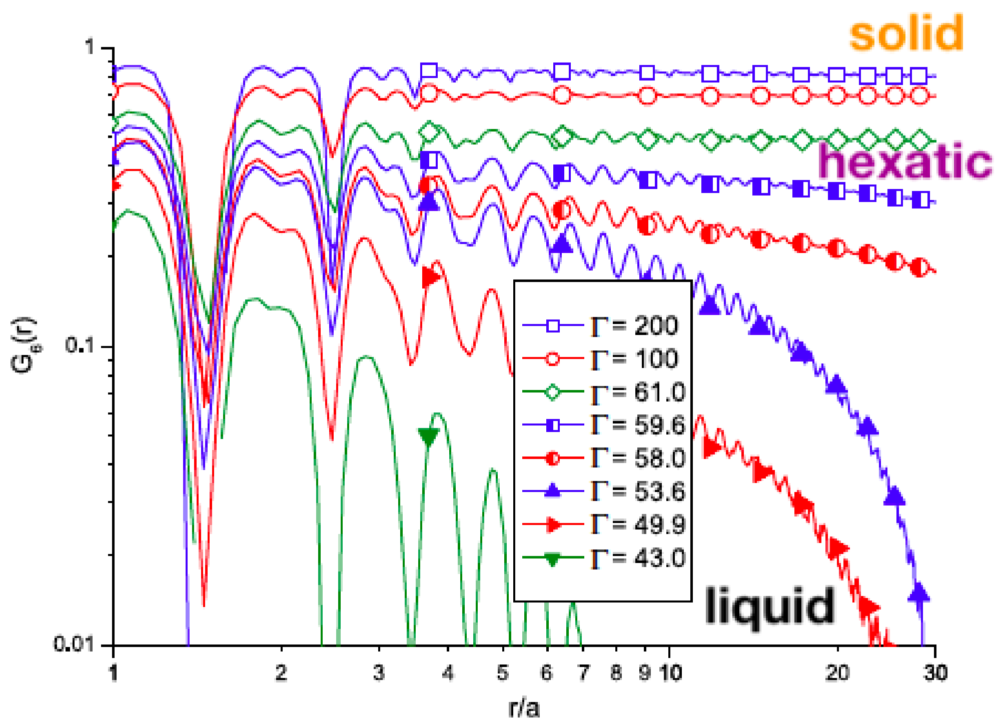

Figure from **Keim, Maret & von Grünberg, PRE 75, 031402 (2007)**

What drives the phase transitions ?

Why did we highlight the particles with **5** & **7** neighbours ?

Defects

Unbinding of dislocations : from the solid to the hexatic

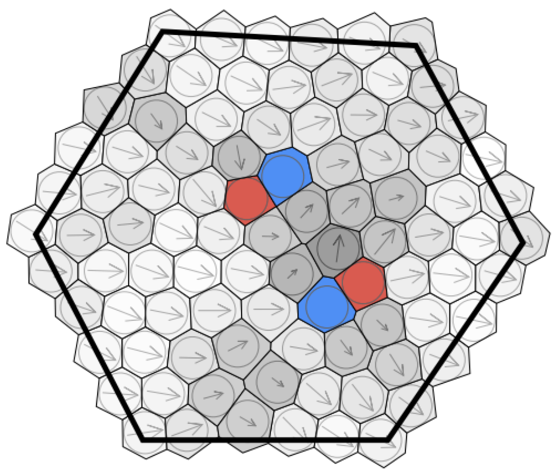

A bound pair of dislocations

In the crystal the centres of the disks form a triangular lattice

The **blue** disks have seven neighbours and the **red** ones have five.

On the left image : the external path closes and forms a perfect hexagon.

The effects of the defects are confined. This is the **solid** phase.

Defects

Unbinding of dislocations: from the solid to the hexatic

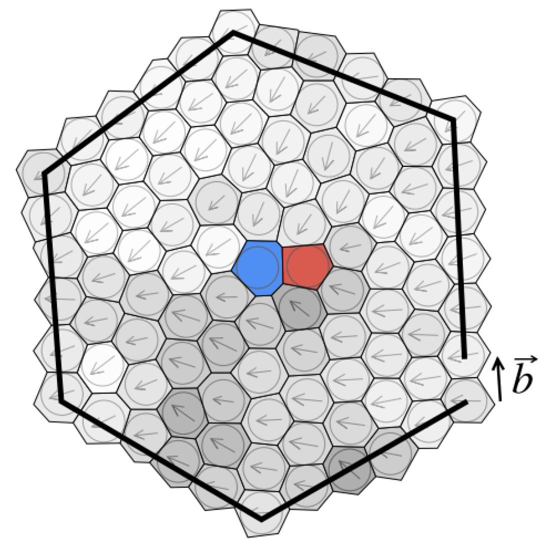

A free dislocation

In the crystal the centres of the disks form a triangular lattice

The **blue** disks have seven neighbours and the **red** ones have five.

On the right image: the external path fails to close, no perfect hexagon.

The effect of the defects spreads & kills translation order: **hexatic** phase.

Defects

Unbinding of dislocations: from the solid to the hexatic

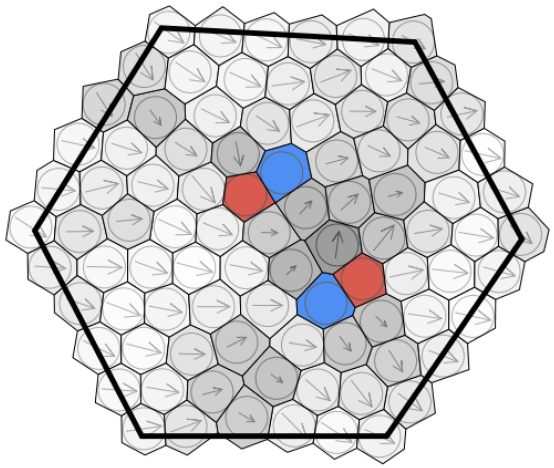

A bound pair of dislocations

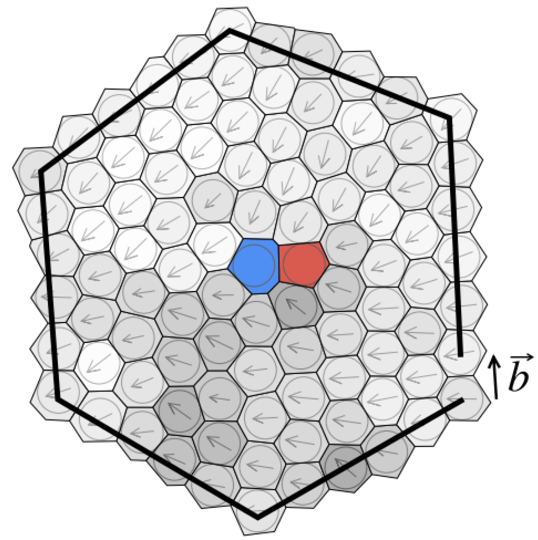

A free dislocation

In the crystal the centres of the disks form a triangular lattice

The **blue** disks have seven neighbours and the **red** ones have five.

Destruction of the **solid** by unbinding of dislocations

Defects

Unbinding of disclinations: from the hexatic to the liquid

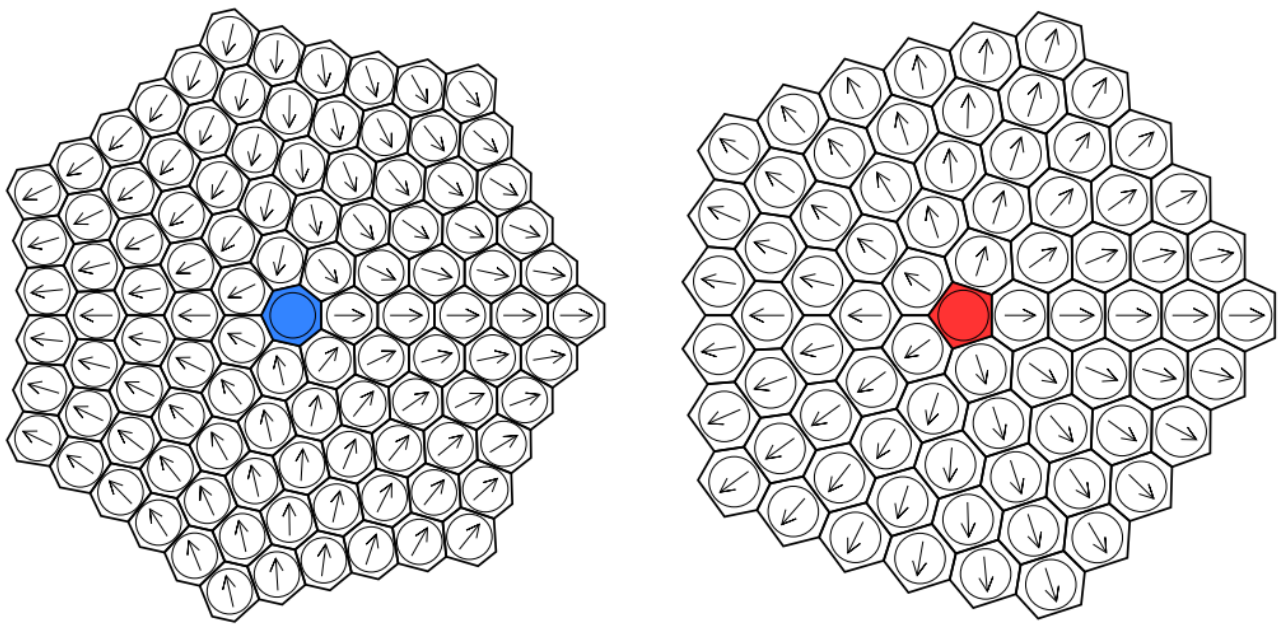

The orientation winds by $\pm 2\pi$ around the **blue** (seven) and **red** (five) defects.

Very similar to the vortices in the $2d$ XY magnetic model.

Halperin, Nelson & Young scenario: the unbinding of disclinations drives a second BKT-like transition to the **liquid**.

Freezing/Melting

Mechanisms in $2d$

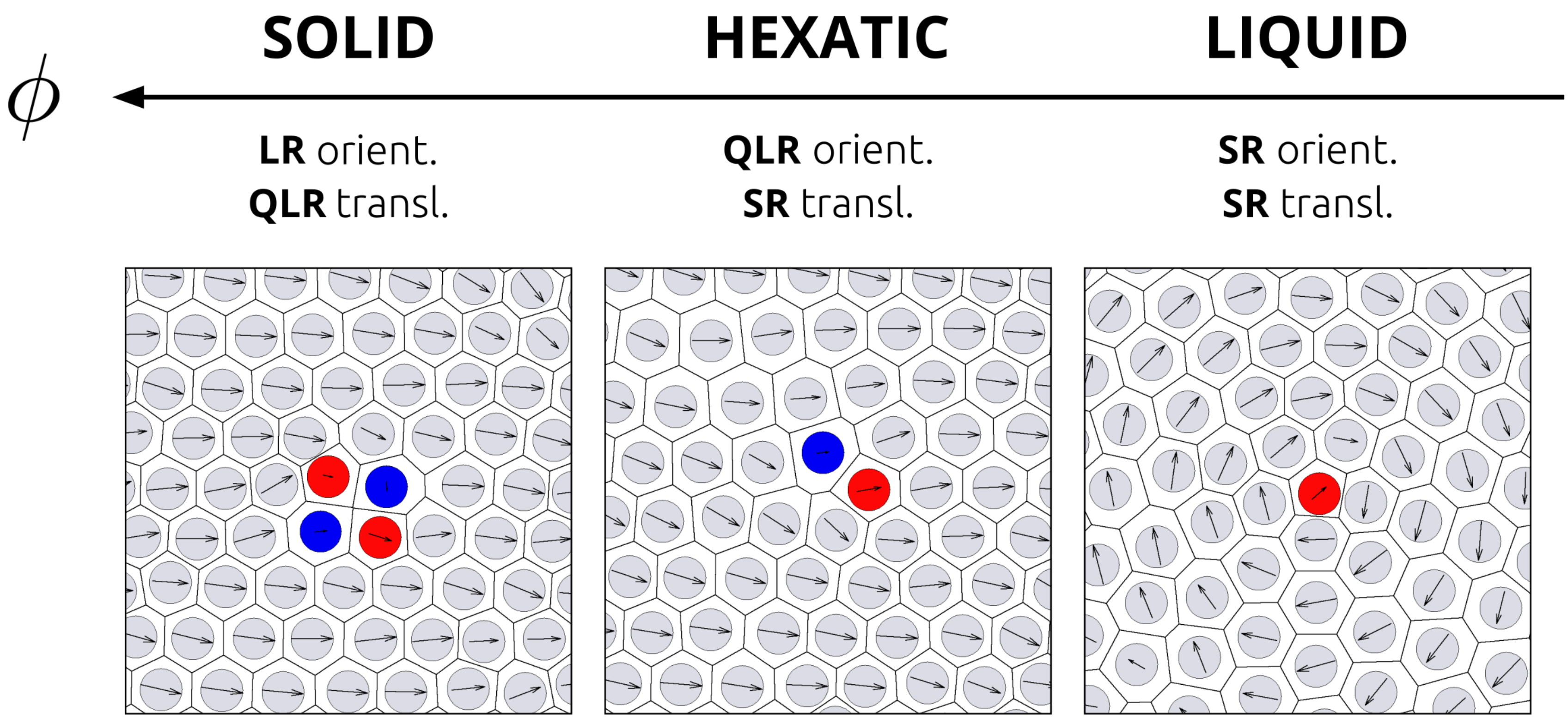

Arrows oriented (LR) less oriented (QLR) order lost

five neighbours seven neighbours

Voronoi tesselation

Phases & transitions

Berezinskii, Kosterlitz, Thouless, Halperin, Nelson & Young 70s

	BKT-HNY
Solid	QLR positional & LR orientational
transition	BKT (unbinding of dislocations)
Hexatic phase	SR positional & QLR orientational
transition	BKT (unbinding of disclinations)
Liquid	SR positional & orientational

Two infinite order, $\xi \propto e^{\delta^{-\nu}}$ with $\delta \to 0$,

Berenzinskii, Kosterlitz & Thouless

transitions

Berezinskii-Kosterlitz-Thouless

The $2d$ XY model

At very high temperature one expects disorder.

At very low temperature the harmonic approximation is exact and there is quasi long-range order.

There must be a transition in between.

Assumption : the transition is continuous and it is determined by the unbinding of vortices (topological defects).

Proved with RG, assuming a continuous phase transition.

The correlation length diverges exponentially $\xi_{\rm eq} \simeq e^{a/|T-T_{\rm BKT}|^{-\nu}}$ at $T_{\rm BKT}$ and it remains infinite in the phase with quasi long-range order.

Berezinskii-Kosterlitz-Thouless

Lack of universality of the transition in XY models

The RG proof yields, actually, an upper limit for the stability of the quasi long-range ordered phase.

A first order phase transition at a lower T can preempt the BKT one.

It does for sufficiently steep potentials:

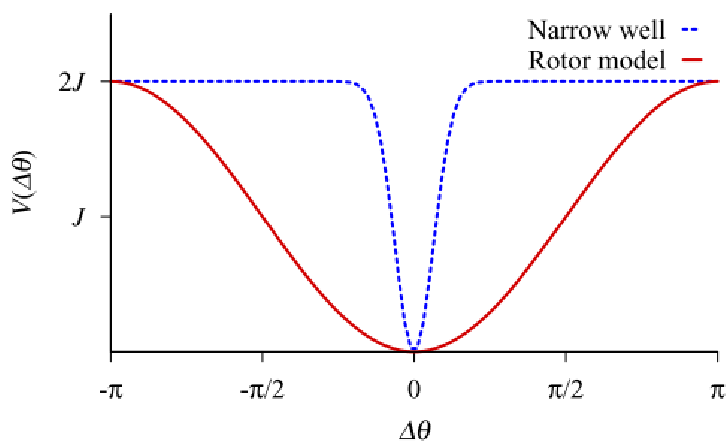

"First order phase transition in an XY model with nn interactions"

Domany, Schick & Swendsen, Phys. Rev. Lett. 52, 1535 (1984)

Hard disks

Pressure loop and finite N dependence: evidence for 1st order

Hexatic **Liquid**

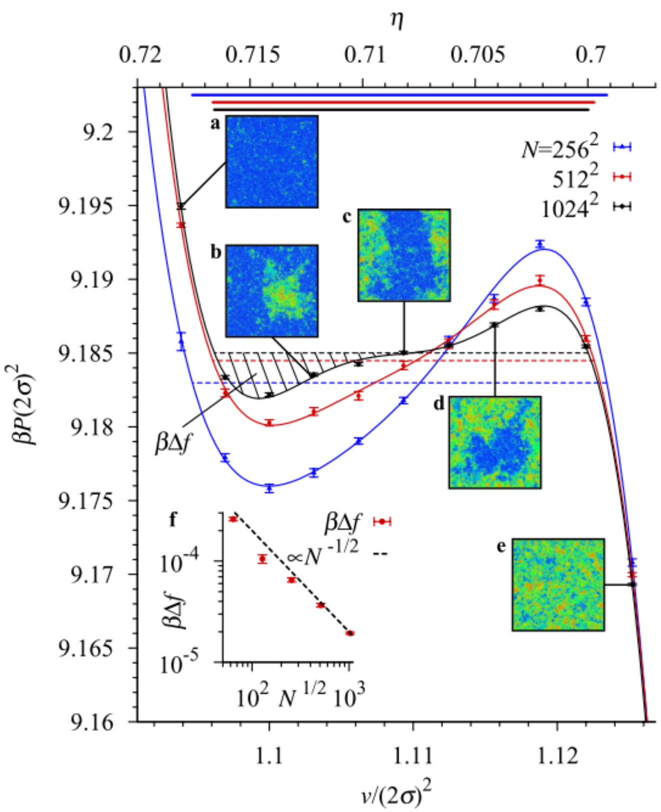

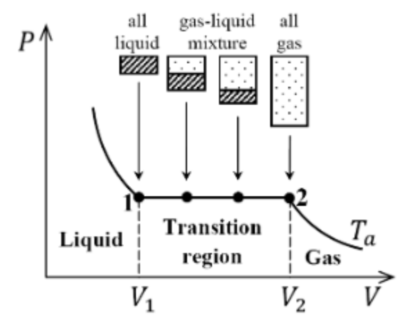

Similar to Van der Waals model for 1st order phase transitions

P cannot increase with V (stability): phase separation *via* Maxwell construction

Hard disks

Coexistence

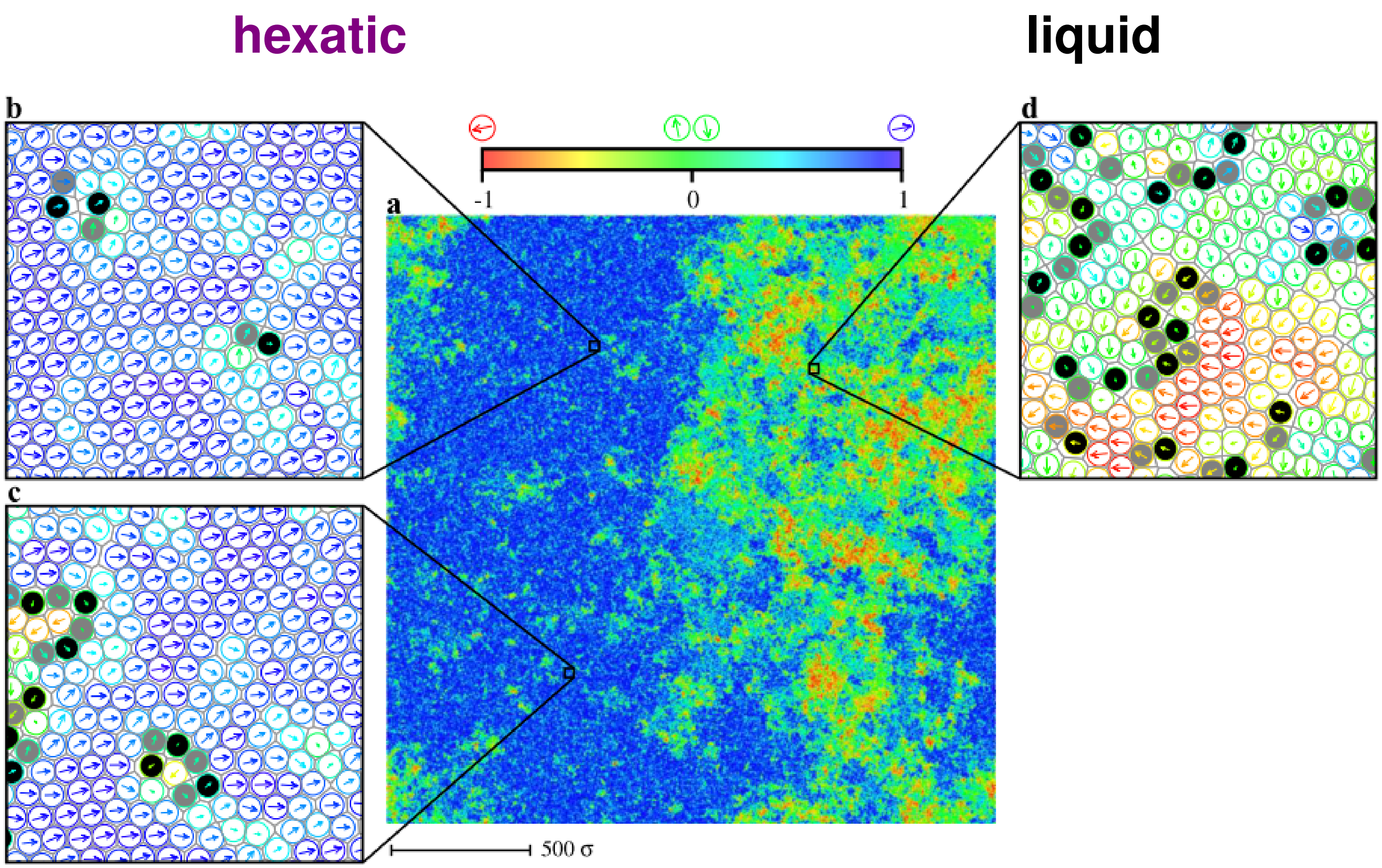

"Two-step melting in two dimensions : first-order liquid-hexatic transition"

Bernard & Krauth, PRL 107, 155704 (2011)

Phases & transitions

BKT-HNY *vs.* a new scenario by Bernard & Krauth 2011

	BKT-HNY	BK
Solid	QLR pos & LR orient	QLR pos & LR orient
transition	BKT (unbinding of dislocations)	BKT
Hexatic phase	SR pos & QLR orient	SR pos & QLR orient
transition	BKT (unbinding of disclinations)	**1st order**
Liquid	SR pos & orient	SR pos & orient

Basically, the phases are the same, but the **hexatic**-**liquid** transition is different, allowing for **coexistence of the two phases** for **hard enough particles**

Event driven MC simulations. Sketches from **Bernard's** thesis.

Rather hard disks

Lennard-Jones $\mapsto$ Mie potential

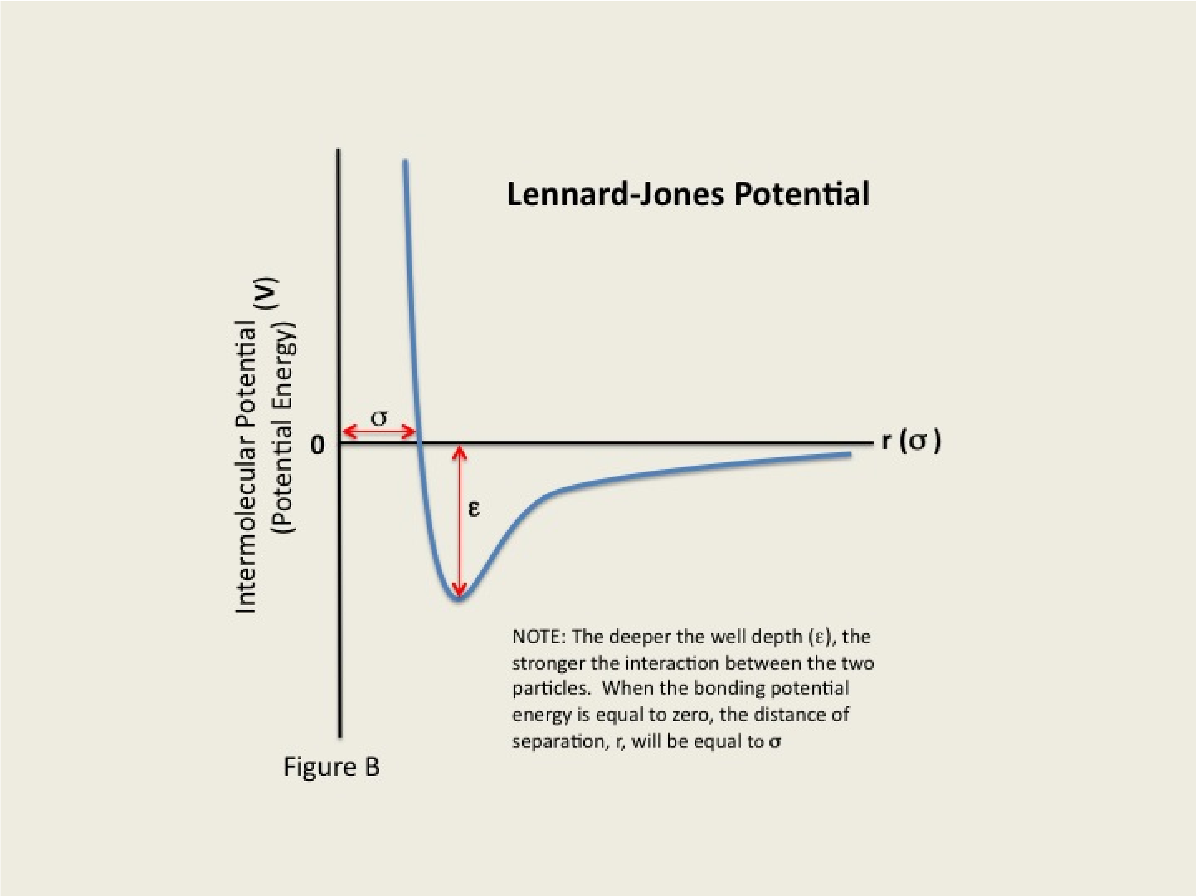

LJ $4\epsilon[(\sigma/r)^{2n} - (\sigma/r)^n]$ with $n = 6$ Mie $n = 32$

Rather hard disks

Molecular dynamics of overdamped Brownian particles

$$m\ddot{\mathbf{r}}_i + \gamma\dot{\mathbf{r}}_i = -\nabla_i \sum_{j(\neq i)} U_{\rm Mie}(r_{ij}) + \boldsymbol{\xi}_i \ ,$$

$\mathbf{r}_i$ position of the centre of the ith particle

$r_{ij} = |\mathbf{r}_i - \mathbf{r}_j|$ inter-part distance

$m \ll \gamma$ over-damped limit

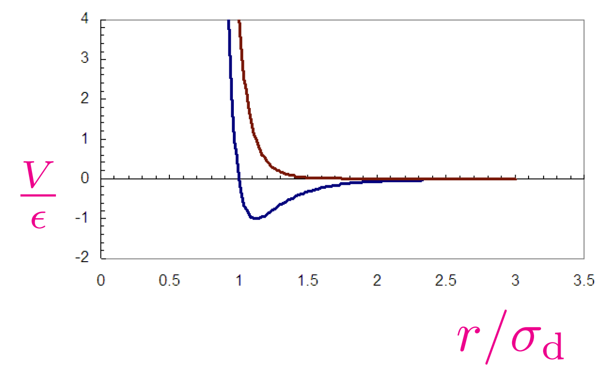

very short-ranged, purely repulsive, Mie potential (truncated Lennard-Jones)

$\boldsymbol{\xi}$ zero-mean Gaussian noise with $\langle \xi_i^a(t)\, \xi_j^b(t') \rangle = 2\gamma k_B T \delta_{ij}^{ab} \delta(t-t')$

packing fraction $\phi = \pi\sigma_d^2 N/(4S)$

parameters $\gamma = 10$ and $k_B T = 0.05$

Digregorio et al. PRL (2018)

Rather hard disks

Phase diagram

ϕ

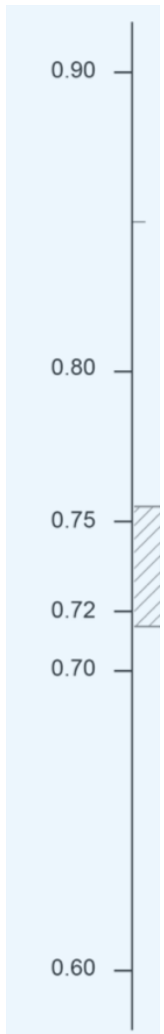

ϕ_{CP}

ϕ_{RCP}

solid

hexatic

co-existence

Really ?

liquid

Rather hard disks

Two local observables

Space-point dependent normalized density

$$\rho(\mathbf{r}_0) = \frac{1}{N} \sum_{k=1}^{N} \delta(\mathbf{r}_0 - \mathbf{r}_k)$$

averaged over a volume ℓ^d around the point $\mathbf{r}_0$ or the position of a particle i

Particle dependent hexatic order parameter – a vector –

$$\psi_{6j} = \frac{1}{N_{\rm nn}^j} \sum_{k=1}^{N_{\rm nn}^i} e^{6{\rm i}\theta_{jk}}$$

projected on a preferred direction – the averaged one or a reference axis – and averaged over a volume ℓ^d around a point $\mathbf{r}$ or the position of a particle i

Rather hard disks

Local density & local hexatic parameter

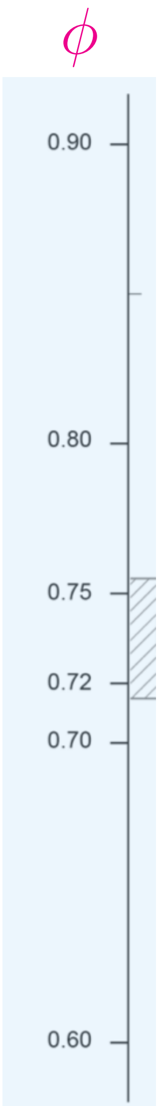

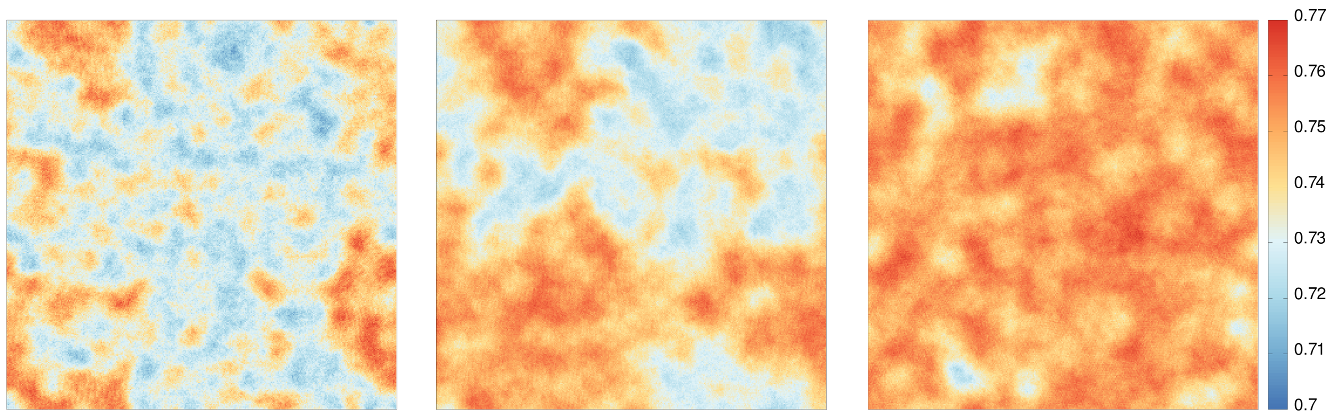

(co-existence) (co-existence) (upper limit of co-existence)

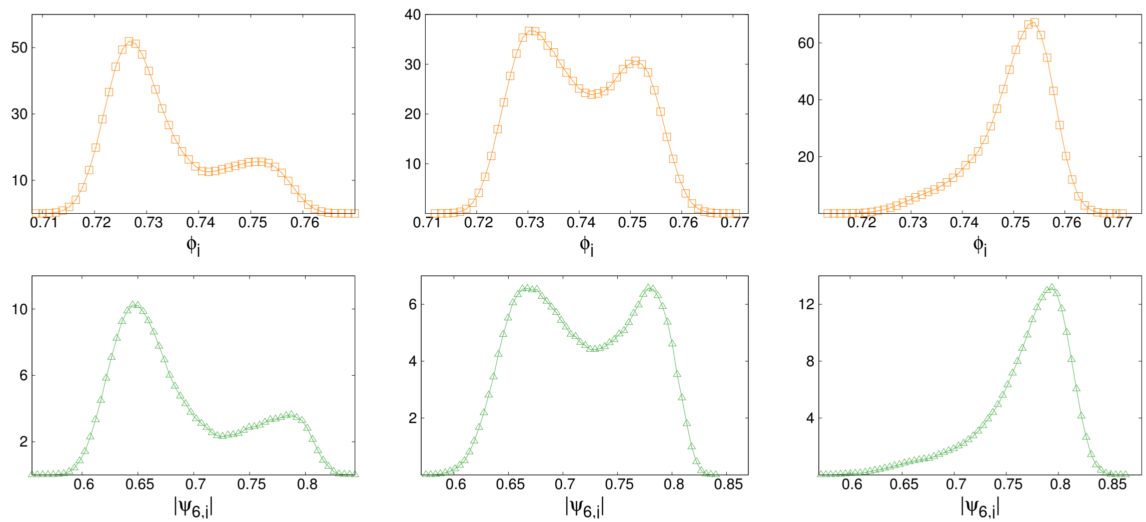

What happens with the defects?

Unbinding of defects

Solid-hexatic transition & the emergence of the liquid

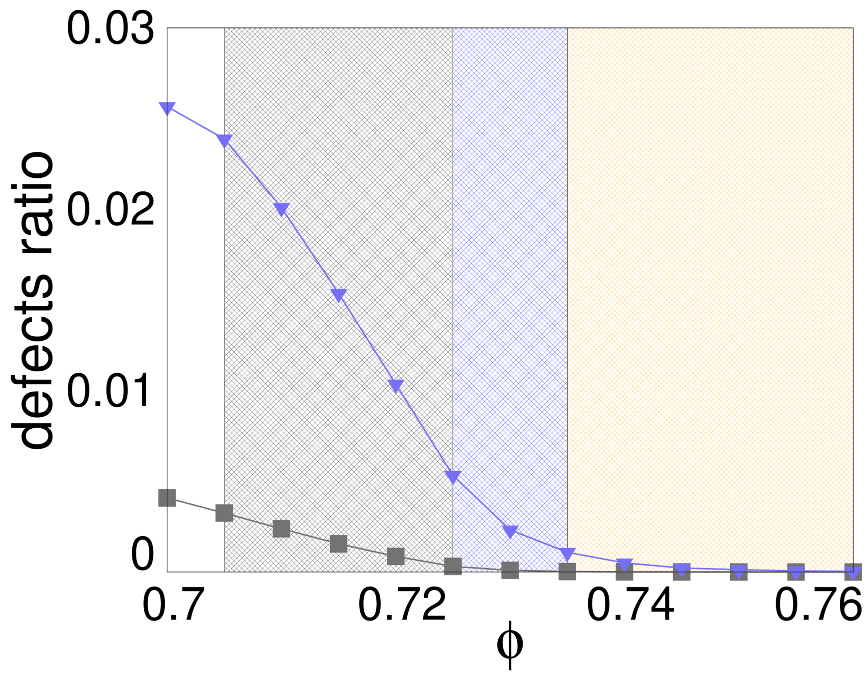

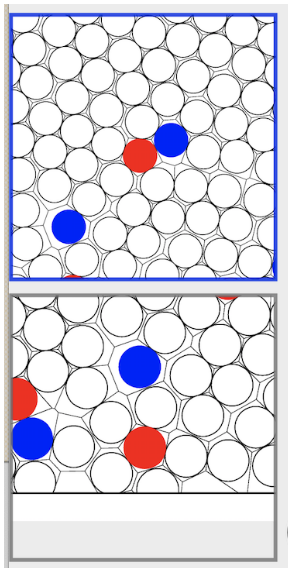

Dislocations ▼

Disclinations ■

Dislocations ▼ unbind at the **solid** - **hexatic** transition as in BKT-HNY

Disclinations ■ unbind when the liquid appears in the co-existence region

Digregorio, Levis, LFC, Gonnella & Pagonabarraga, arXiv:2106.03454

BKT-HNY theory

Solid-hexatic transition & the emergence of the liquid at Pe = 0

Exponential decrease of the number density of defects at the transition coming from the disordered side

$$\rho_d \sim a \ \exp\left[-b\left(\frac{\phi_c}{\phi_c-\phi}\right)^{\nu}\right]$$

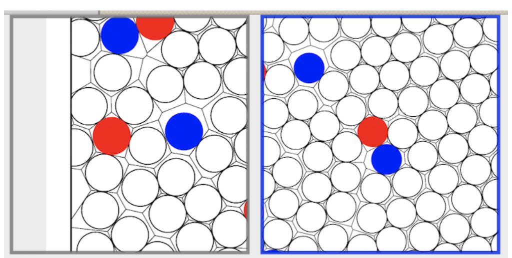

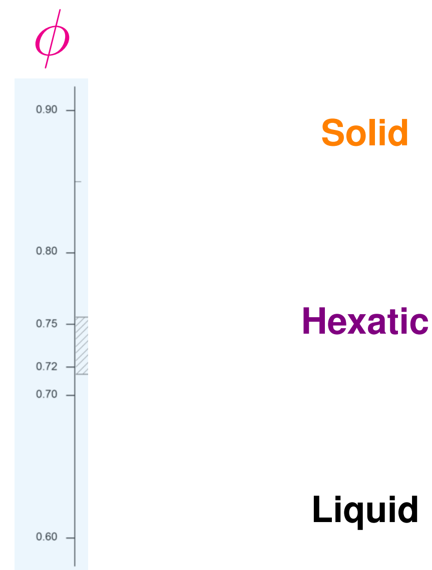

with $\nu = 0.37$ for dislocations at the **solid** - **hexatic** transition

and $\nu = 0.5$ for disclinations at the **hexatic** - **liquid** transition

Dislocations

At the Pe = 0 solid-hexatic transition

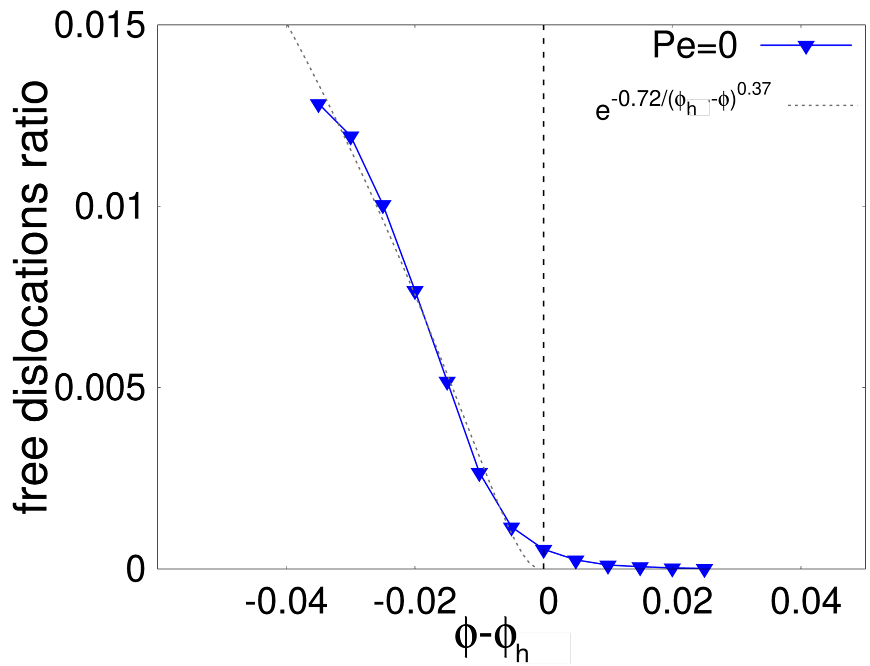

Dislocations ▼ unbind close to the **solid** - **hexatic** transition

ϕ_h from the measurement of correlation functions and other observables,

Dotted line exponential form with $\nu = 0.37$ and ρ_d forced to vanish at ϕ_h

Dislocations

At the Pe = 0 solid-hexatic transition

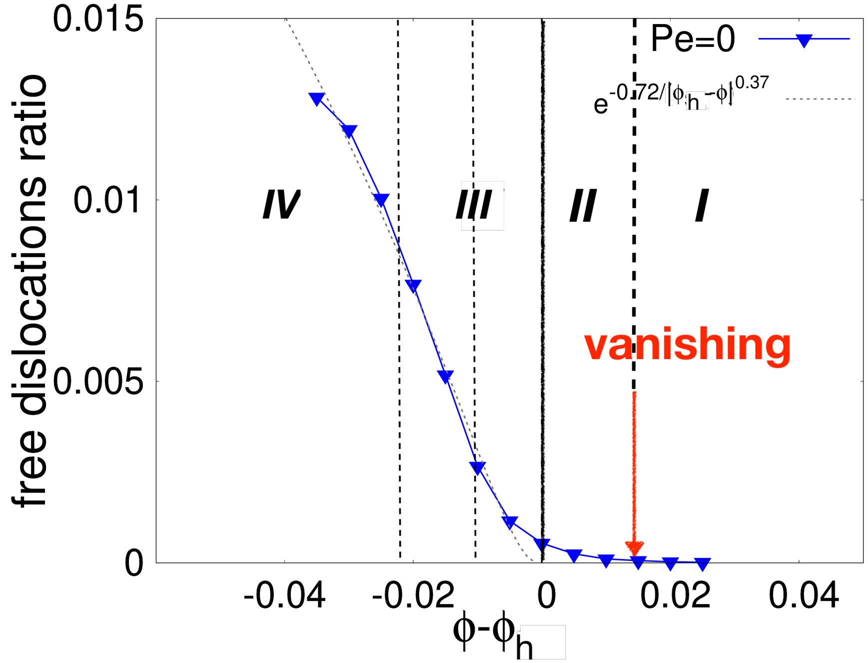

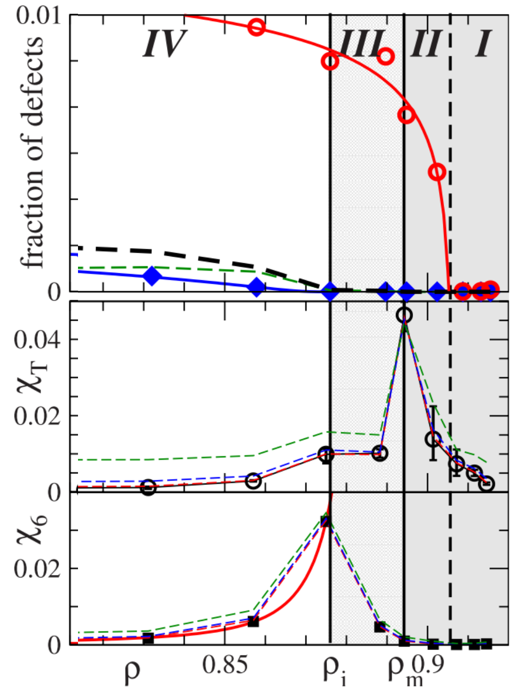

Do **dislocations ▼** really unbind at the **solid** - **hexatic** transition ϕ_h ?

Even experimentally $\phi_c > \phi_h$ & $\rho_d(\phi > \phi_c)$ is much larger than for us

though $\nu = 0.37$ is acceptable (effect of parameter b quite large)

Han, Ha, Alsayed, & Yodh, PRE 77, 041406 (2008) Short-range & repulsive microgel

Disclinations

At Pe = 0 close to the 1st order hexatic - liquid transition

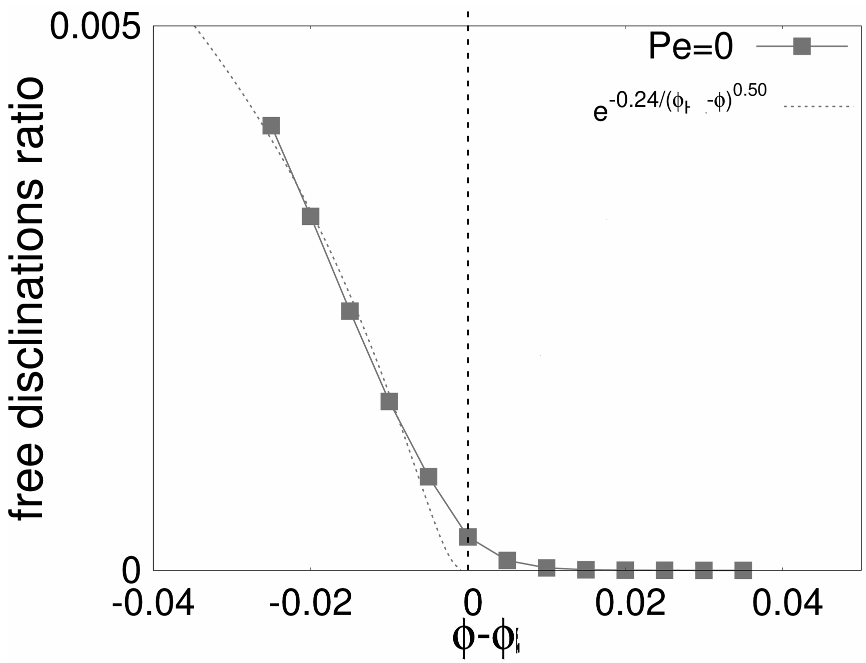

Disclinations ■ unbind close to where the **liquid** appears in co-existence at ϕ_l

Dotted line with $\nu = 0.5$ and ρ_d forced to vanish at ϕ_l, the upper limit of the co-existence region

Disclinations

At Pe = 0 close to the 1st order hexatic-liquid

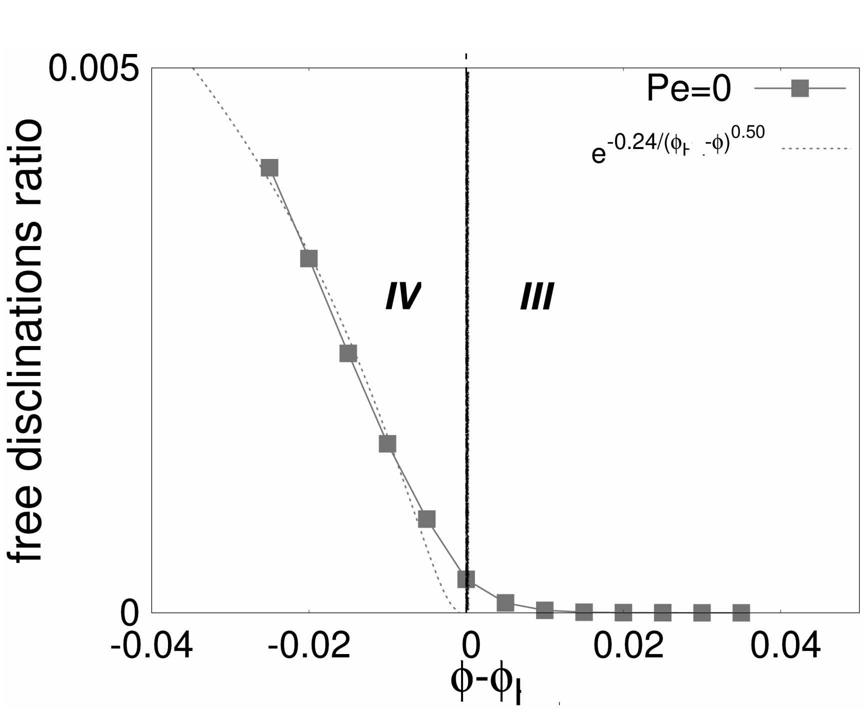

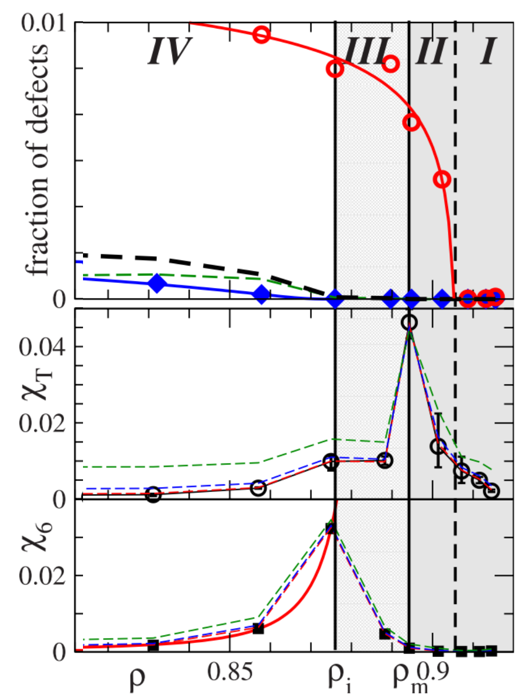

Disclinations ■ unbind close to where the **liquid** appears in co-existence at ϕ_l

Dotted line with $\nu = 0.5$ forced to vanish at ϕ_l

Han, Ha, Alsayed, & Yodh, PRE 77, 041406 (2008) Short-range & repulsive microgel

Do not identify a 1st order transition

Disclinations

At Pe = 0 close to the 1st order hexatic-liquid

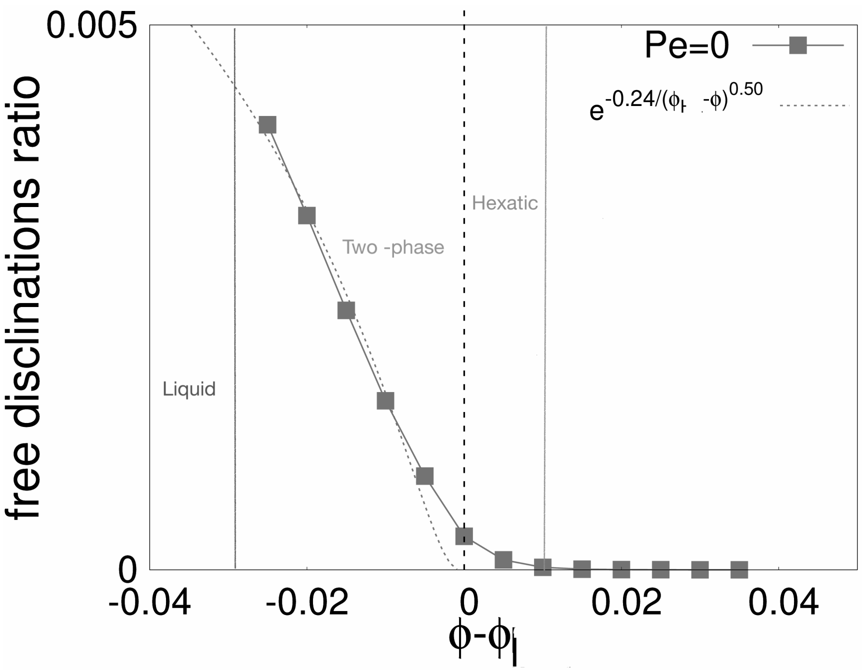

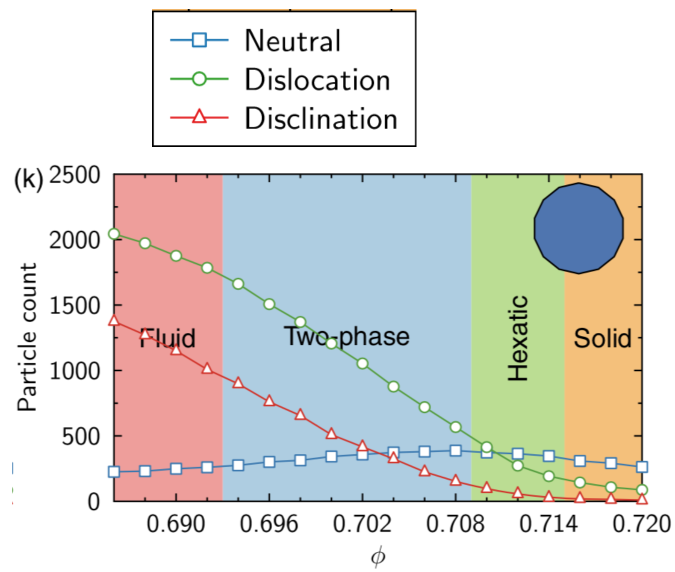

0.15

Disclinations ■ unbind close to where the **liquid** appears in co-existence at ϕ_l

Dotted line with $\nu = 0.5$ forced to vanish at ϕ_l (upper co-existence)

Anderson, Antonaglia, Millan, Engel & Glotzer, PRX 7, 021001 (2017) MC hard

$N = 16384 \implies \rho_d \sim 0.01$ at ϕ_l also more than us but we use $N = 260000$

Disclinations

At the hexatic - liquid transition ϕ_l at all Pe

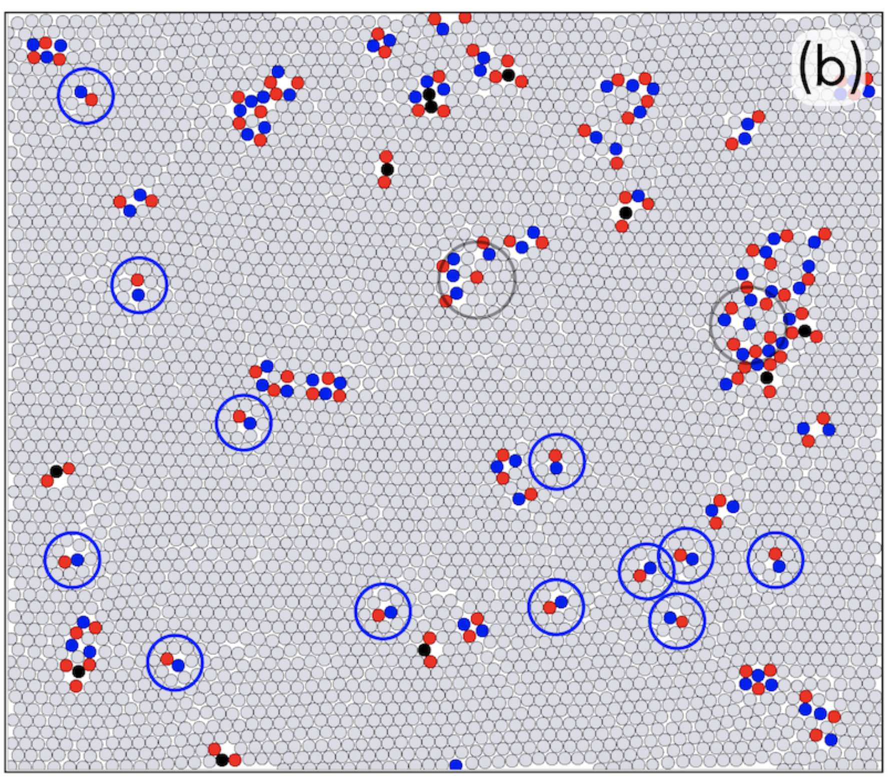

dislocations

disclinations

Very few disclinations, and always very close to other defects, so **not free**

Grain boundaries & clusters

Classification

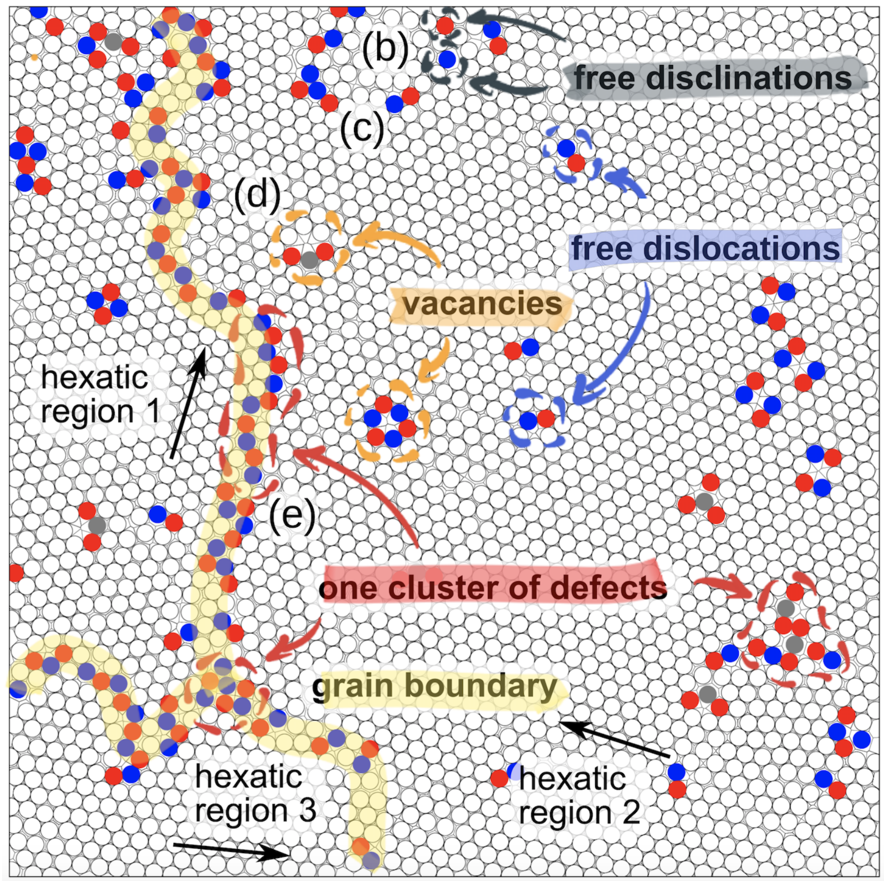

The classification in **Pertsinidis & Ling, PRL 87, 098303 (2001)**

Coarse graining

Square boxes with $\ell = 3\sigma_d$

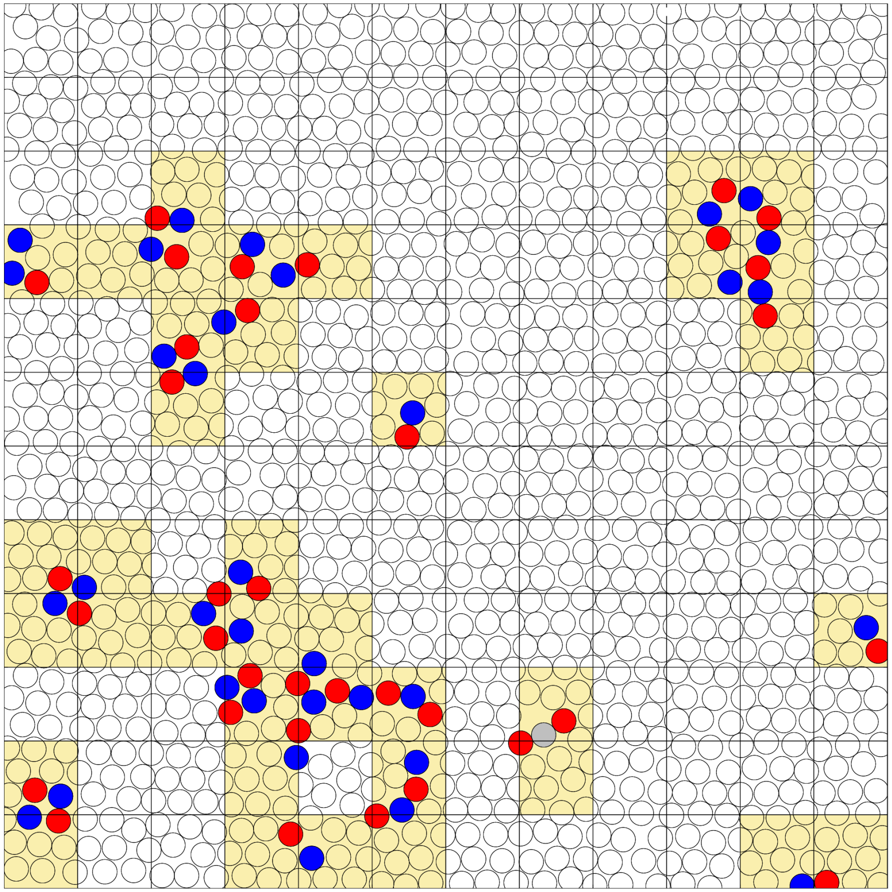

Clusters

Close to the hexatic - liquid transition

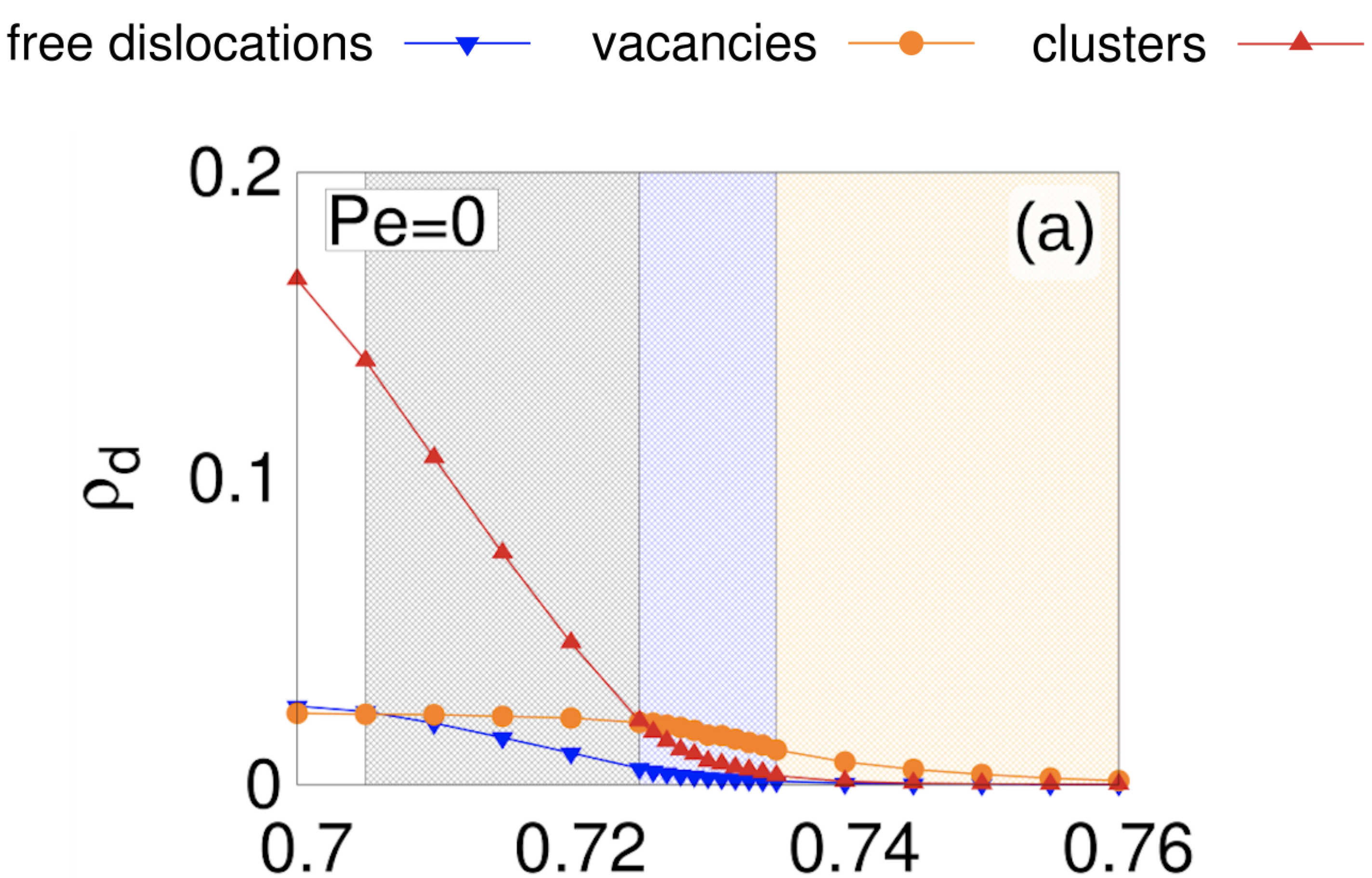

As soon as the liquid appears in co-existence, **defects in clusters dominate**

Clusters

Within the co-existence region at Pe = 0

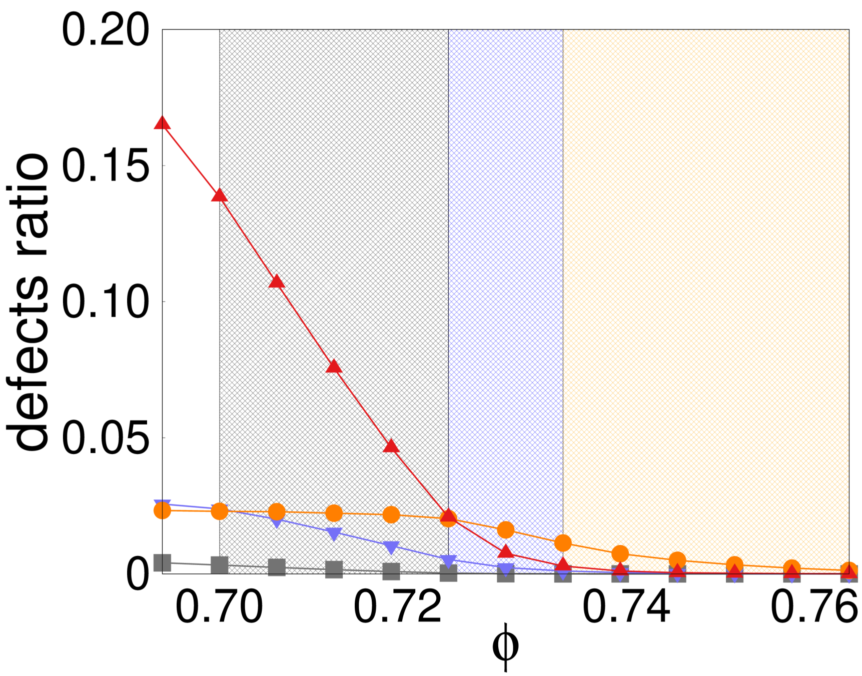

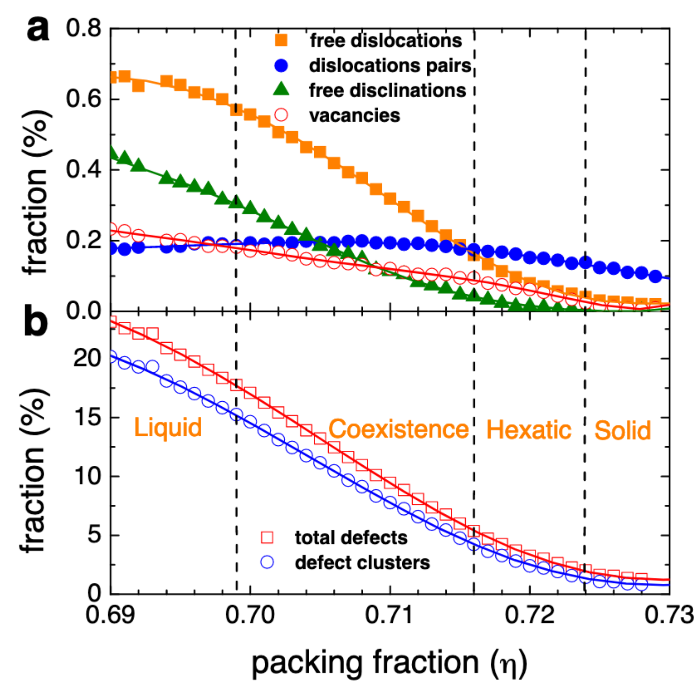

Clusters ▲ proliferate within the co-existence region

Vacancies ● remain approximately constant within the co-existence region

Qi, Gantapara & Dijkstra, Soft Matter 10, 5419 (2014) Event drive MD hard disks

Clusters

Percolation : finite size scaling

The probability of there being a wrapping cluster ($d_s = 3\sigma_d$)

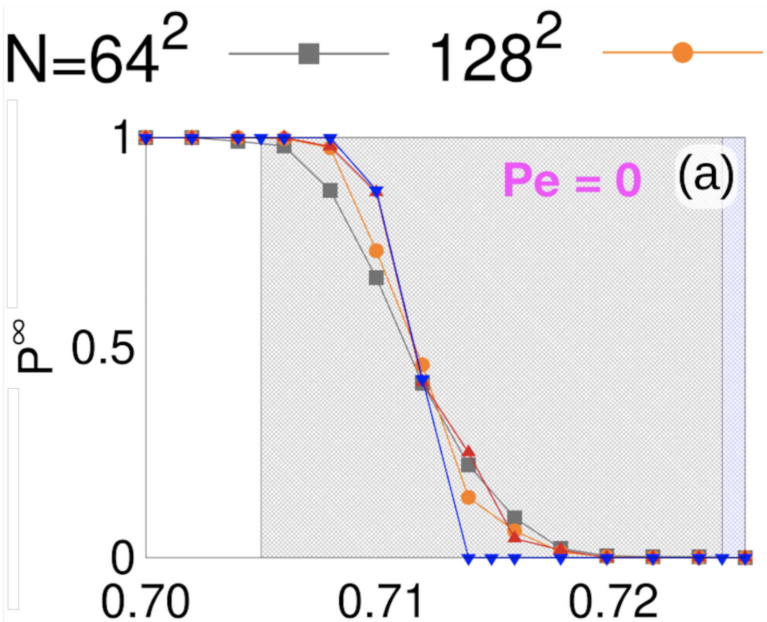

The curves cut at a single point: finite size scaling indicates this is the critical parameter

At ϕ_p close but below the ϕ_l where the **liquid** first appears.

Clusters

Hexatic - liquid transition

Hexatic order

heat map

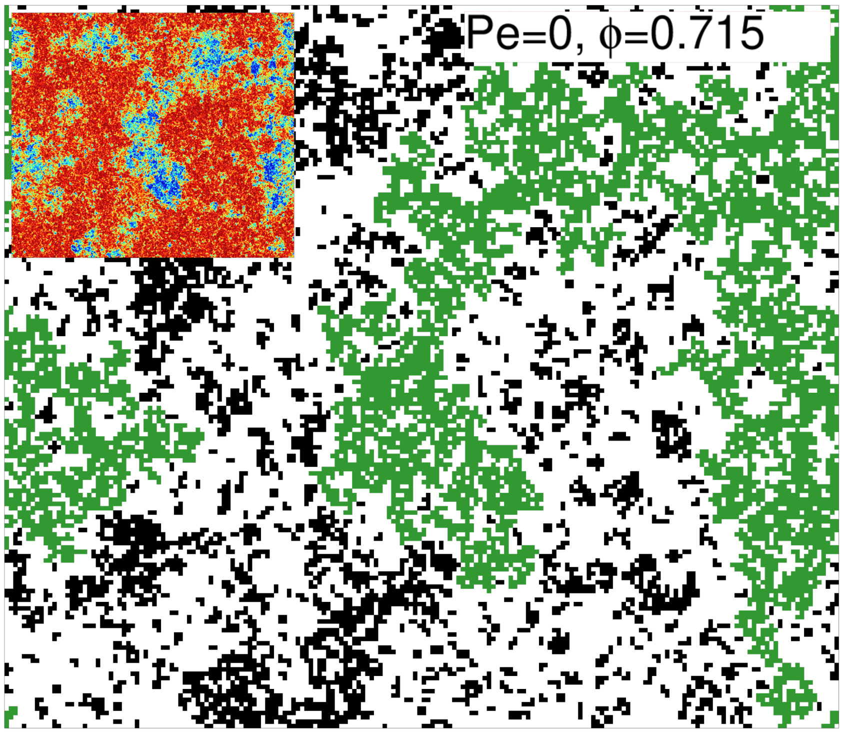

The green cluster of defects percolates (vertically)

Invation of liquid phase (on the defect cluster) within the hexatic one

Rather hard disks

$\sim$ Algebraic distribution of defect cluster sizes

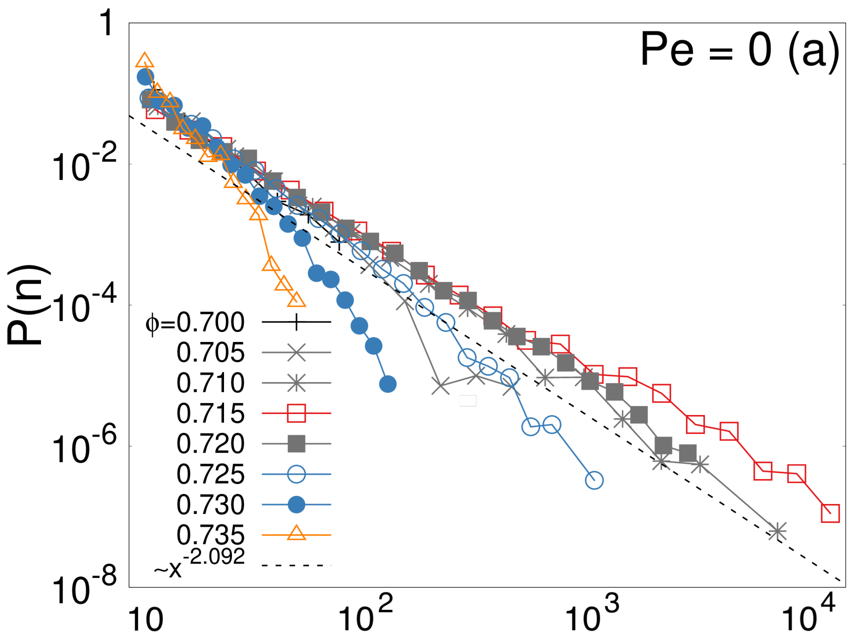

$\phi = 0.715$

within the coexistence region

aspects of critical percolation of clusters of defects

Though, careful, recall geometric vs. Fortuin-Kasteleyn clusters in Ising model, Potts for various q, etc. Still to be better understood.

Is this really related to the 1st order nature of the transition ?

Soft disks

Defect ratio & size distribution

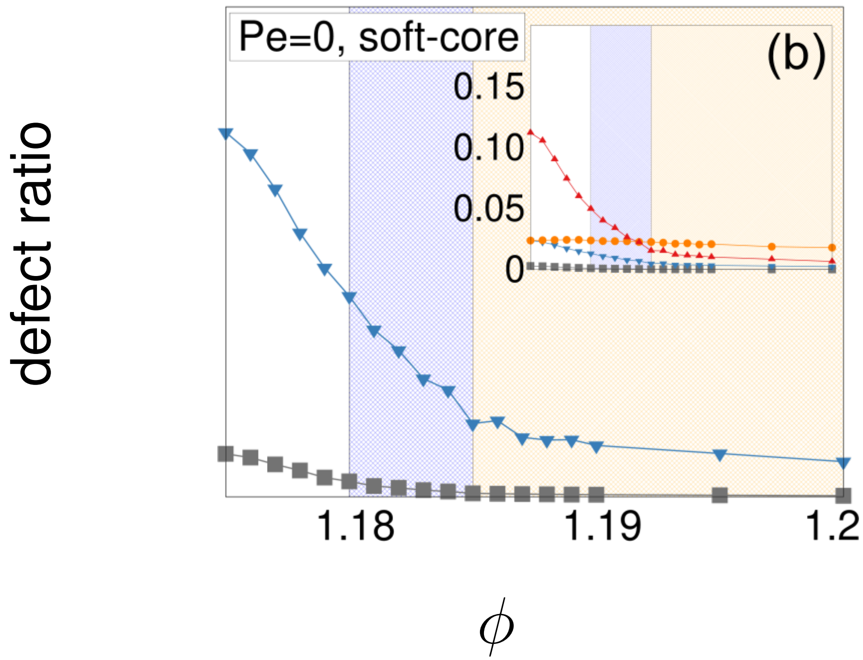

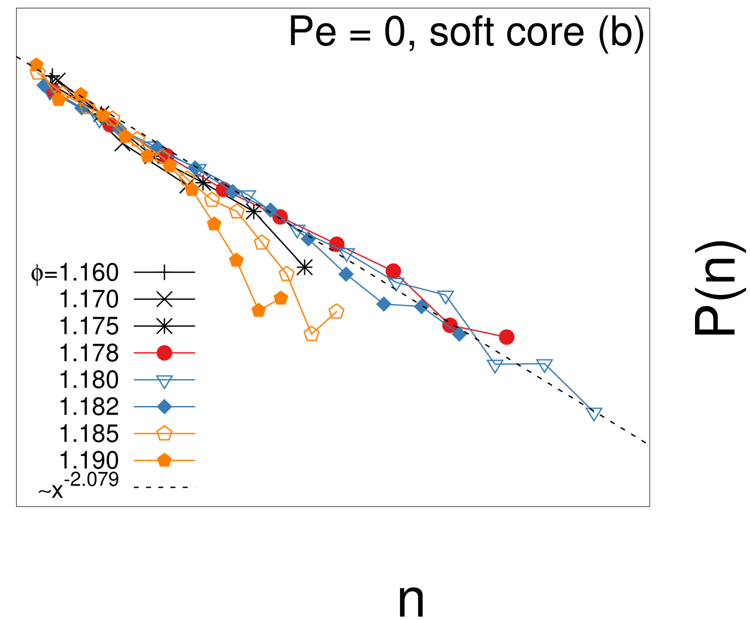

For soft disks the **hexatic**-**liquid** transition is **continuous**, no signature of co-existence. Still, similar picture ; proliferation of clusters with aspects of critical percolation at the hexatic-liquid transition.

Plan

1. Equilibrium phases : solidification/melting

   Special in two-dimensions

   Solid, hexatic & liquid phases

   Phase transitions

   Topological defects

2. **Active matter**

   Self-propelled Brownian disks in $2d$

   Phase diagram

   Solid, hexatic & liquid phases ; motility induced phase separation

   Topological defects

Active matter

Definition

Active matter is composed of large numbers of active "agents", each of which consumes energy in order to move or to exert mechanical forces.

Due to the energy consumption, these systems are intrinsically out of thermal equilibrium.

Uniform energy injection within the samples (and not from the borders).

Coupling to the environment (bath) allows for the dissipation of the injected energy.

Active matter

Realisations & modelling

- Wide range of scales: macroscopic to microscopic

  Natural examples are birds, fish, cells, bacteria.

- Also artificial realisations: Janus particles, granular, etc.

- $3d$, $2d$ and $1d$.

- Modelling: very detailed to coarse-grained or schematic.

  — microscopic or *ab initio* with focus on active mechanism,

  — *mesoscopic*, just forces that do not derive from a potential,

  — *Cellular automata* like in the Vicsek model.

Active matter

Natural & artificial systems

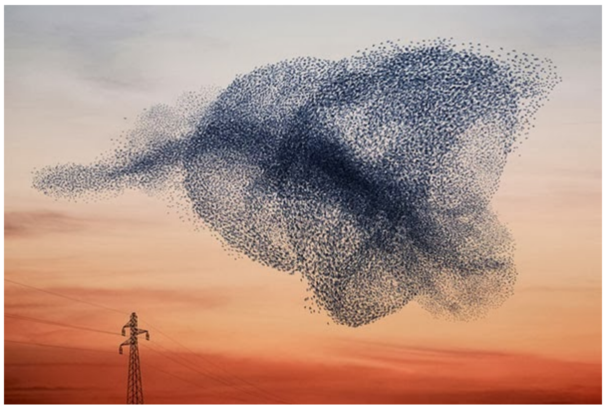

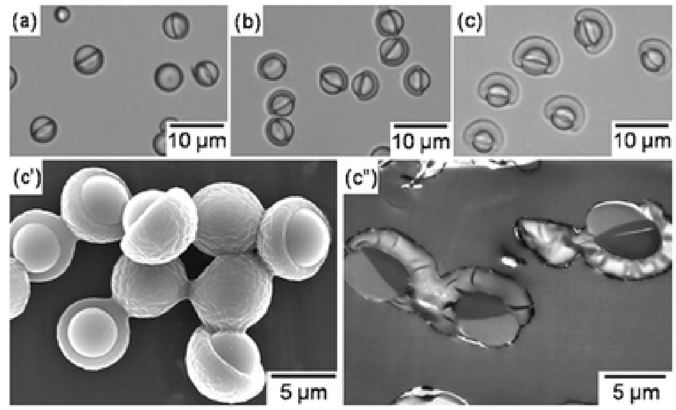

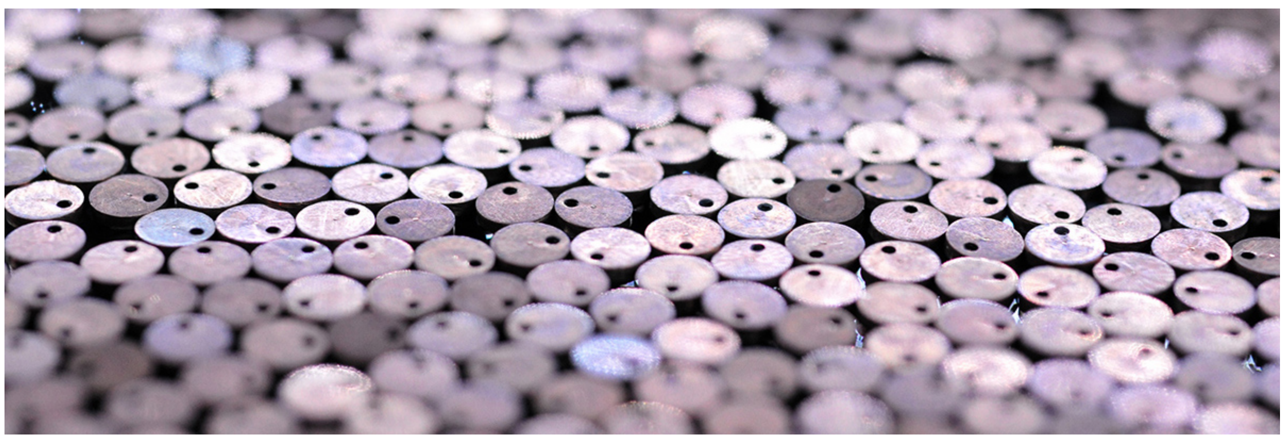

Experiments & observations **Bartolo et al.** Lyon, **Bocquet et al.** Paris, **Cavagna, et al.** Roma, **di Leonardo et al.** Roma, **Dauchot et al.** Paris, just to mention some Europeans

Active disks

Overdamped Brownian particles (the standard model)

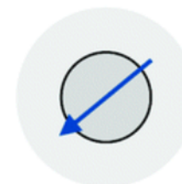

Active force $\mathbf{F}_{\rm act}$ along $\mathbf{n}_i = (\cos\theta_i(t), \sin\theta_i(t))$

$$m\ddot{\mathbf{r}}_i + \gamma\dot{\mathbf{r}}_i = F_{\rm act}\mathbf{n}_i - \nabla_i \sum_{j(\neq i)} U_{\rm Mie}(r_{ij}) + \boldsymbol{\xi}_i \ , \qquad \dot{\theta}_i = \eta_i \ ,$$

$\mathbf{r}_i$ position of the centre of ith part & $r_{ij} = |\mathbf{r}_i - \mathbf{r}_j|$ inter-part distance,

short-ranged repulsive Mie potential, over-damped limit $m \ll \gamma$

$\boldsymbol{\xi}$ and η zero-mean Gaussian noises with
$\langle \xi_i^a(t)\, \xi_j^b(t')\rangle = 2\gamma k_B T \delta_{ij}^{ab}\delta(t-t')$ and $\langle \eta_i(t)\, \eta_j(t')\rangle = 2D_\theta\delta_{ij}\delta(t-t')$.

The units of length, time and energy are given by $\sigma_{\rm d}$, $\tau_p = D_\theta^{-1}$ and ε

$D_\theta = 3k_BT/(\gamma\sigma_d^2)$, $\phi = \pi\sigma_d^2 N/(4S)$, $\gamma = 10$ and $k_BT = 0.05$

Péclet number Pe = $F_{\rm act}\sigma_{\rm d}/(k_BT)$ measures activity

Repulsive hard potential

Mie form

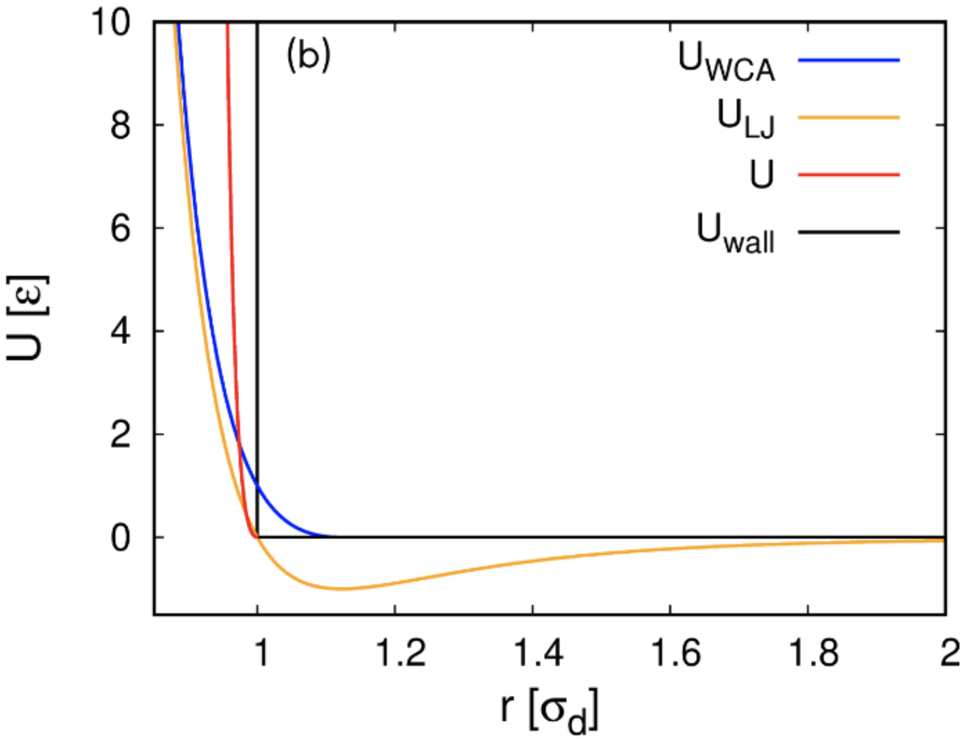

$$4\epsilon[(\sigma/r)^{2n} - (\sigma/r)^{n}] + \epsilon \quad \text{with} \quad n = 32$$

Active Brownian disks

The typical motion of particles in interaction

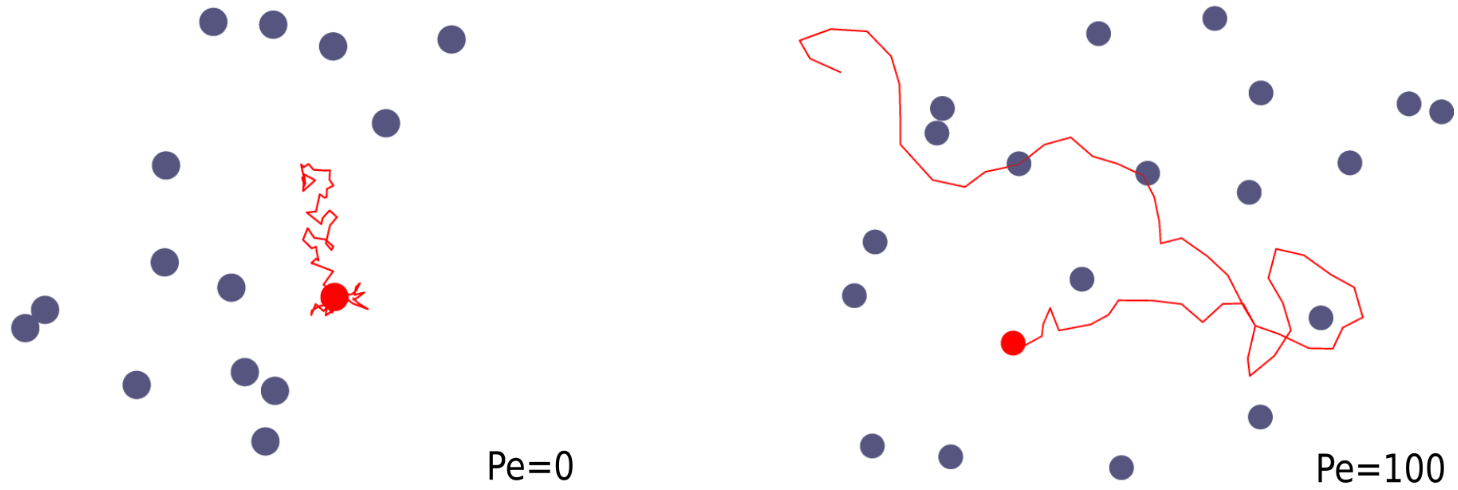

Pe induces a persistent motion

$$\tau_p = D_\theta^{-1}$$

Weak activity

Active disks

Phase diagram with solid, hexatic, co-existence & liquid

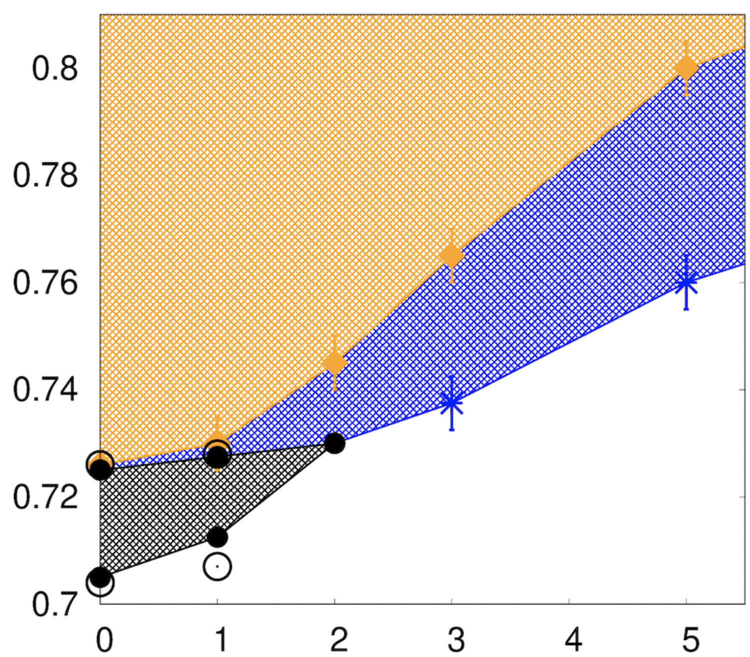

Weak energy injection

small Pe

From pressure $P(\phi)$, correlations G_T & G_6, distributions of ϕ_i & ψ_{6i} at $k_B T = 0.05$

Digregorio, Levis, Suma, LFC, Gonnella & Pagonabarraga, PRL 121, 098003 (2018)

Active disks

Correlation functions in solid, hexatic and liquid phases

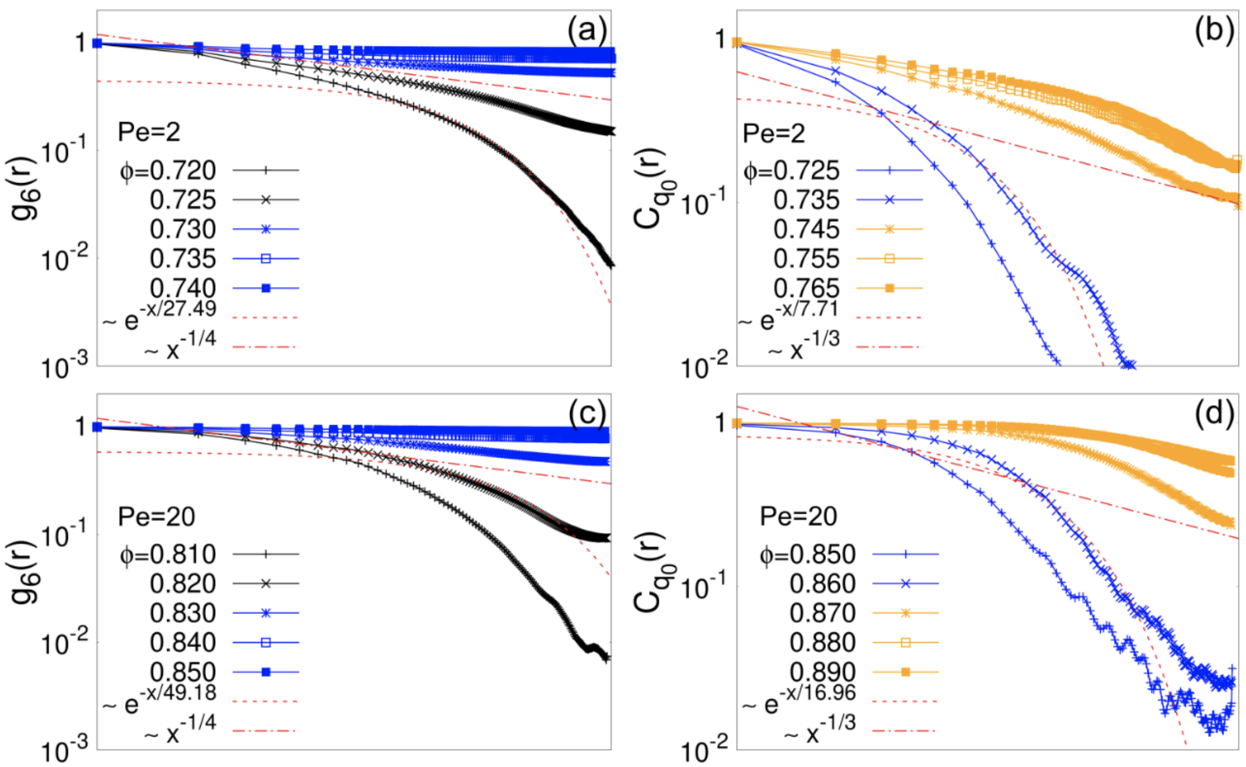

Active hard disks

Distribution of the local density

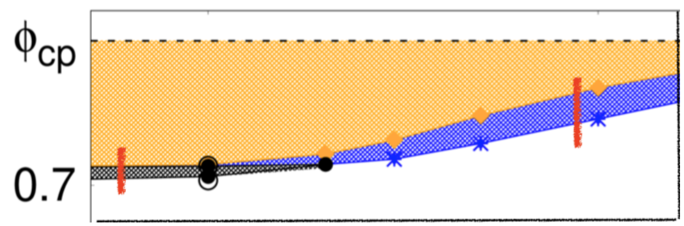

Pe = 1 Pe = 10

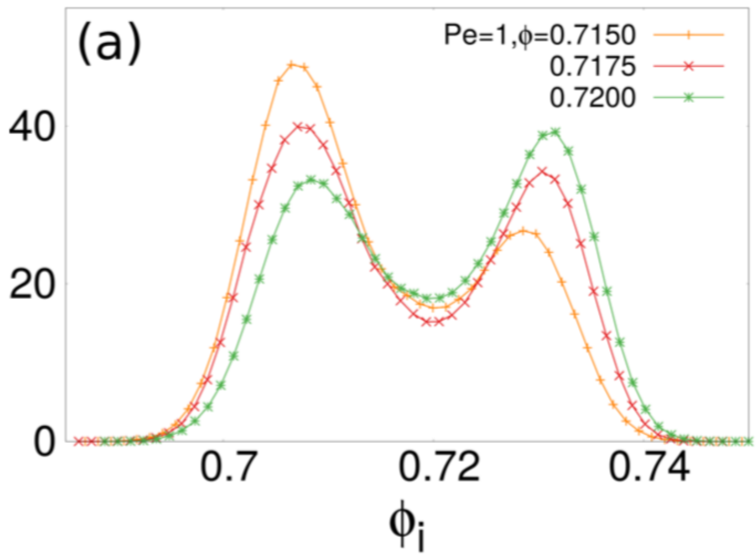

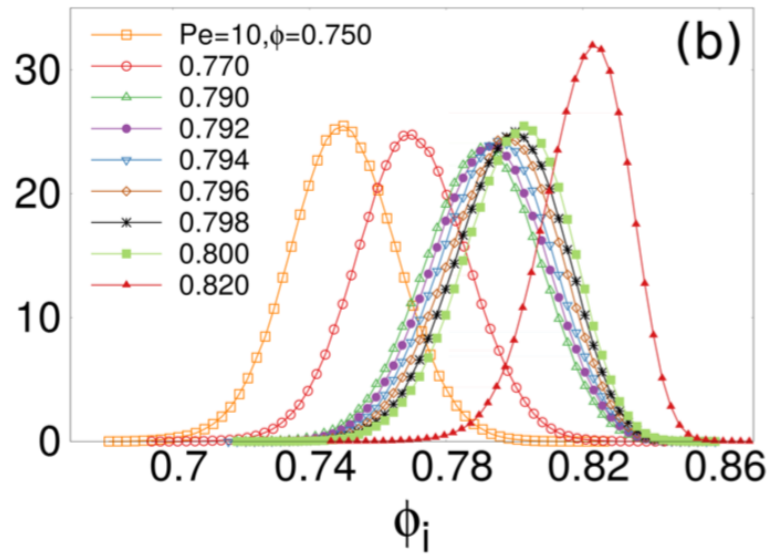

First order - coexistence

Second order

Dislocations

At the solid-hexatic transition at weak Pe

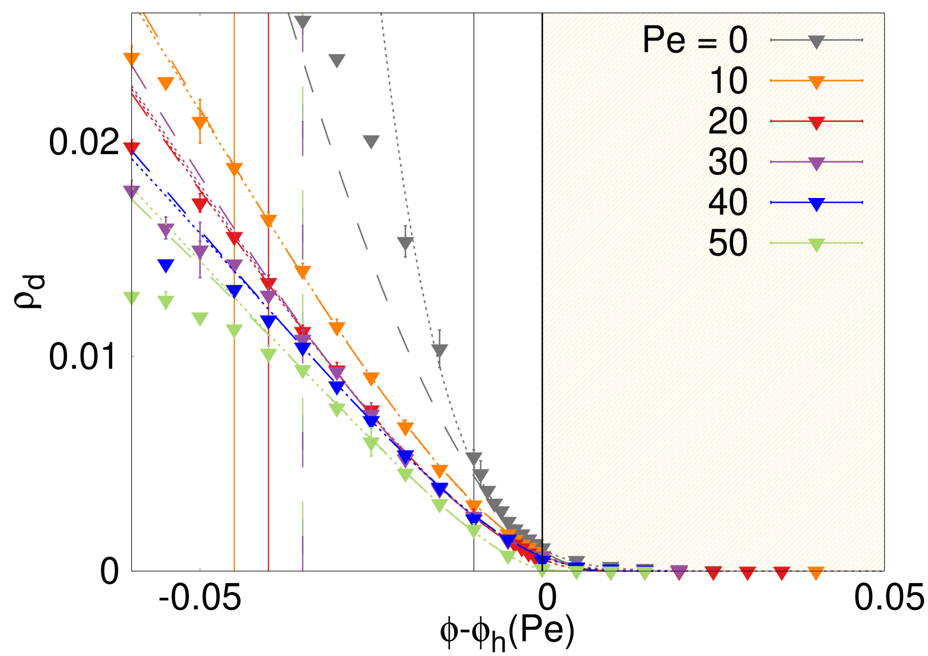

Four (ϕ_c, ν, a, b dotted) vs. three ($\phi_c, \nu = 0.37, a, b$ dashed) parameter fits on data in the hexatic & solid phases only. Criteria to support $\nu = 0.37$:

– χ^2 ... but not clear which one is better

– closeness between ϕ_c and ϕ_h

Batrouni et al for $2d$XY

– not crazy values for a, b but crazy values for ν if let to be fitted

Dislocations

At the solid-hexatic transition at weak Pe

$\nu = 0.37$

Pe	ν	a	b	ϕ_c	ϕ_h	χ^2/ndf
0	0.37	8	2	0.75	0.735	1.61
10	0.37	1.5	1.61	0.853	0.840	2.76
20	0.37	1.2	1.59	0.883	0.870	1.34
30	0.37	2	1.9	0.897	0.880	2.08
40	0.37	0.81	1.47	0.898	0.885	0.791
50	0.37	0.38	1.17	0.895	0.890	0.493

✓

ν free

Pe	ν	a	b	ϕ_c	ϕ_h	χ^2/ndf
0	9	13	0.002	1	0.735	0.920
10	0.6	0.4	0.7	0.857	0.840	2.89
20	0.3	5	3	0.881	0.870	1.39
30	0.8	0.2	0.3	0.909	0.880	2.08
40	0.7	0.2	0.4	0.90	0.885	0.924
50	0.2	7	3	0.892	0.890	0.461

✗

Dislocations

Effect of coarse-graining: the notion of freedom

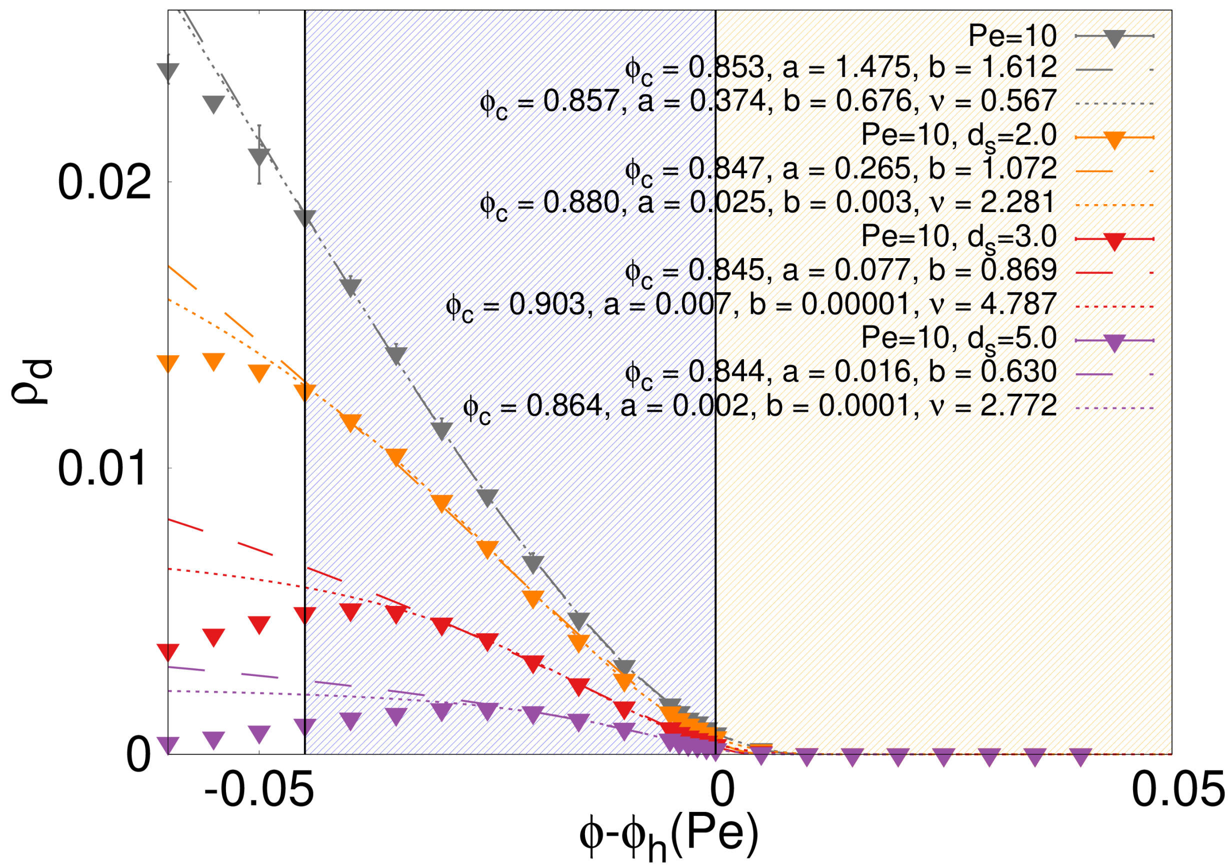

Pe = 10

$\phi_h = 0.84$

$\phi_c = 0.853 \ \ (0)$

$\phi_c = 0.847 \ \ (2)$

$\phi_c = 0.845 \ \ (3)$

$\phi_c = 0.844 \ \ (5)$

Disclinations

At the hexatic - liquid transition at weak Pe

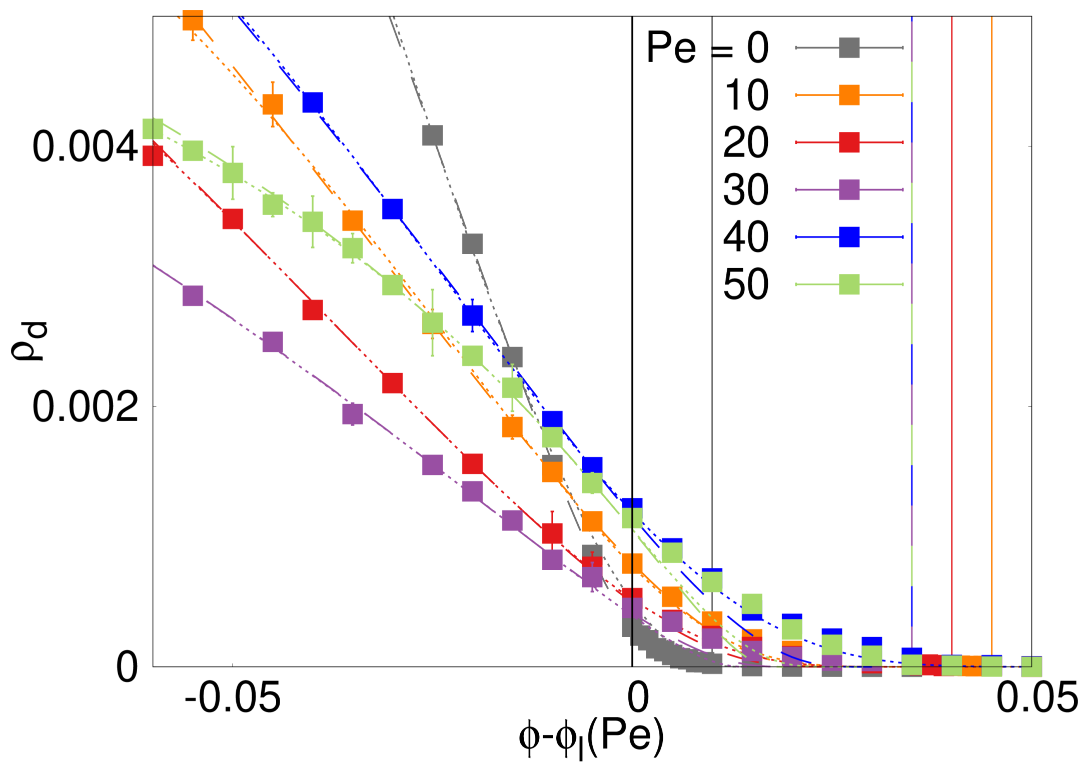

Messier than for dislocations

ϕ_l upper limit of co-existence at Pe = 0 & critical **hexatic** - **liquid** at Pe $\neq 0$

Dotted and broken lines show three (a, b, ϕ_c) and four (also ν) parameter fits.

Vertical lines are at ϕ_h (end of the hexatic phase)

Disclinations

At the hexatic - liquid transition at weak Pe

$\nu = 0.50$

Pe	ν	a	b	ϕ_c	ϕ_l	χ^2/ndf	ϕ_h
0	0.5	0.072	0.62	0.734	0.725	0.430	0.735
10	0.5	0.06	0.81	0.823	0.795	1.09	0.840
20	0.5	0.05	0.8	0.857	0.830	0.710	0.870
30	0.5	0.025	0.64	0.866	0.845	0.895	0.880
40	0.5	0.053	0.71	0.880	0.850	0.809	0.885
50	0.5	0.016	0.41	0.874	0.855	0.233	0.890

✓

ν free

Pe	ν	a	b	ϕ_c	ϕ_l	χ^2/ndf
0	0.4	0.4	2	0.7	0.725	3.24
10	2	0.012	0.03	0.85	0.795	0.859
20	1	0.02	0.2	0.9	0.830	0.858
30	0.3	0.09	2	0.86	0.845	0.965
40	2	0.013	0.01	0.96	0.850	0.661
50	0.9	0.008	0.1	0.88	0.855	0.288

✗

Disclinations

Effect of coarse-graining: basically, no free disclinations

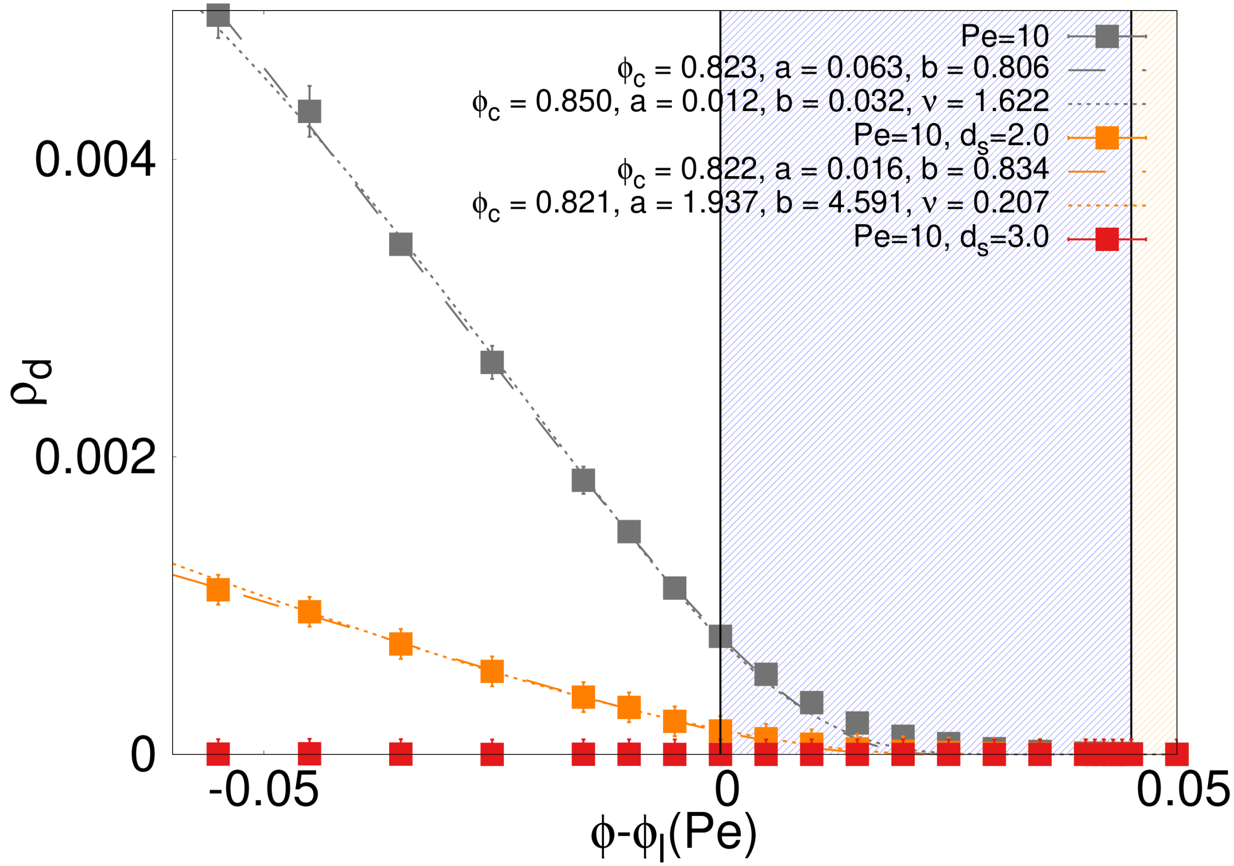

Pe = 10

$\phi_l = 0.795$

d_s	ϕ_c
0	0.823
2	0.822
3	0.821

No more

Clusters

Percolation : finite size scaling

The probability of there being a wrapping cluster ($d_s = 3\sigma_d$)

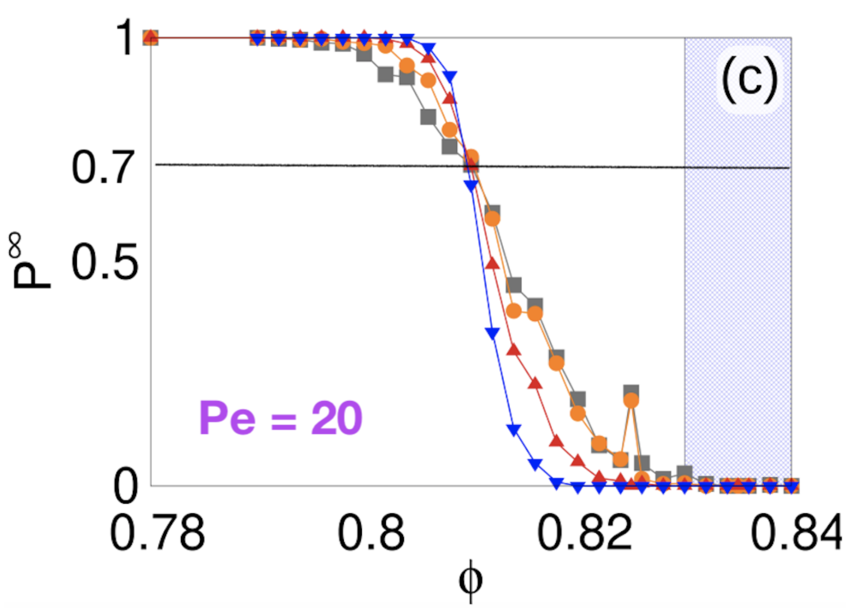

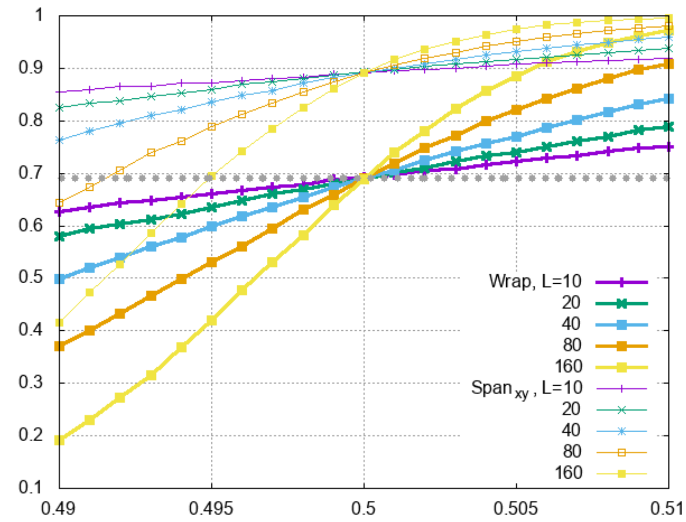

At ϕ_p close but below the ϕ_l where the **liquid** first appears.

Critical site percolation data from **M. Picco**

Clusters

Percolation : cluster size distribution

$P(n) \sim n^{-\tau}$ with $\tau = 1 + d/d_\mathrm{f} = 187/91 \sim 2.05$

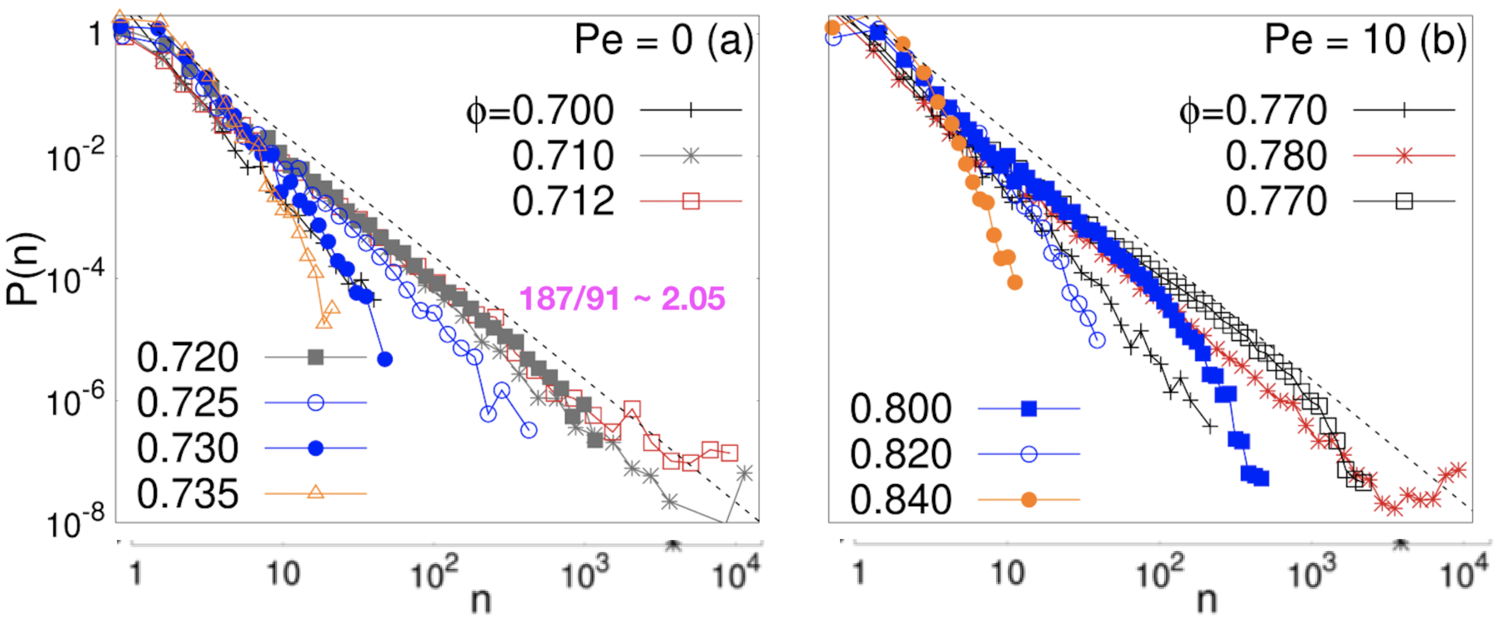

Red data points at ϕ_p within the co-existence region at Pe = 0, and slightly below ϕ_l at Pe $\neq 0$.

Clusters

Percolation: (in)dependence of coarse-graining Pe = 10

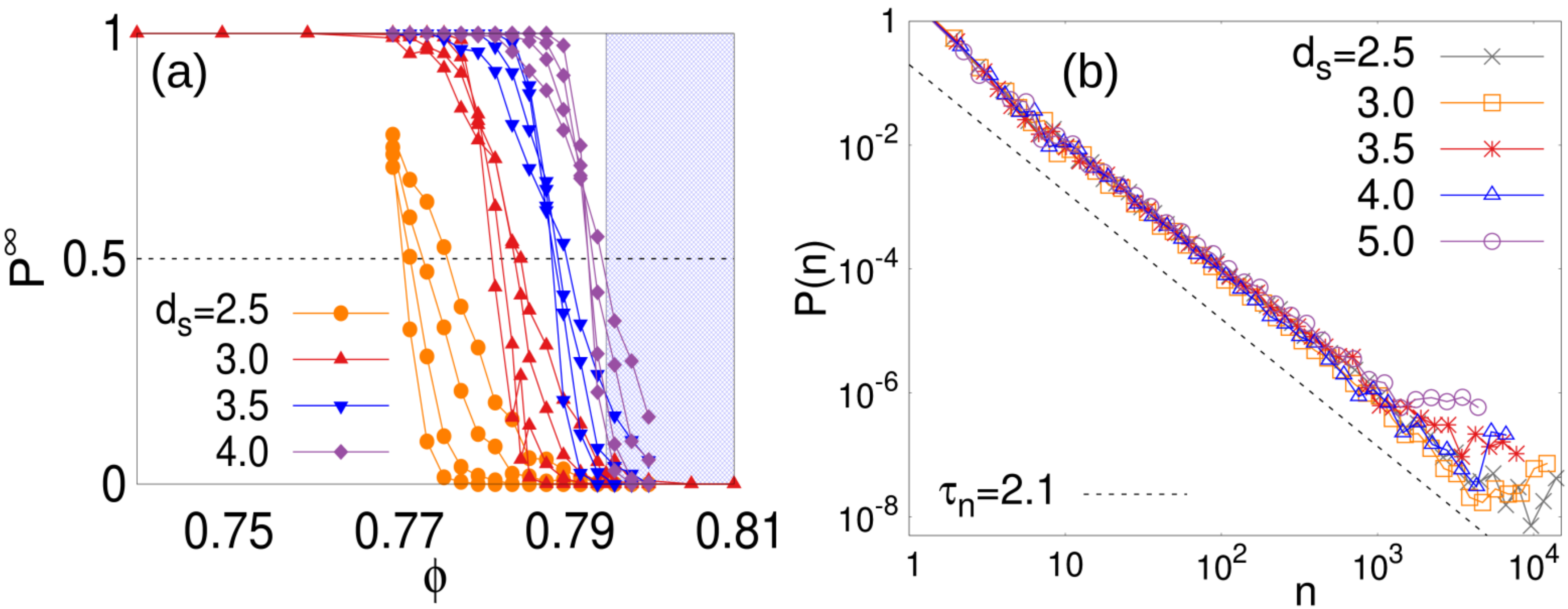

ϕ_p displaces towards larger values with increasing d_s but $d_{\rm f}, \tau$ do not change.

Clusters

Percolation : fractality

Binned scatter plot of the mass of each cluster n_C against its radius of gyration R_{g_C}

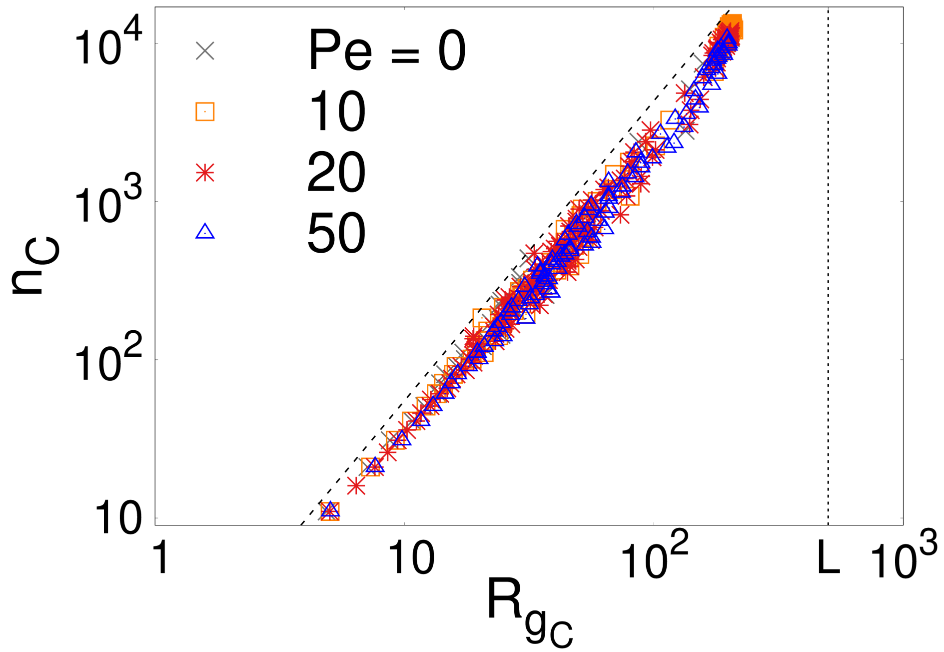

At ϕ_p close but below ϕ_l where the **liquid** first appears.

Dashed inclined line $n_C \sim R_{g_C}^{d_f}$ with $d_f \sim 1.90$

Clusters

Percolation : the critical curve

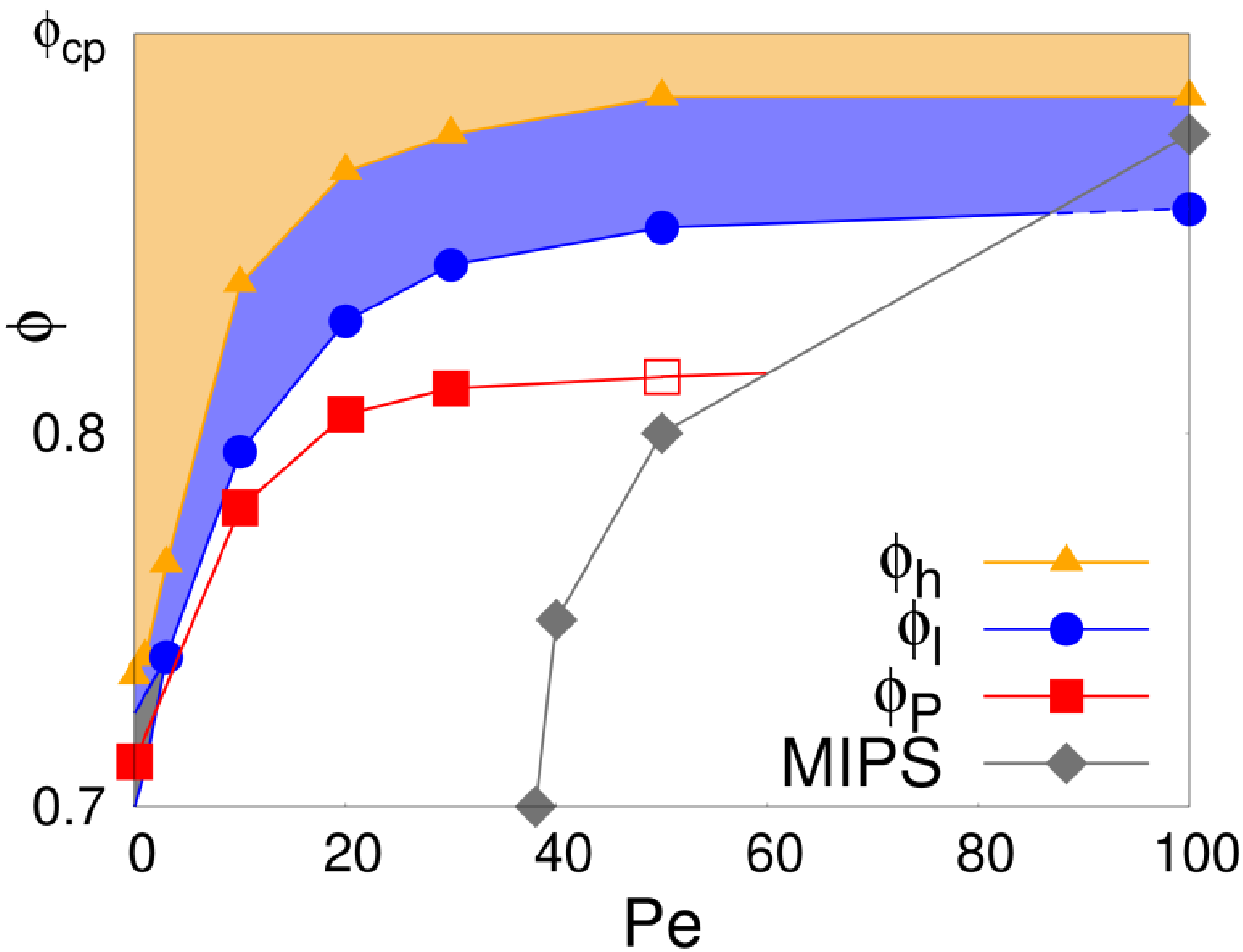

Strong activity

Active disks

Phase diagram with solid, hexatic, liquid, co-existence and MIPS

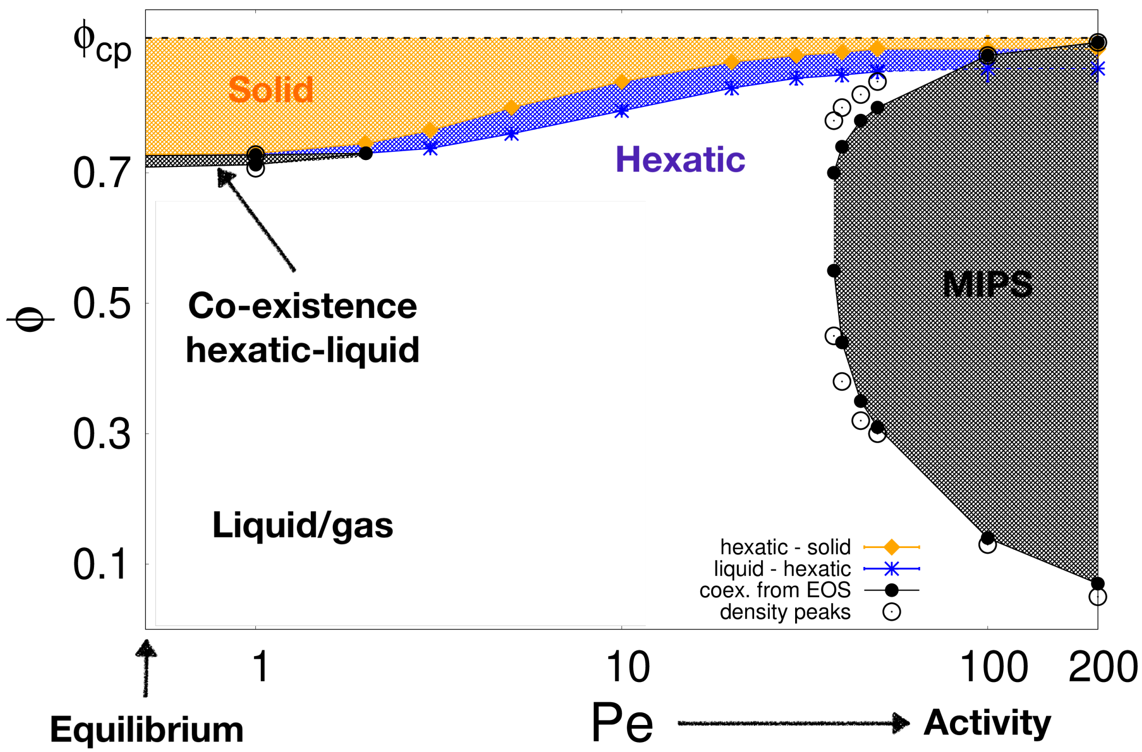

Motility induced

phase separation

gas & dense

Cates & Tailleur

Ann. Rev. CM 6, 219 (2015)

Farage, Krinninger & Brader

PRE 91, 042310 (2015)

Pressure $P(\phi, \text{Pe})$ (EOS), correlations $G_T(r)$, $G_6(r)$, and distributions of ϕ_i, $|\psi_{6i}|$

Digregorio, Levis, Suma, LFC, Gonnella & Pagonabarraga, PRL 121, 098003 (2018)

Active disks

Motility induced phase separation

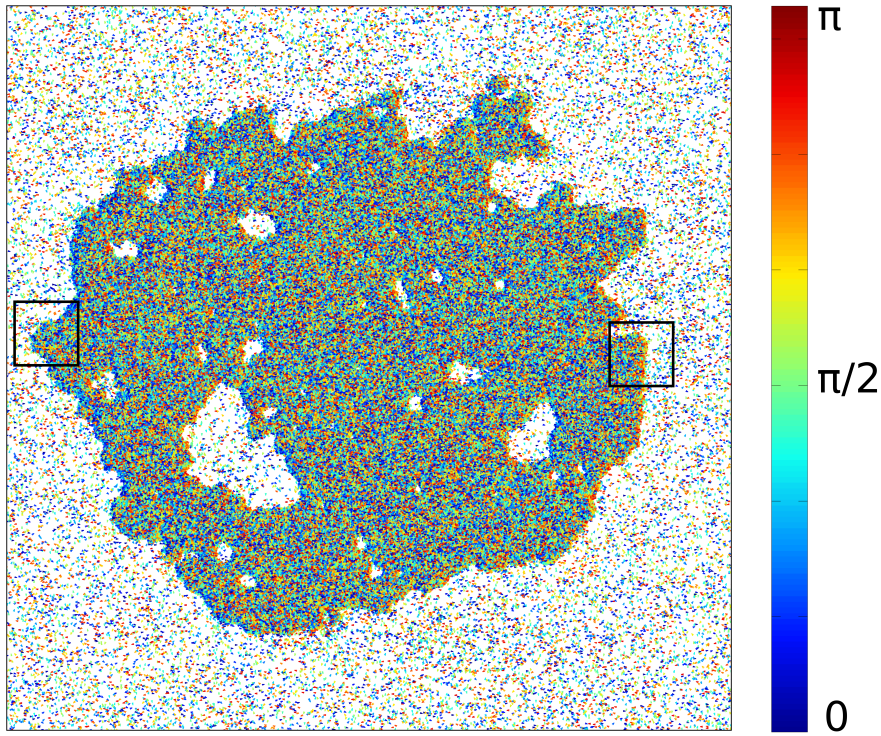

$\longrightarrow$ **blue 0** $\qquad\qquad$ $\longleftarrow$ **red π**

The colours indicate the direction along which the particles are pushed by the active force $\boldsymbol{F}_{\rm act}$

Active disks

Motility induced phase separation

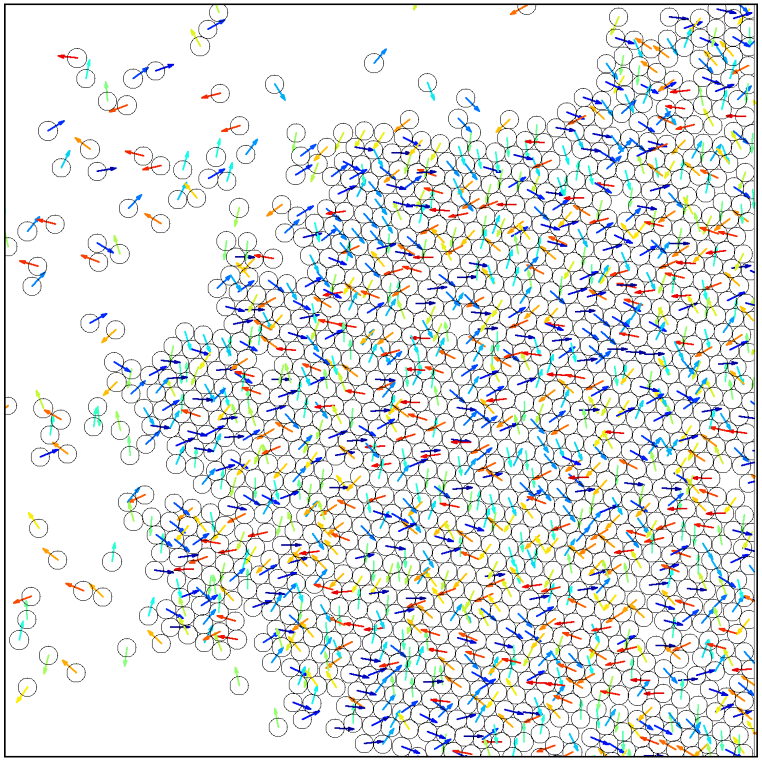

Zoom over left border $\to 0$

Active disks

Motility induced phase separation

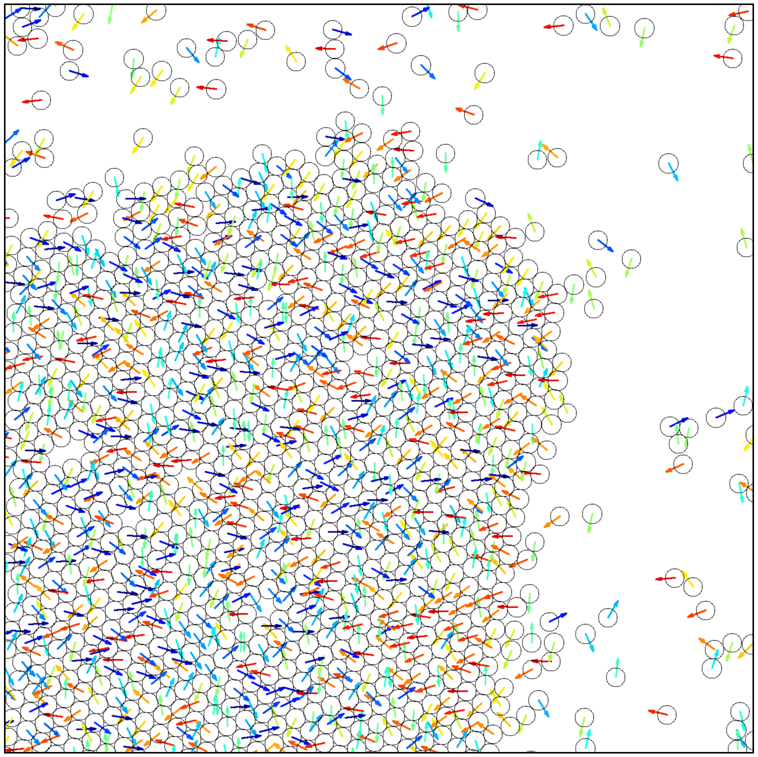

Zoom over right border $\leftarrow \pi$

Active disks

Motility induced phase separation

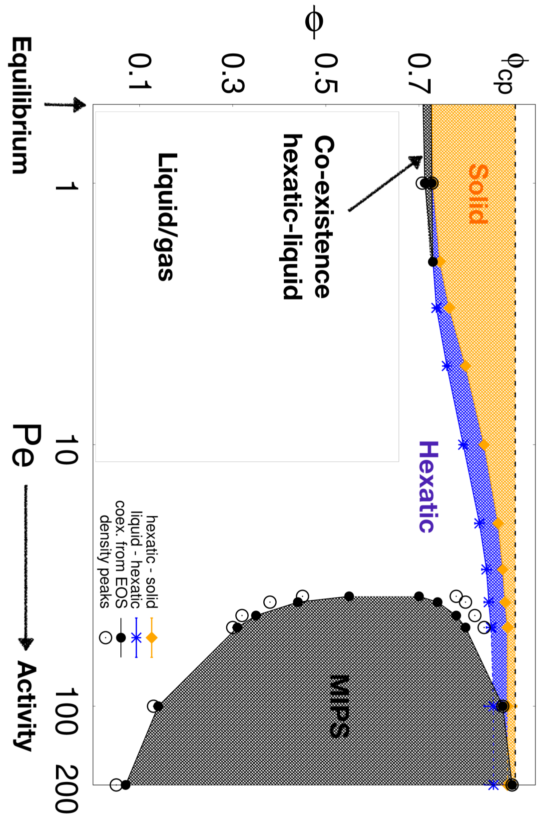

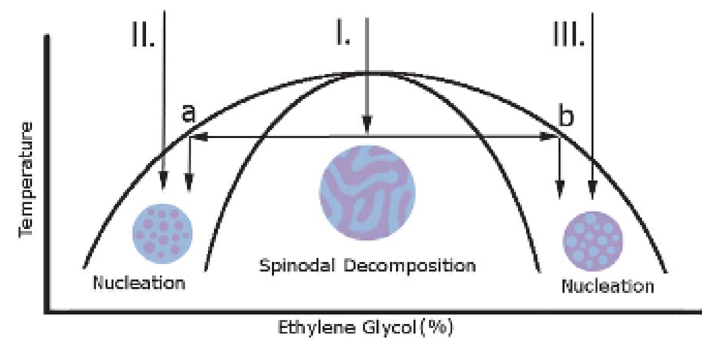

Similar to phase separation with percentage of system covered by dense and gas phases determined by a level rule

Cates & Tailleur (2012)

Active disks

Motility Induced Phase Separation

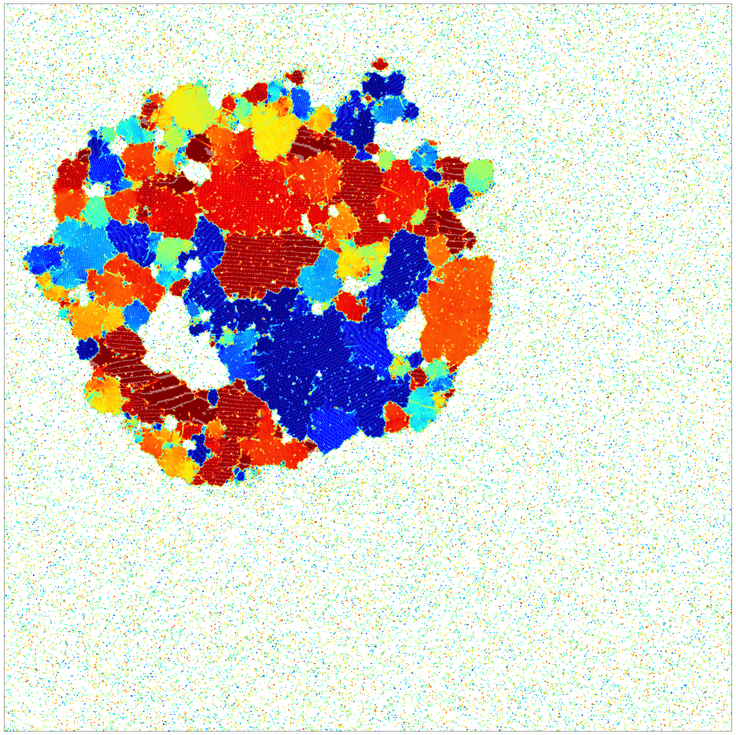

Dense/dilute separation[1]

For low packing fraction ϕ

a single round droplet.

A mosaic of different

hexatic orders[2] with

gas bubbles[2,3,4]

Defects ?

[1] Cates & Tailleur, Annu. Rev. Cond. Matt. Phys. 6, 219 (2015)

[2] Caporusso, Digregorio, Levis, LFC & Gonnella, PRL 125, 178004 (2020)

[3] Tjhung, Nardini & Cates, PRX 8, 031080 (2018)

[4] Shi, Fausti, Chaté, Nardini & Solon, PRL 125, 168001 (2020)

Active disks

Modulus of the local hexatic order parameter

Pe = 1 Pe = 200

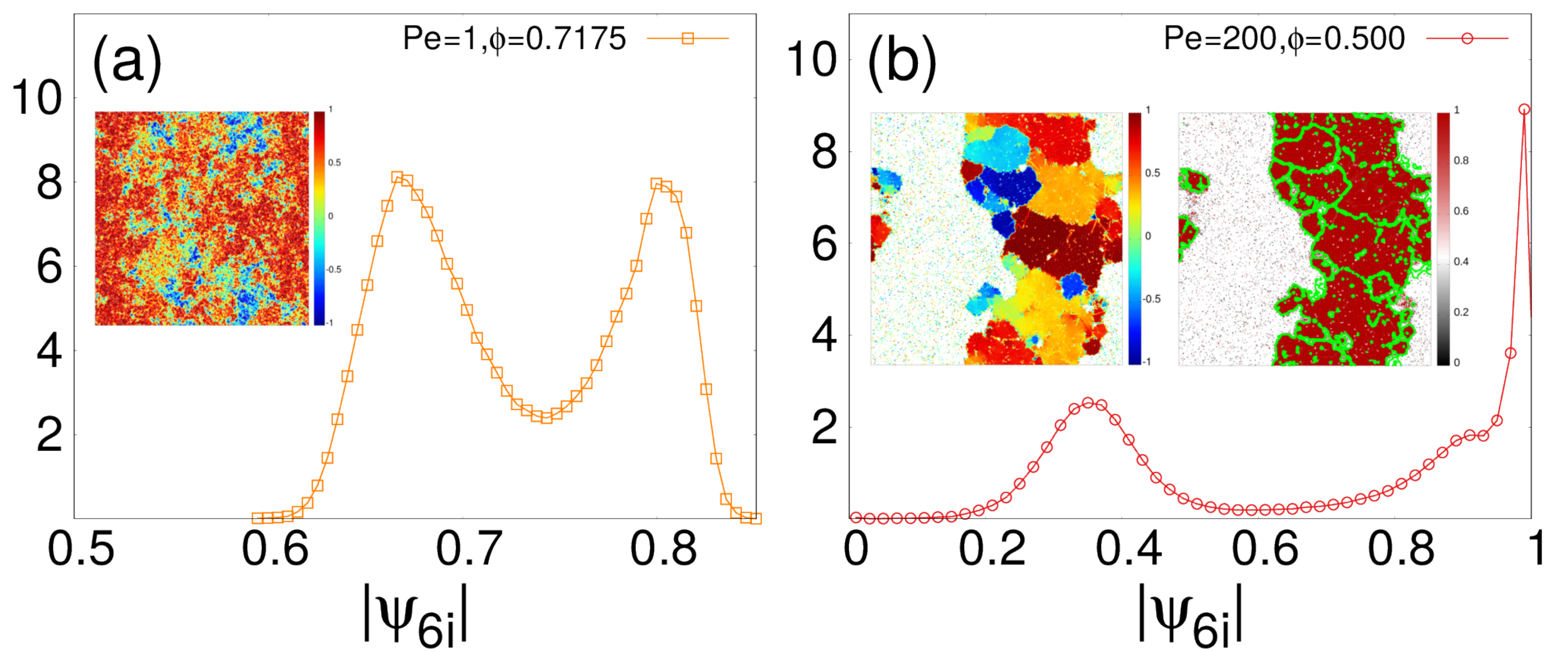

Co-existence in passive limit and in MIPS

Active disks

Local density distributions across MIPS

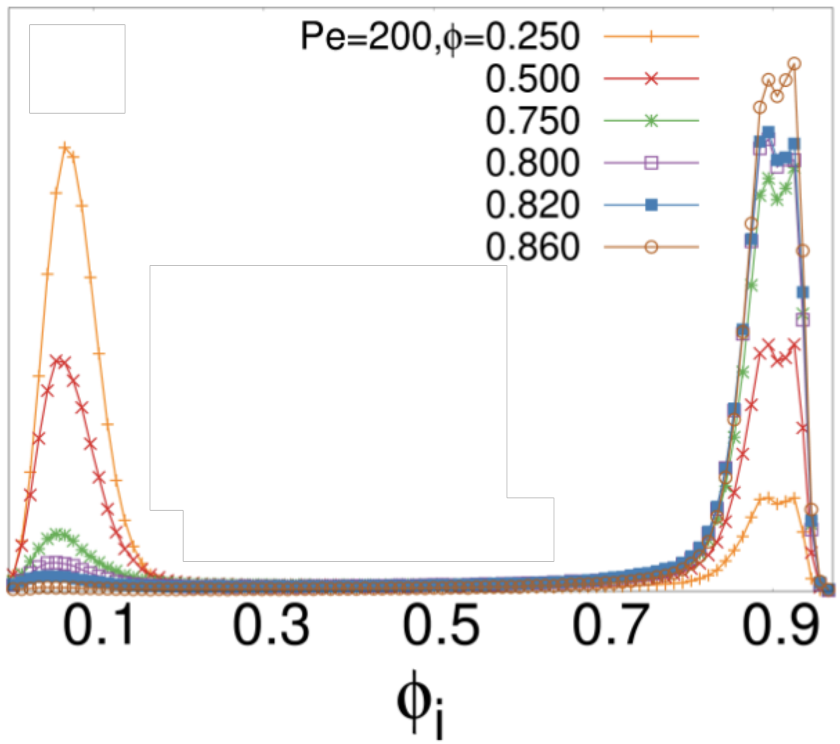

The position of peaks does not change while changing the global packing fraction ϕ but the relative height of them does. Transfer of mass from gas to dense component as ϕ increases

MIPS

Point-like defects

A zoom over high ϕ

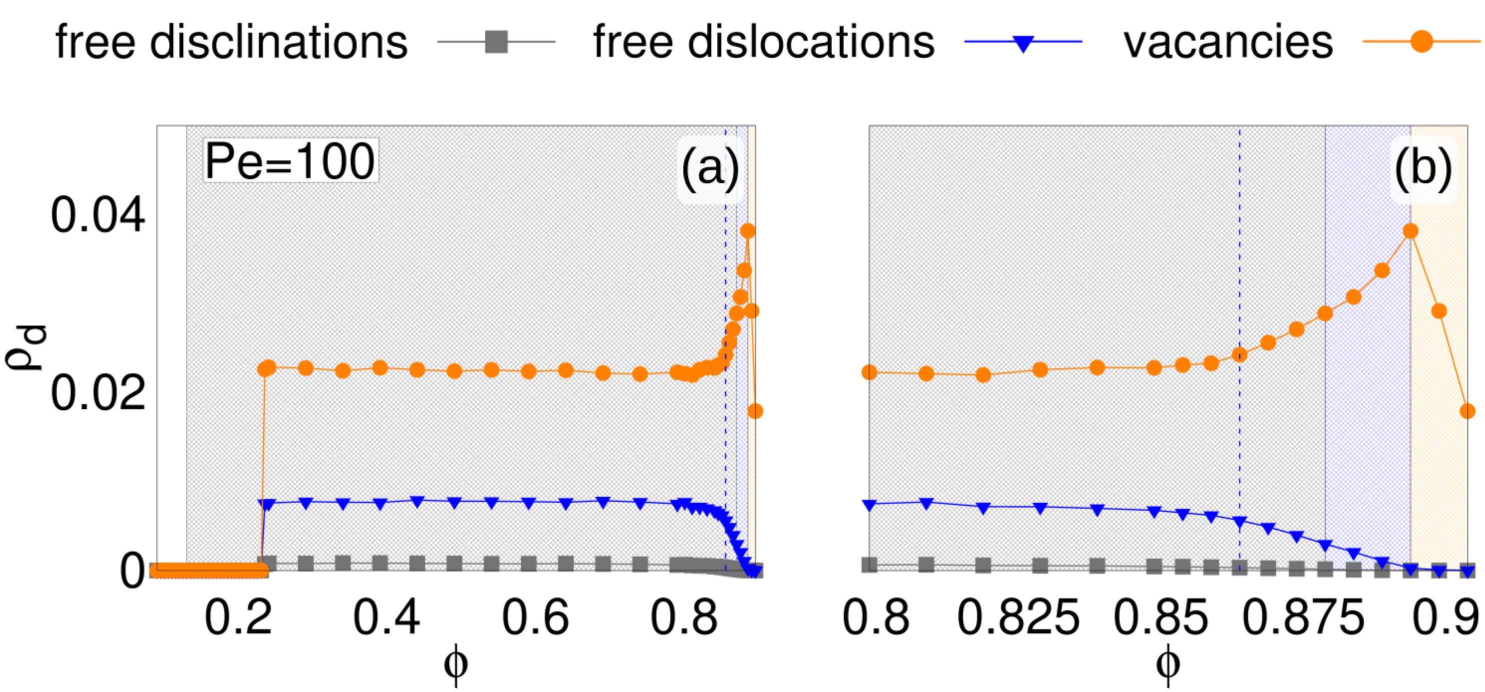

Densities ρ_d are quite independent of ϕ in the bulk of the **MIPS** phase

MIPS

Configuration

Hexatic order map

Defects

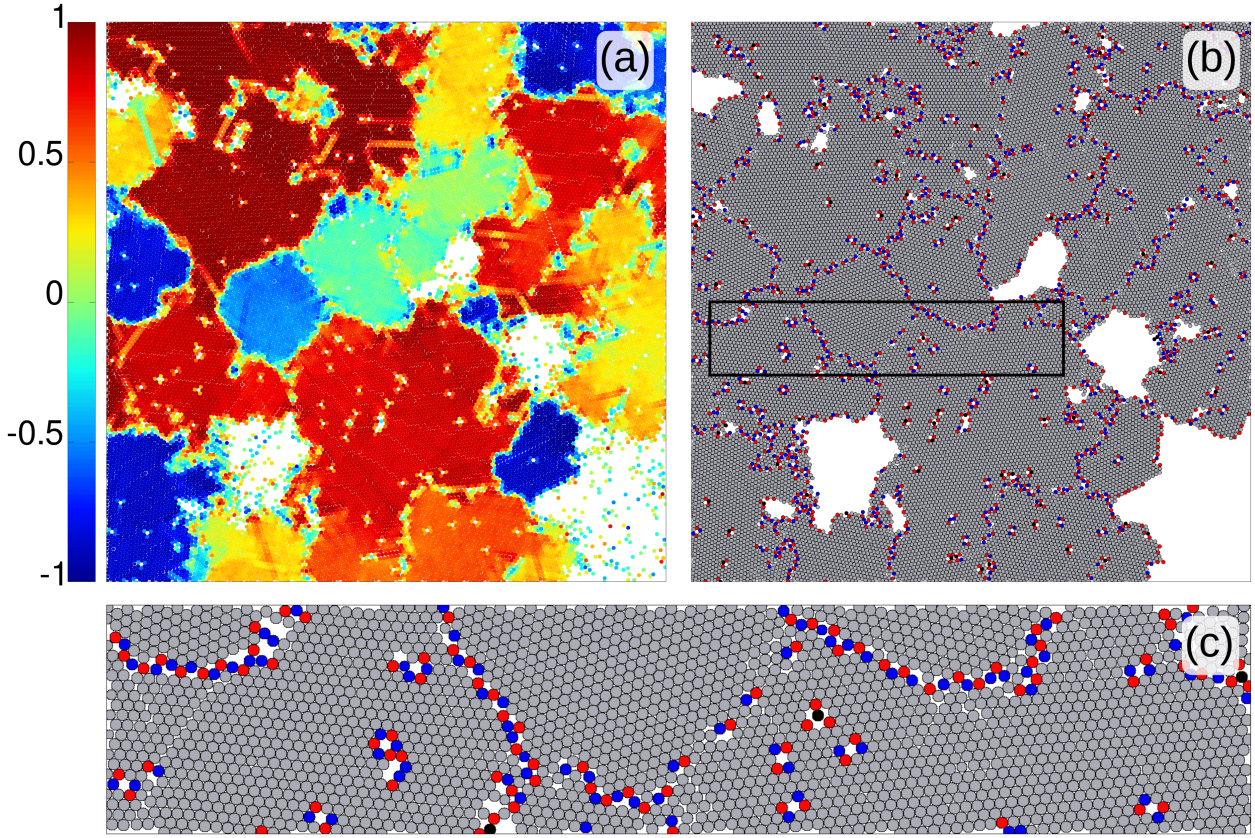

Zoom over the rectangular selection

Clusters

Probability distribution of sizes

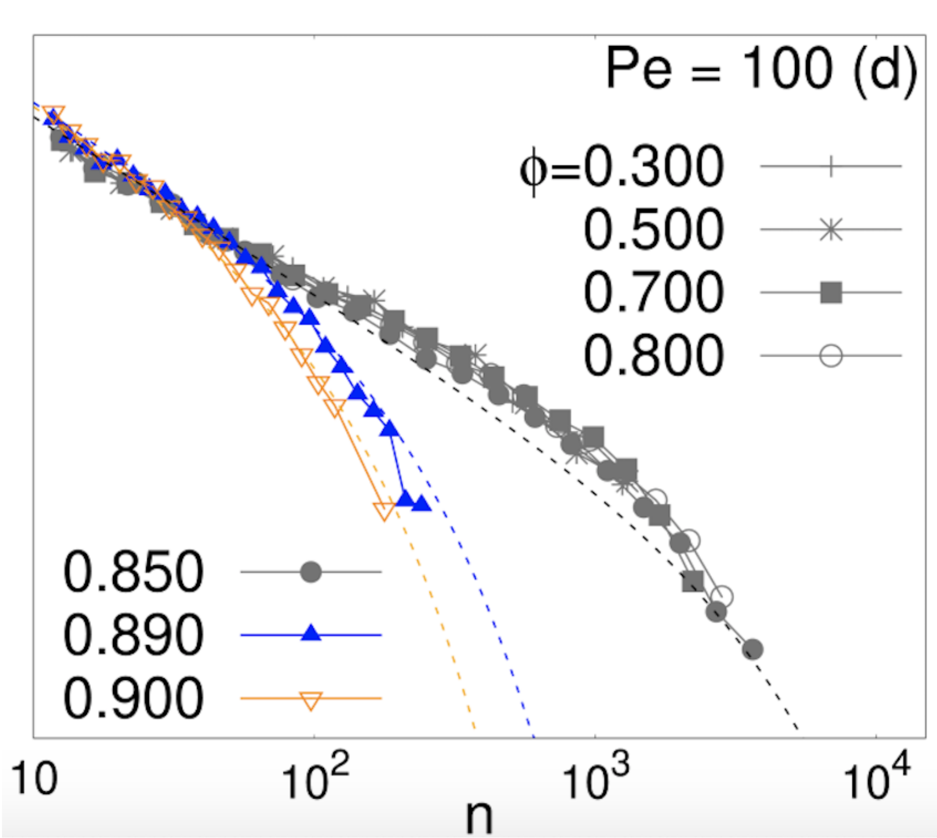

$$P(n) \simeq n^{-\tau} e^{-n/n^*}$$

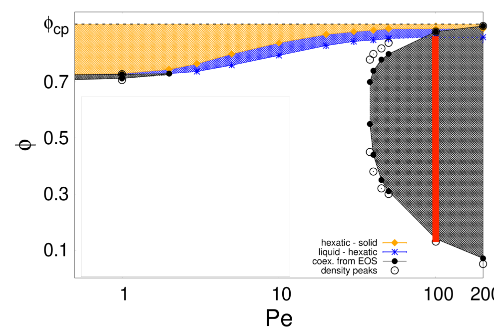

Independence of ϕ at fixed Pe within MIPS

MIPS

No criticality due to gas bubbles in cavitation

Percolation transition

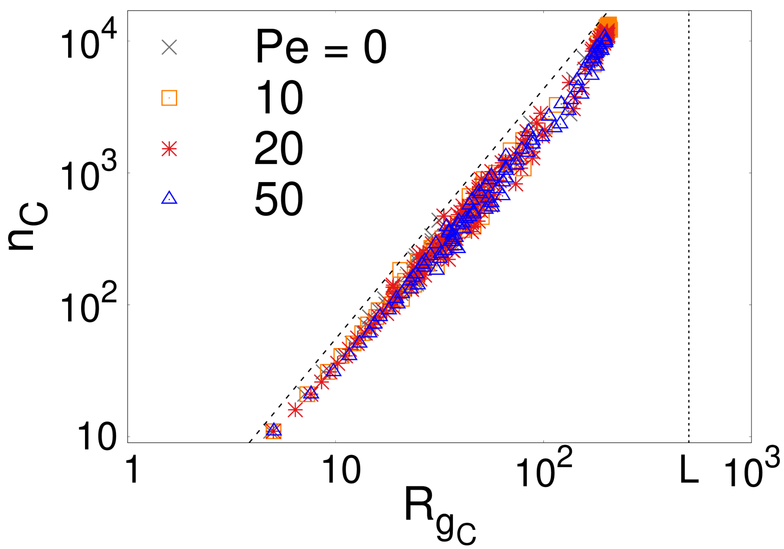

MIPS

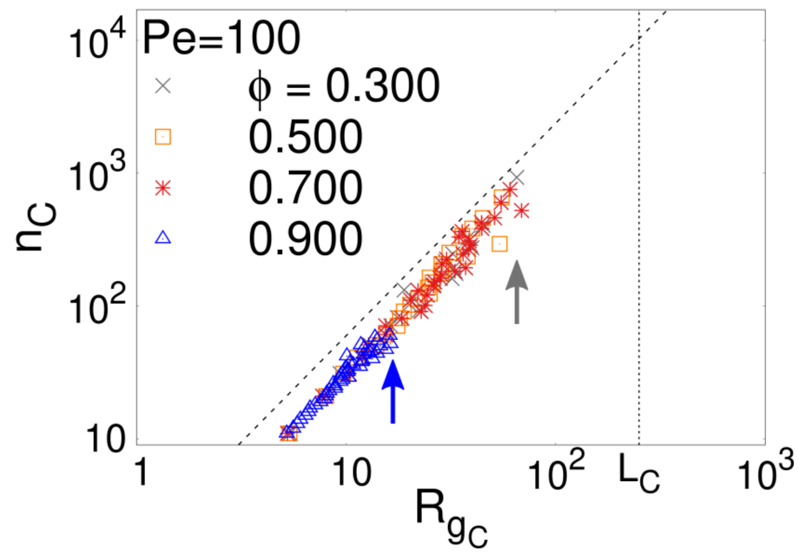

No ϕ dependence in MIPS

L_C estimated linear size of dense phase

MIPS

Bubbles in cavitation

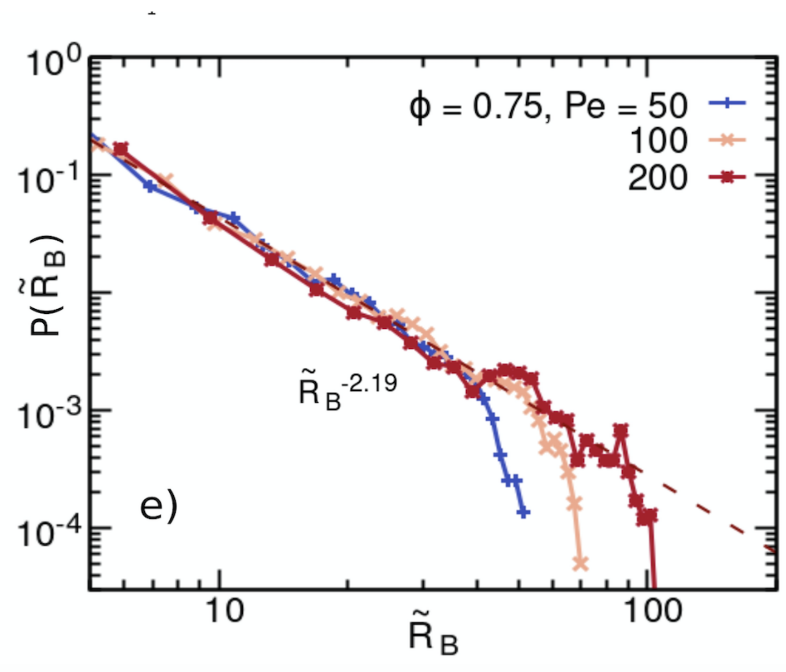

Algebraic distribution of bubble sizes with an exponential cut-off

Results

Summary

- **Solid** - **hexatic** à la BKT-HNY even quantitatively (ν) and independently of Pe. Universality.
- **Hexatic** - **liquid** very few disclinations and not even free. Breakdown of the BKT-HNY picture for all Pe.
- Close to, but in the liquid, **percolation** of clusters of defects, with properties of uncorrelated critical percolation ($d_{\rm f}, \tau$).
- In **MIPS**, network of defects on top of the interfaces between hexatically ordered regions, interrupted by the gas bubbles in cavitation.

Growth

MIPS: regimes

Multinucleation, evaporation/coagulation, scaling regime, saturation

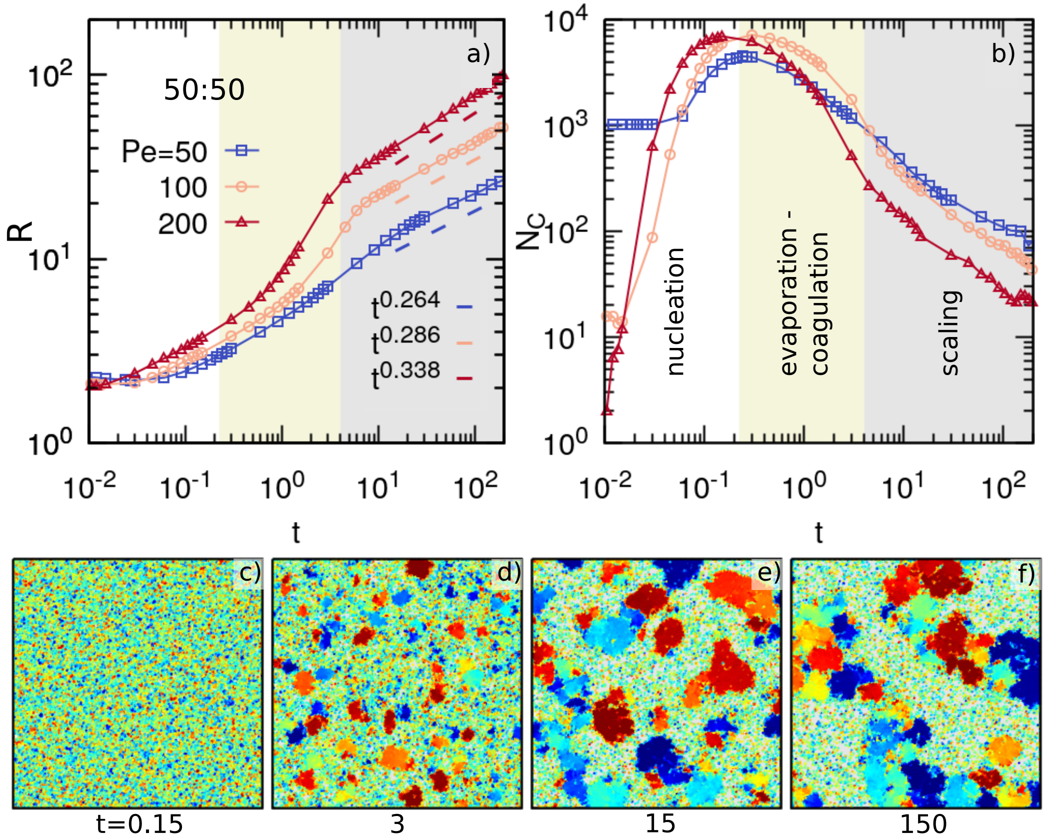

On the scaling regime: **Redner, Hagan & Baskaran, PRL 110, 055701 (2013)**

Stenhammar, Marenduzzo, Allen & Cates, Soft Matter 10, 1489 (2014), etc.

MIPS: regimes

Growth of the dense component, R_G, and hexatic order, R_H

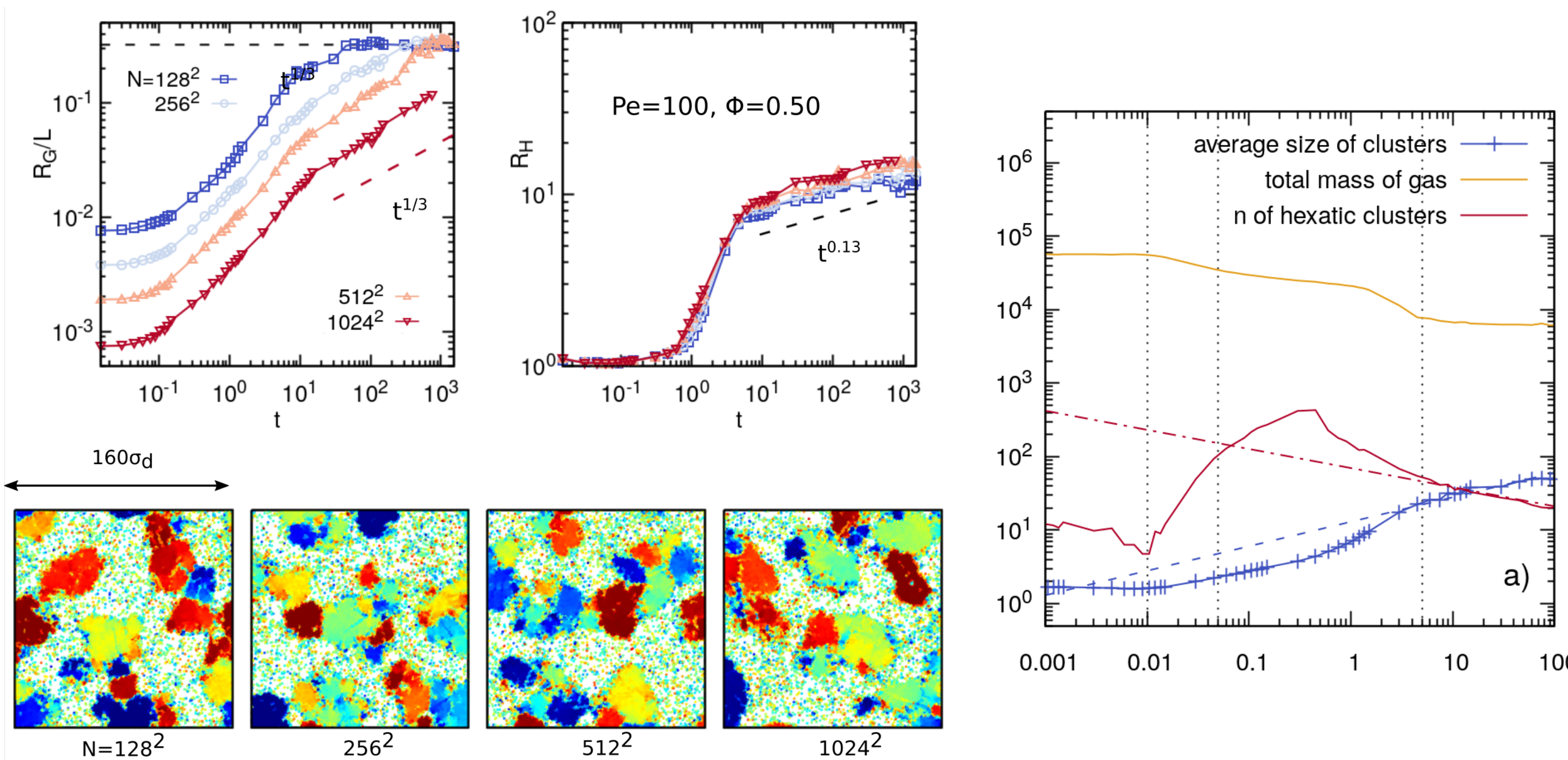

$R_G \simeq t^{1/3}$ in the scaling regime (à la **Lifshitz-Slyozov-Wagner**), and $R_G \to c\,L$

$R_H \simeq t^{0.13}$ in the scaling regime and $R_H \to R_H^{\rm st} \ll L$ (similar to pattern formation, e.g. **Vega et al. PRE 71, 061803 (2005)**)

MIPS : macro vs micro

Stationary state, zoom over the box, or video disk, slab, random

Local hexatic order map   Local density map

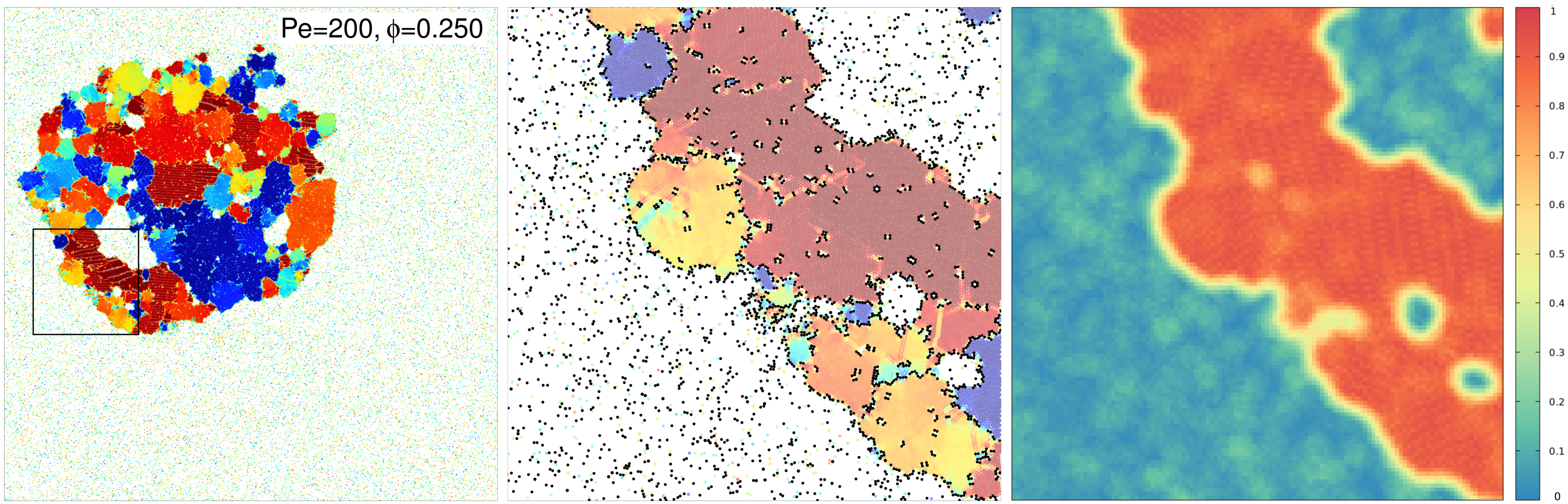

Local hexatic order saturates to a size independent value

Defects on the boundaries between different hexatic ordered patches

Note the bubbles within the dense droplet

MIPS

In the stationary state, size distributions

hexatic patch radii

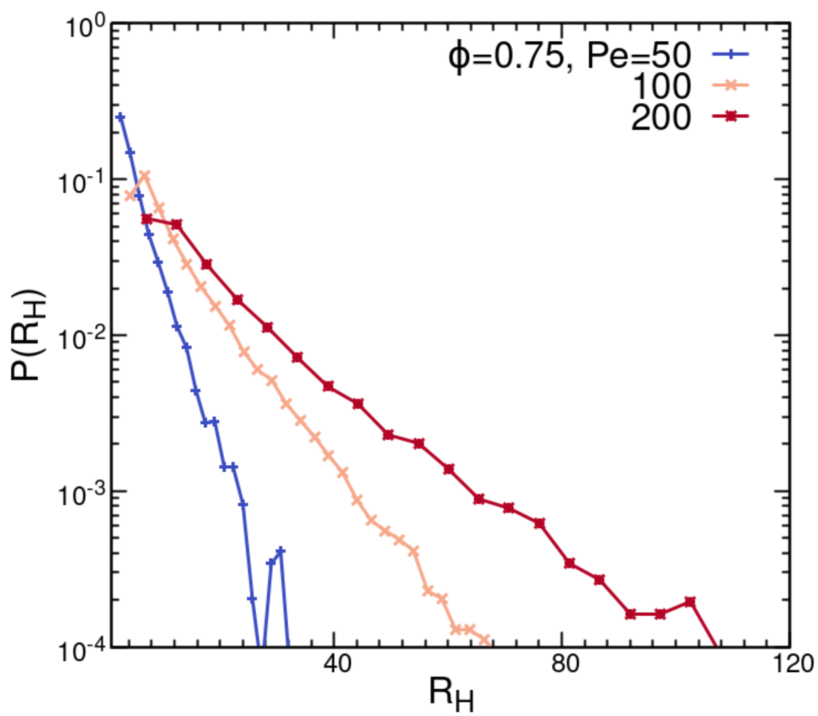

bubble radii

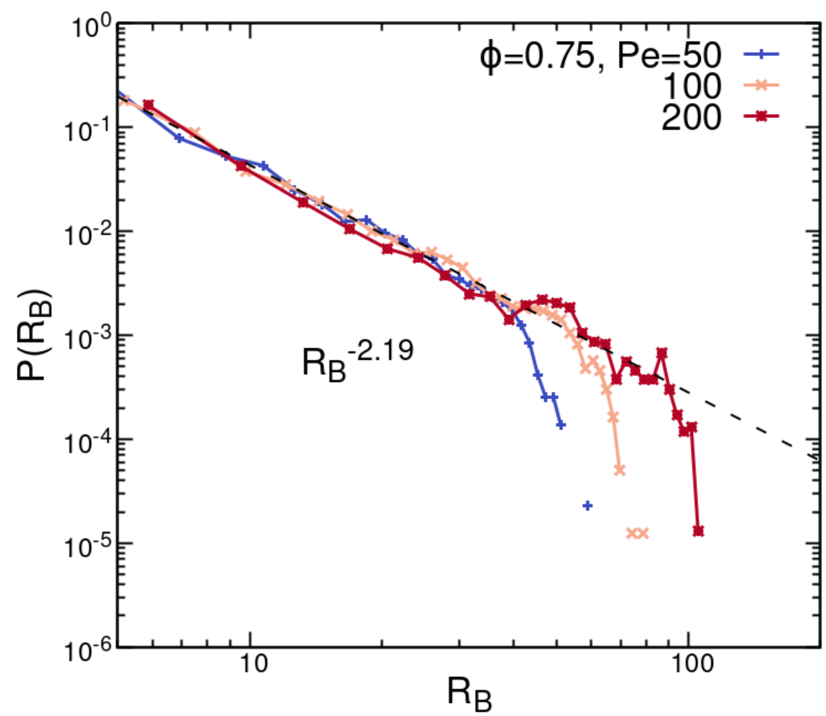

$e^{-R_H/R_H^*(\mathrm{Pe})}$ exponential

$R_B^{-\alpha}\, e^{-R_H/R_B^*(\mathrm{Pe})}$ algebraic w/exp cut-off

Summary & conclusions

There is still a lot to be understood in the very "classic" problem of melting of passive systems in two dimensions.

New picture with a first order phase transition towards the liquid.

The standard lore on topological effects is only partially verified.

Effects of activity?

We established the phase diagram of active Brownian particles

we studied the statistics of topological defects

and the coarsening dynamics

This is a problem in which numerical simulations have been of great help.

Active Brownian systems

Phase diagrams & plenty of interesting facts

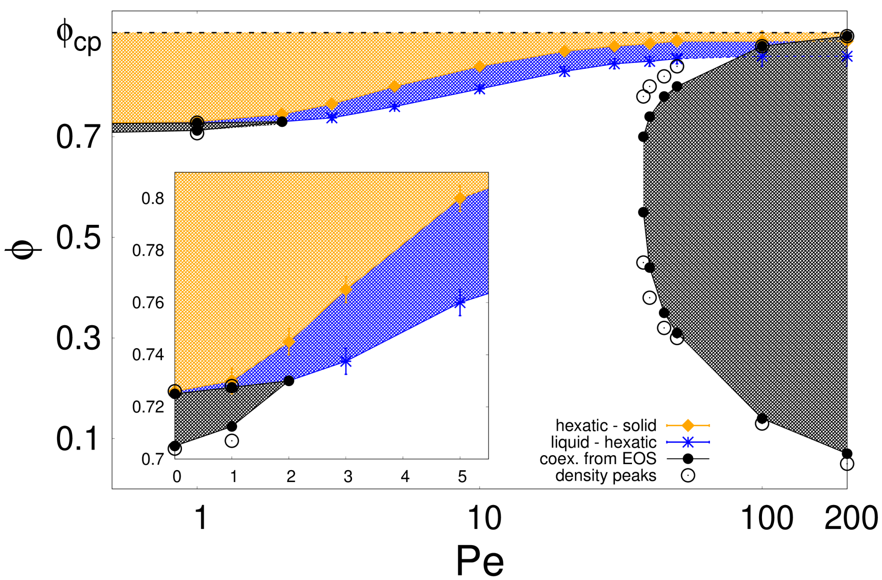

Disks

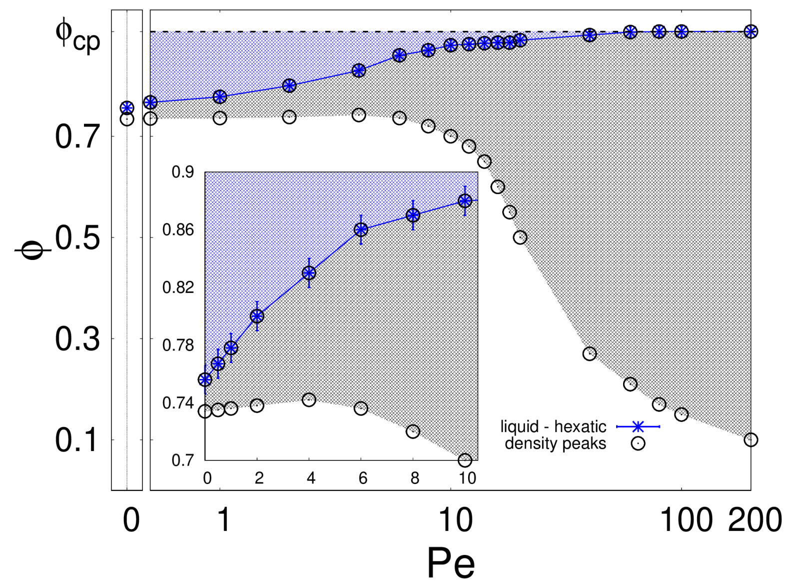

Dumbbells

Summary

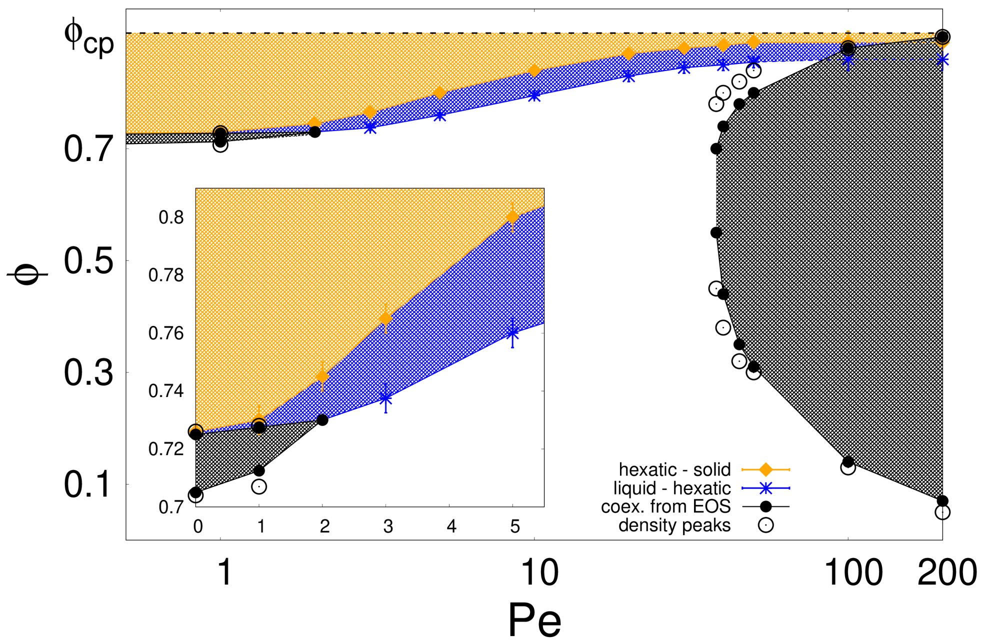

ϕ_{cp}
0.7
0.5
0.3
0.1
ϕ
1
10
100
200
Pe
0.8
0.78
0.76
0.74
0.72
0.7
0
1
2
3
4
5
hexatic - solid
liquid - hexatic
coex. from EOS
density peaks

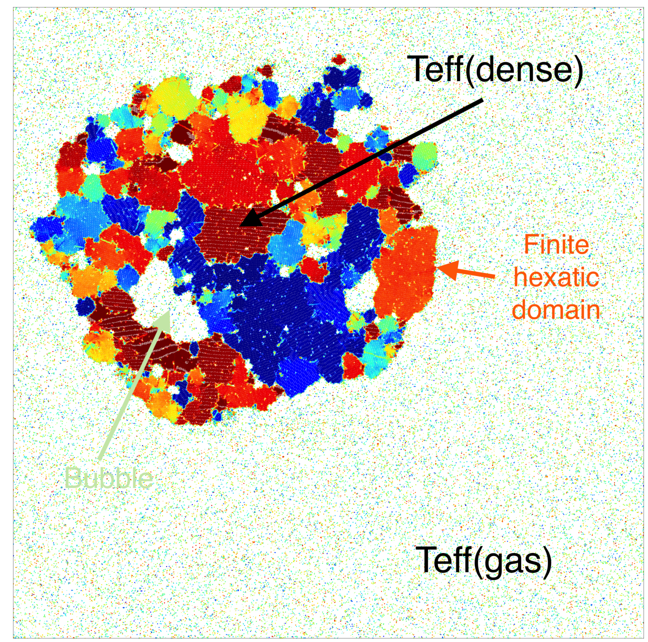

Teff(dense)
Finite hexatic domain
Bubble
Teff(gas)

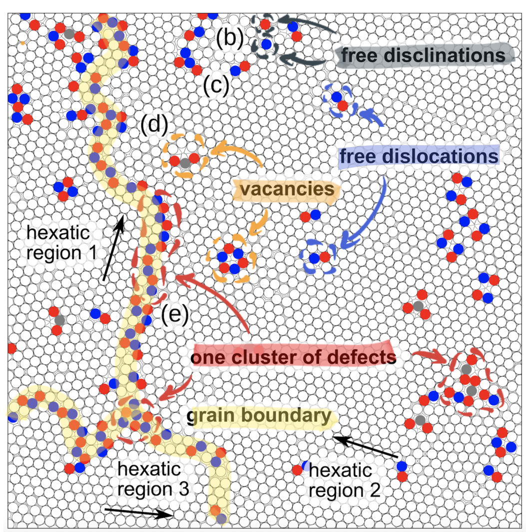

(b)
(c)
(d)
(e)
free disclinations
free dislocations
vacancies
hexatic region 1
one cluster of defects
grain boundary
hexatic region 3
hexatic region 2

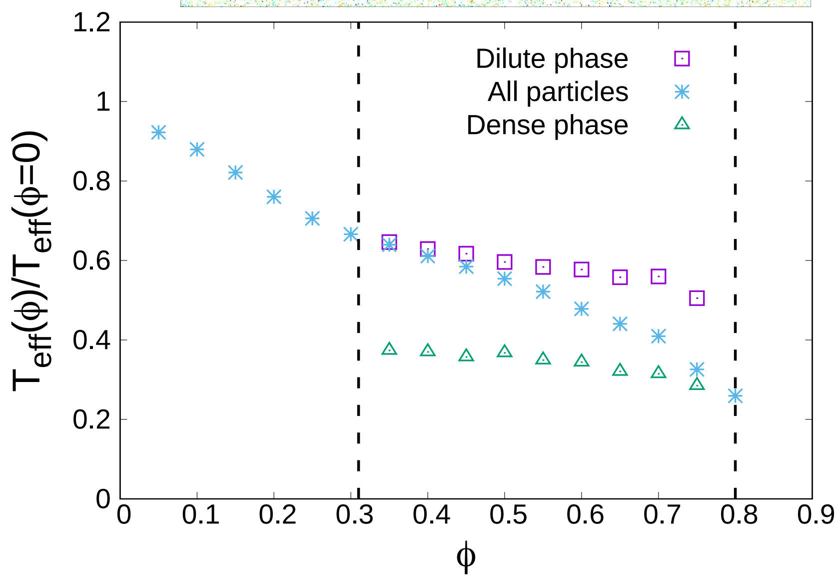

$T_{eff}(\phi)/T_{eff}(\phi=0)$
ϕ
Dilute phase
All particles
Dense phase
1.2
1
0.8
0.6
0.4
0.2
0
0.1
0.2
0.3
0.4
0.5
0.6
0.7
0.8
0.9

Fluctuation-dissipation

Linear relation between χ and Δ^2 in equilibrium

$$\boxed{P(\zeta, t_w) \to P_{\mathrm{eq}}(\zeta)}$$

- The dynamics are stationary

$$\Delta^2_{AB}(t,t_w) = \langle [A(t) - B(t_w)]^2 \rangle = [C_{AA}(0) + C_{BB}(0) - 2C_{AB}(t-t_w)]$$

$$\to \Delta^2_{AB}(t-t_w)$$

- The fluctuation-dissipation theorem between spontaneous (Δ^2_{AB}) and induced (R_{AB}) fluctuations

$$R_{AB}(t-t_w) = \frac{1}{2k_BT} \frac{\partial \Delta^2_{AB}(t-t_w)}{\partial t} \, \theta(t-t_w)$$

holds and implies

$$\boxed{\chi_{AB}(t-t_w) \equiv \int_{t_w}^{t} dt' \, R_{AB}(t,t') = \frac{1}{2k_BT}[\Delta^2_{AB}(t-t_w) - \Delta^2_{AB}(0)]}$$

Fluctuation-dissipation

Linear relation between χ and Δ^2 out of equilibrium ?

$$P(\zeta, t_w) \neq P_{\rm eq}(\zeta)$$

- The dynamics are stationary

$$\Delta^2_{AB}(t,t_w) = \langle [A(t) - B(t_w)]^2 \rangle = [C_{AA}(0) + C_{BB}(0) - 2C_{AB}(t-t_w)]$$

$$\to \Delta^2_{AB}(t-t_w)$$

- The fluctuation-dissipation theorem between spontaneous (Δ^2_{AB}) and induced (R_{AB}) fluctuations

$$R_{AB}(t-t_w) \neq \frac{1}{2k_BT} \frac{\partial \Delta^2_{AB}(t-t_w)}{\partial t} \, \theta(t-t_w)$$

does not hold but one can propose

$$\chi_{AB}(t-t_w) \equiv \int_{t_w}^{t} dt' \, R_{AB}(t,t') = \frac{[\Delta^2_{AB}(t-t_w) - \Delta^2_{AB}(0)]}{2k_BT_{\rm eff}(t-t_w)}$$

Teff = T

Co-existence in equilibrium

Pe = 0 $\phi = 0.710$

Integrated linear response & mean-square displacement: their ratio (FDT) $\tau = t - t_w$

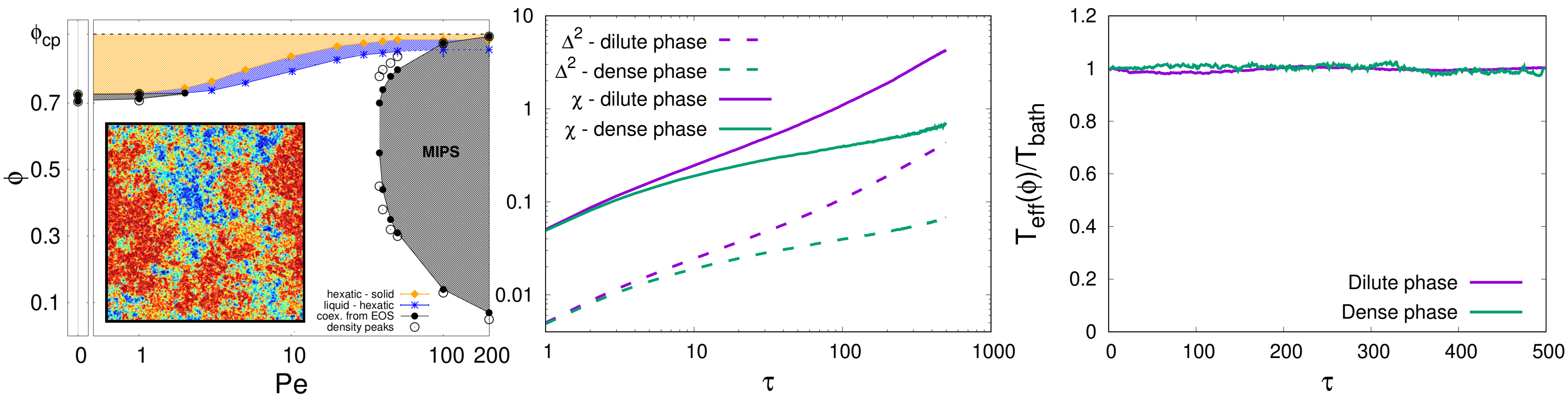

Method: linear response computed with Malliavin weights (no perturbation applied) as proposed by **G. Szamel** for active matter systems.

Petrelli, LFC, Gonnella & Suma, in preparation

Teff $\neq$ T

Co-existence in MIPS

Pe = 50 $\quad \phi = 0.5$

Integrated linear response & mean-square displacement: their ratio (FDR) $\tau = t - t_w$

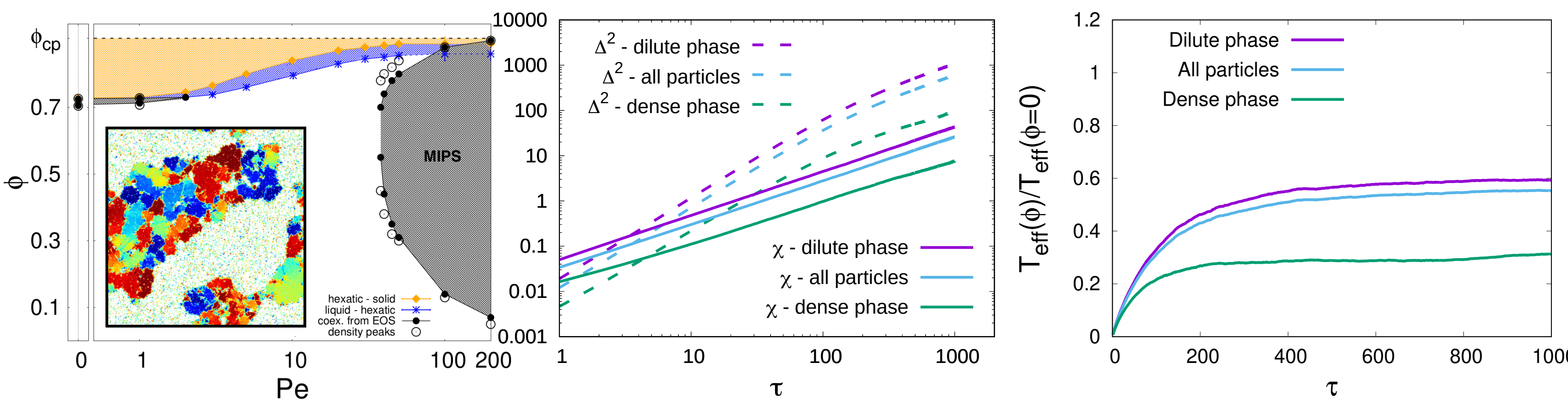

Method: linear response computed with Malliavin weights (no perturbation applied) as proposed by **G. Szamel** for active matter systems.

Petrelli, LFC, Gonnella & Suma, in preparation

Hard disks in two dimensions

Pressure loop and finite N dependence

Hexatic Liquid

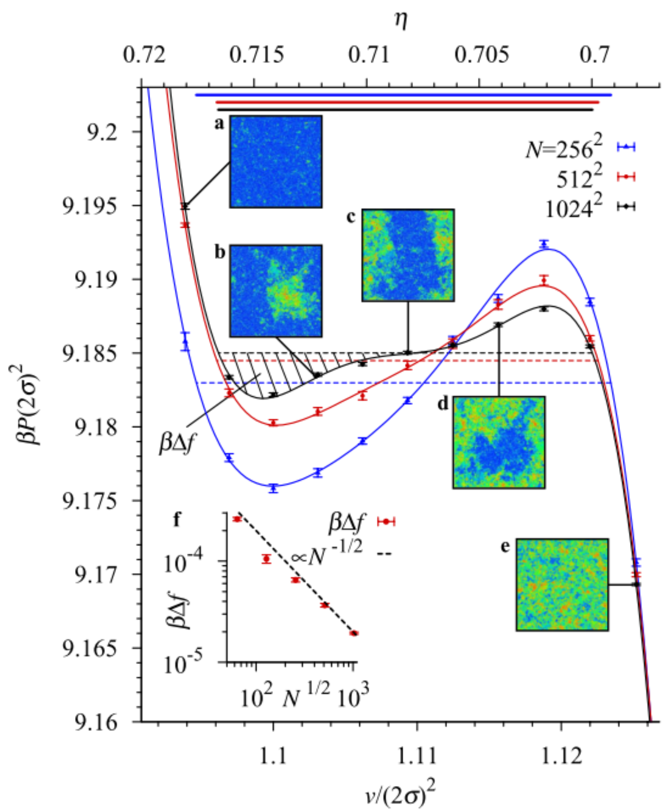

A system with PBCs has a $\sim$ flat interface with surface energy scaling as $S \simeq L^{d-1} = \sqrt{N}$ and $f \simeq N^{-1/2}$. Verified in the inset for $\phi \simeq 0.708$

Passive system

Structure factor - very low and very high density

$\phi = 0.66$

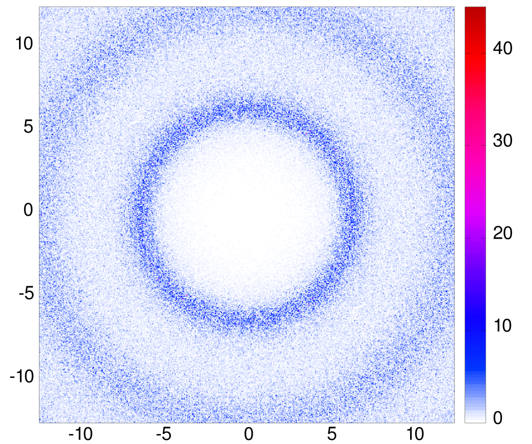

Liquid

$\phi = 0.76$

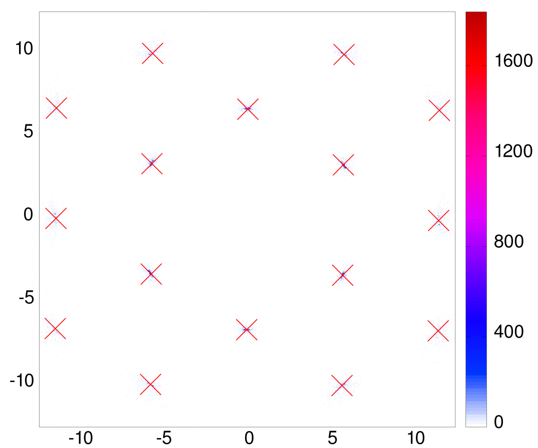

Solid

Bragg peaks

Primitive vectors

$$\boldsymbol{q}_1 = \frac{4\pi}{a\sqrt{3}}\left(\frac{\sqrt{3}}{2}, -\frac{1}{2}\right)$$

$$\boldsymbol{q}_2 = \frac{4\pi}{a\sqrt{3}}(0, 1)$$

Unit of length

$$a = \left(\frac{\pi}{2\sqrt{3}\phi}\right)^{1/2} \sigma_{\rm d}$$

Observables

Structure factor in $2d$: test of positional order

$\boldsymbol{r}_i$ and $\boldsymbol{r}_j$ are the positions of the disks i and j and $\boldsymbol{q}$ is a wave-vector :

$$S(\boldsymbol{q}) = \frac{1}{N} \sum_{ij} e^{\mathrm{i}\boldsymbol{q}\cdot(\boldsymbol{r}_i - \boldsymbol{r}_j)}$$

Visualisation: two dimensional representation in the (q_x, q_y) plane.

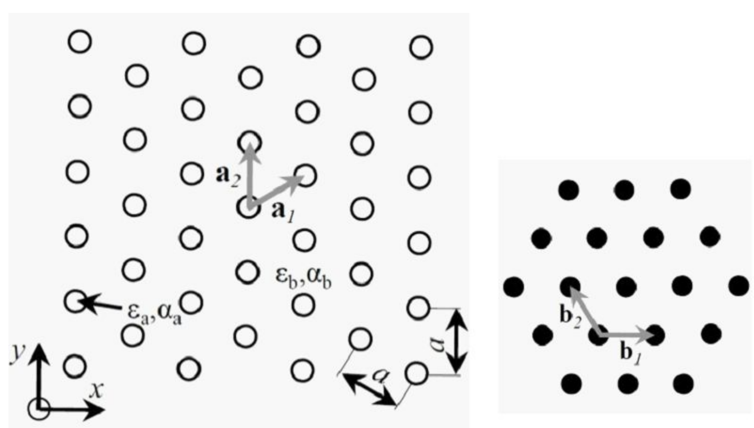

(a) (b)

Triangular lattice in real space Hexagonal lattice in reciprocal space

Passive system

Structure factor - progressive increase in density

$\phi = 0.66$
(liquid)

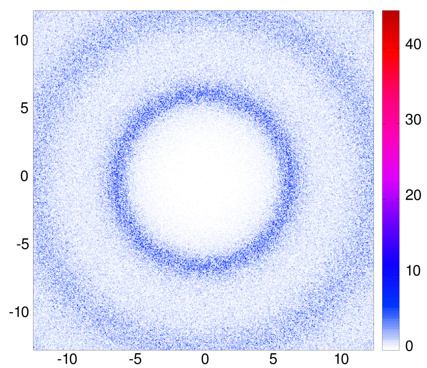

$\phi = 0.72$
(liquid)

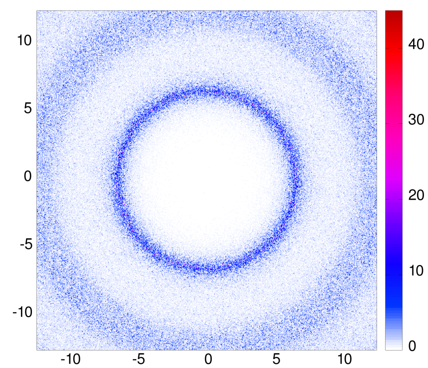

$\phi = 0.76$
(solid)

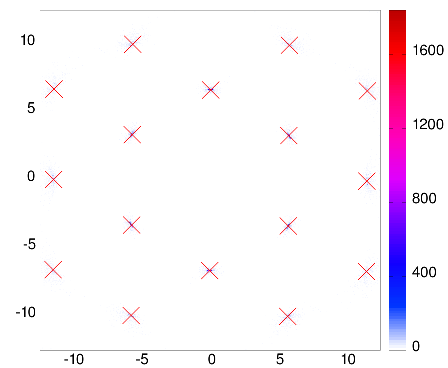

$\phi = 0.734$
(co-existence)

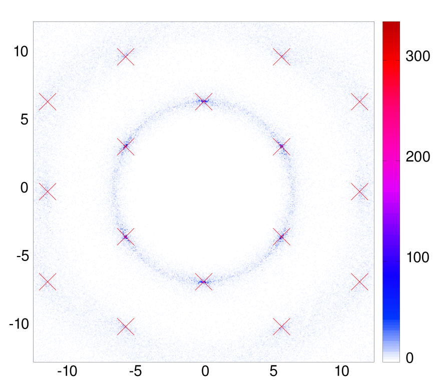

$\phi = 0.74$
(co-existence)

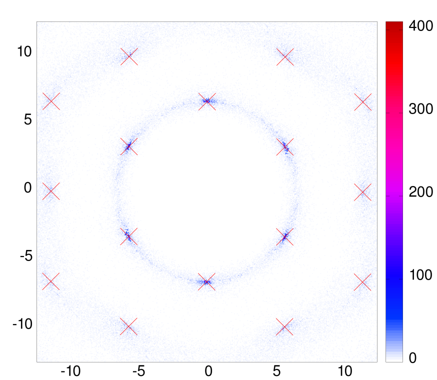

$\phi = 0.75$
(co-existence)

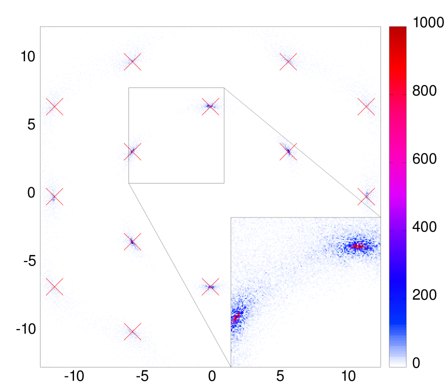

Active system

Structure factor Pe = 10 & Pe = 40

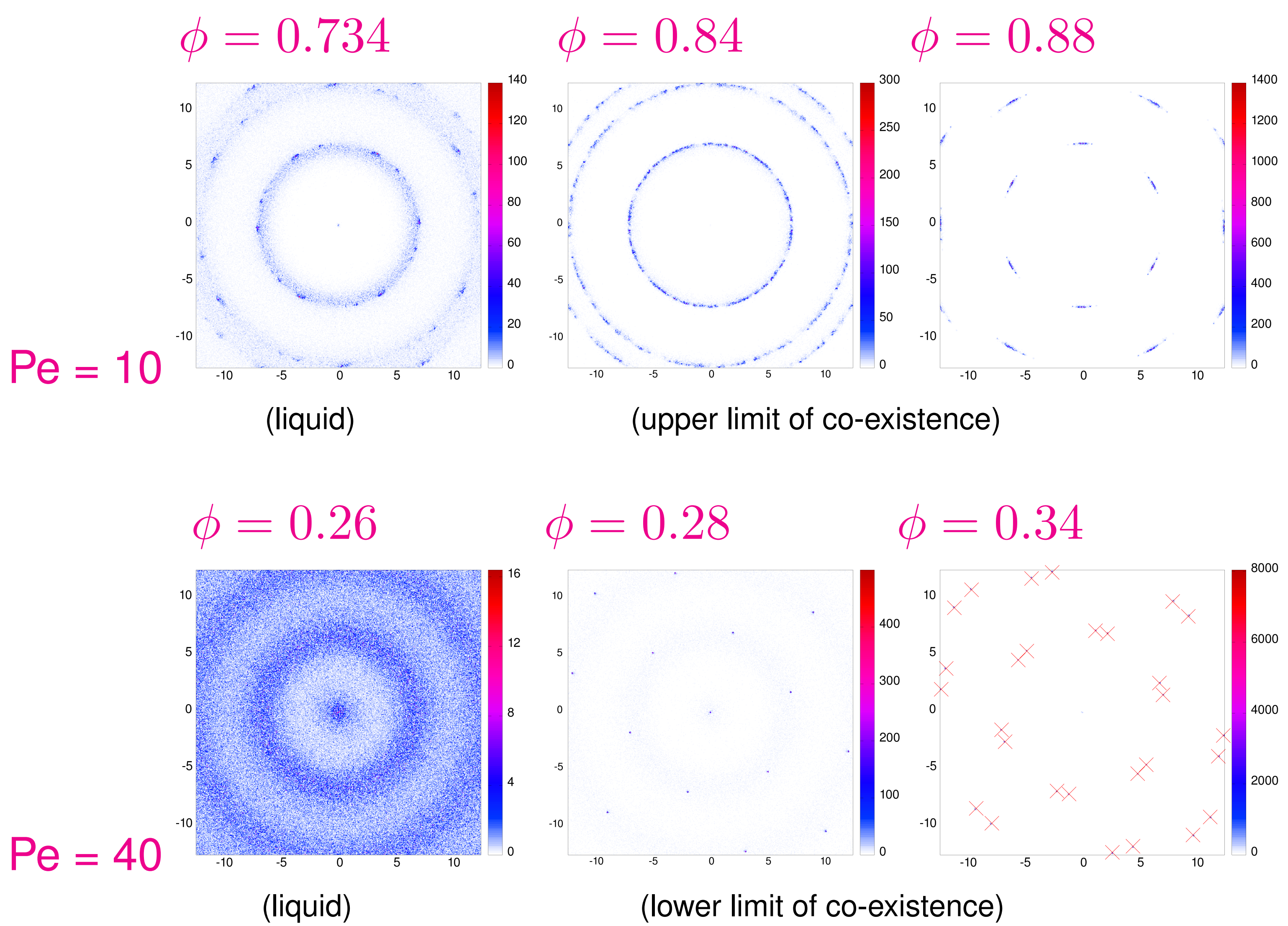

Kinetic energy

Two populations in co-existence region

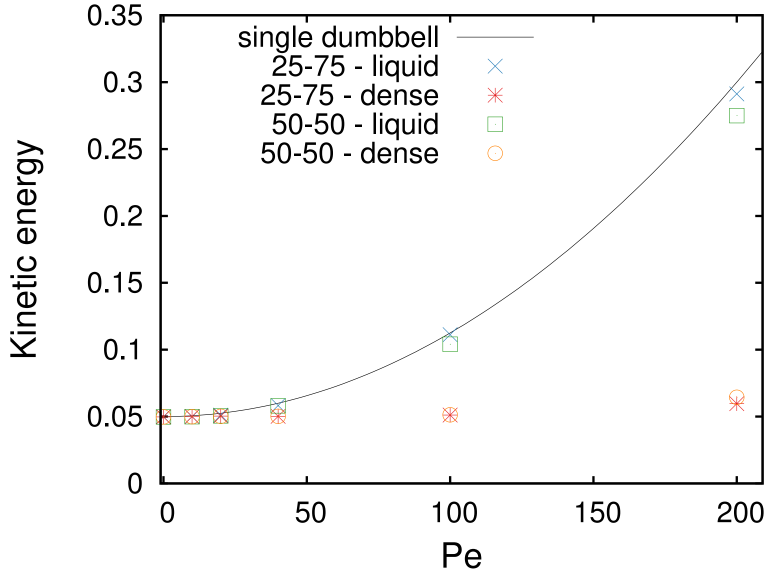

→ Liquid/disordered

→ Dense/hexatic

The averaged hexatic modulus is computed for each particle on a radius of 10 $\sigma_{\rm d}$ around the particle itself, and a particle is considered to be inside a cluster only if this value is greater than 0.75. Those particles contribute to the "dense" branch.

Petrelli, Digregorio, LFC, Gonnella, Suma, Eur. Phys. J. E 41, 128 (2018)

Active dumbbell

Control parameters

Number of dumbbells N and box volume S in two dimensions:

packing fraction $$\phi = \frac{\pi\sigma_{\rm d}^2 N}{2S}$$

Energy scales:

Active work $2\sigma_{\rm d}\, F_{\rm act}$

thermal energy $k_B T$

Péclet number $$\text{Pe} = \frac{2F_{\rm act}\sigma_{\rm d}}{k_B T}$$

Active force $Lv \mapsto \sigma_{\rm d}\, F_{\rm act}/\gamma$

viscous force $\nu \mapsto \gamma\sigma_{\rm d}^2/m_{\rm d}$

Reynolds number $$\text{Re} = \frac{m_{\rm d} F_{\rm act}}{\sigma_{\rm d}\gamma^2}$$

Pe $\in [0, 200]$ Re $< 10^{-2}$

$$N = 512^2 \simeq 2.6 \times 10^5$$

Stiff molecule limit: vibrations frozen.

Interest in the ϕ, $F_{\rm act}$ and $k_B T$ dependencies, $k_B T = 0.05$ fixed.

Active disks

Equation of state (eos) : pressure

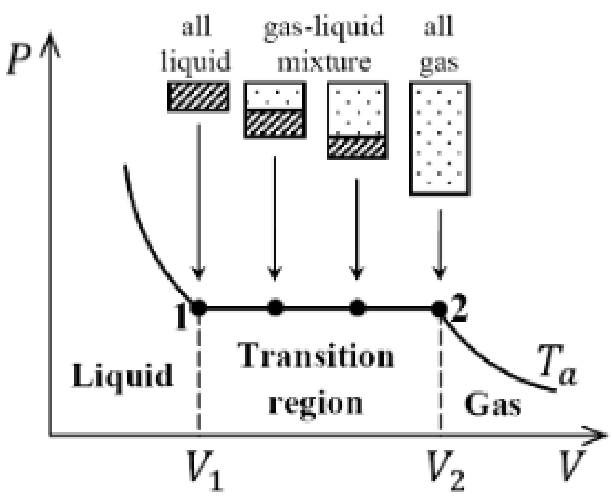

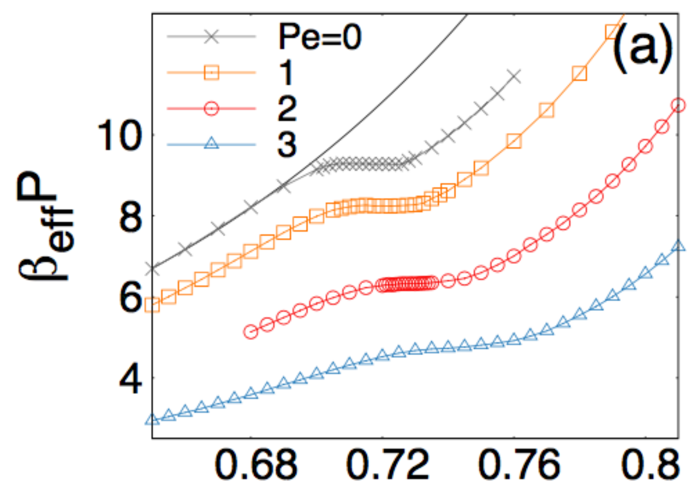

$$\Delta P = P - P_{gas} = \frac{F_{act}}{2V}\sum_i \langle \mathbf{n}_i \cdot \mathbf{r}_i \rangle - \frac{1}{4V}\sum_{i,j}\langle \nabla_i U(r_{ij}) \cdot (\mathbf{r}_i - \mathbf{r}_j)\rangle$$

Positional order

Experiments & simulations of liquids

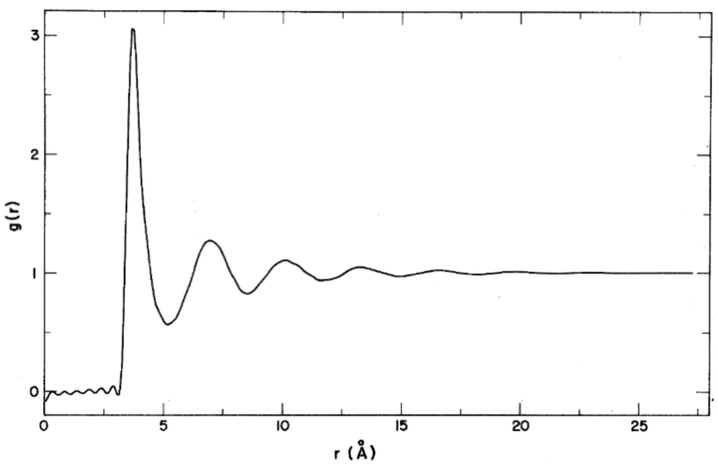

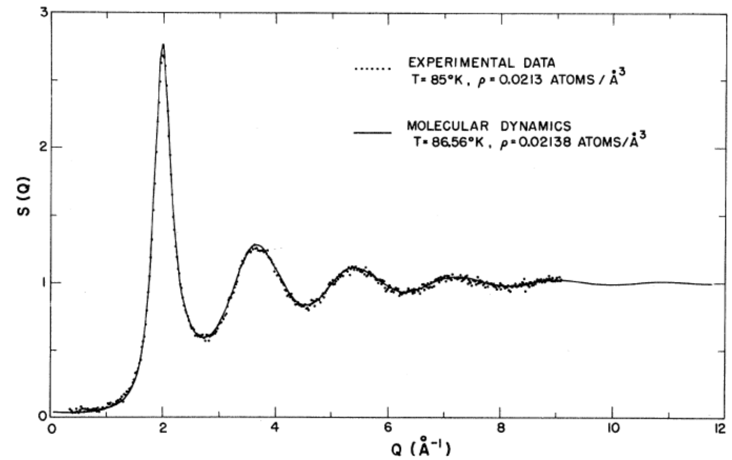

Inter-peak distance between the peaks in $g(r)$ is $\Delta r \simeq \sigma \simeq 3\text{Å}$

Position of the first peak in $S(q)$ is at $q_0 \simeq 2\pi/\Delta r \simeq 2\ \text{Å}^{-1}$

“Structure Factor and Radial Distribution Function for Liquid Argon at 85K”,

Yarnell, Katz, Wenzel & König, Phys. Rev. Lett. 7, 2130 (1973)

Defect clusters

Percolation features $P(n) \sim n^{-\tau}$

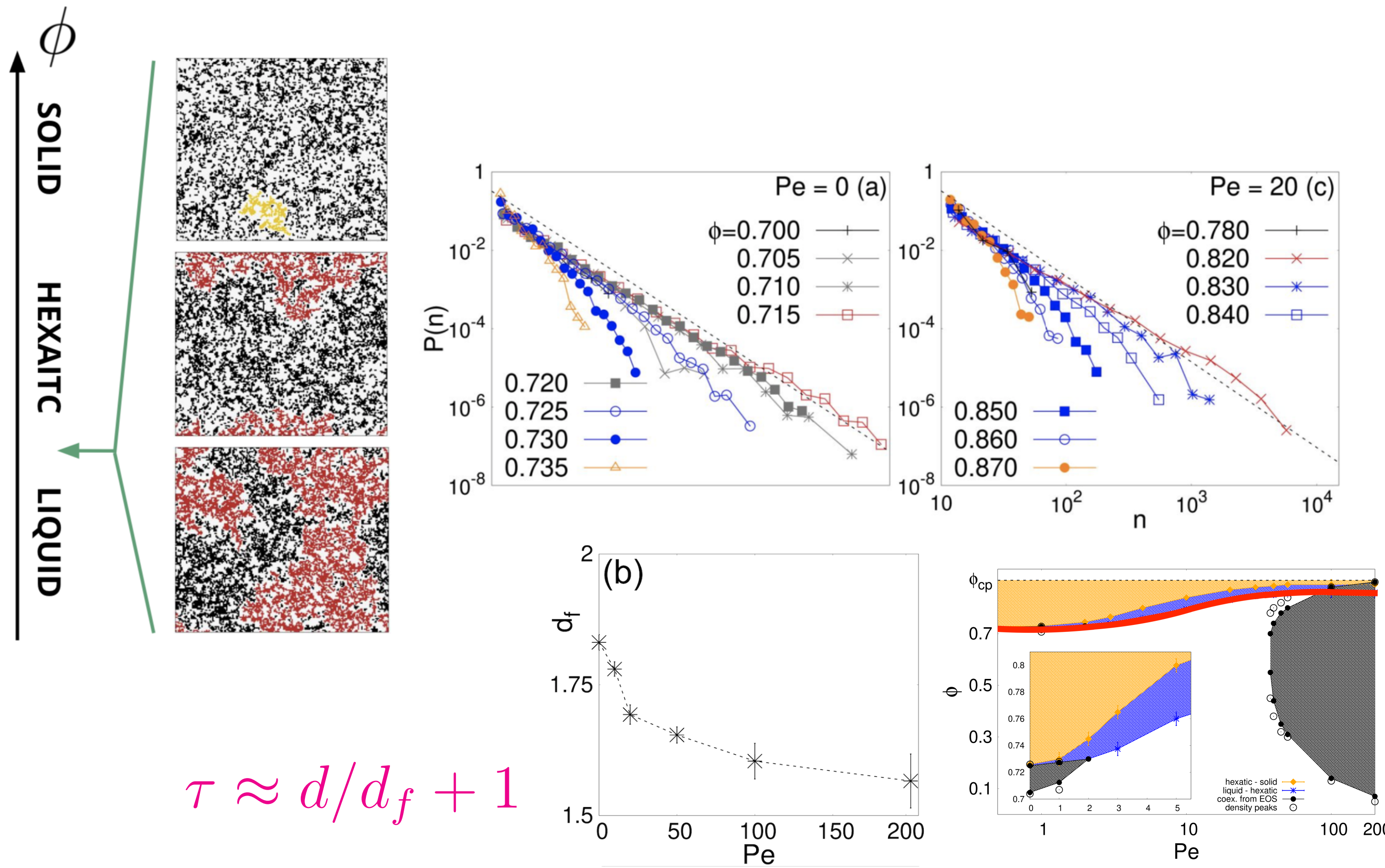

$\tau \approx d/d_f + 1$

d_f from the radius of gyration of the clusters

Active disks

Solid, hexatic, liquid & MIPS

1st order
w/co-existence

à la KTHNY

free dislocations at solid-hex

free disclinations in the liquid

in MIPS

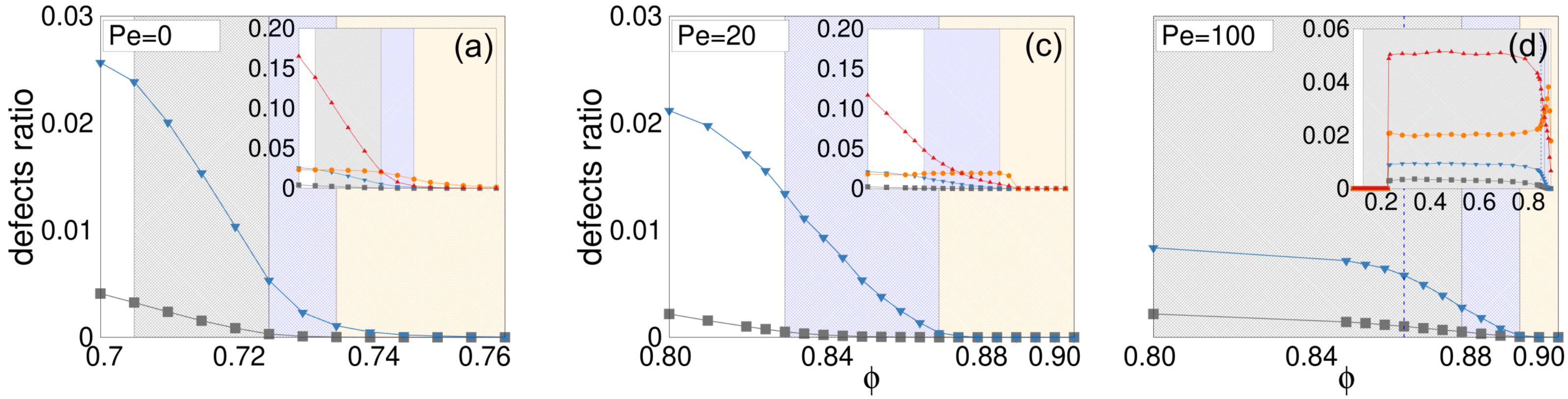

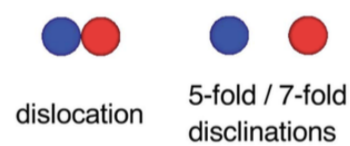

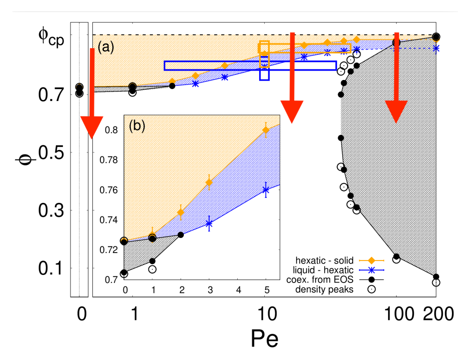

Digregorio, Levis, LFC, Gonnella & Pagonabarraga, arXiv:1911.06366

Clusters

Percolation: hexatic color maps & clusters

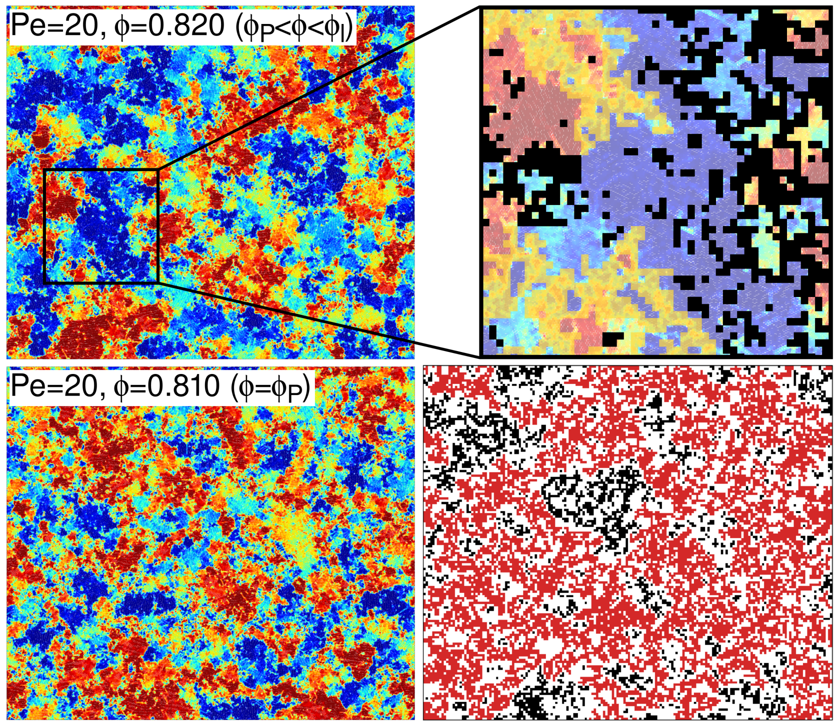

The liquid permeates the sample through the interfaces between local hexatically ordered patches

But, are these the most relevant critical clusters? Recall Fortuin-Kasteleyn

MIPS

Stationary state

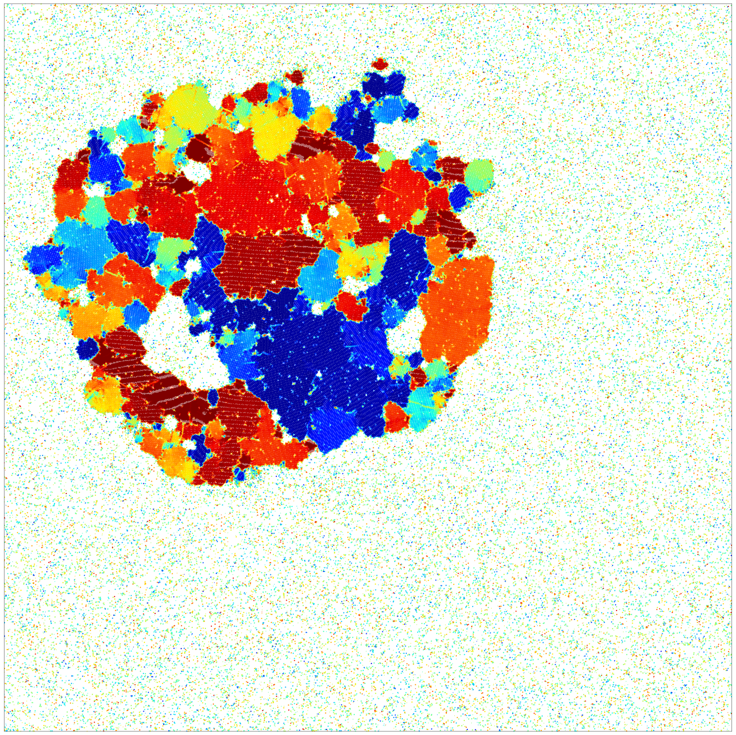

Dense/dilute separation[1]

For low packing fraction ϕ

a single round droplet.

A mosaic of different

hexatic orders[2] with

gas bubbles[2,3,4]

Defects ?

[1] Cates & Tailleur, Annu. Rev. Cond. Matt. Phys. 6, 219 (2015)

[2] Caporusso, Digregorio, Levis, LFC & Gonnella, PRL 125, 178004 (2020)

[3] Tjhung, Nardini & Cates, PRX 8, 031080 (2018)

[4] Shi, Fausti, Chaté, Nardini & Solon, PRL 125, 168001 (2020)